# University of Alberta

Modulation of Chemotransduction in Type I (Glomus) Cells of Rat Carotid Bodies by Adenosine 5'-Triphosphate (ATP), Adenosine, and Pituitary Adenylate Cyclase-Activating Polypeptide (PACAP)

by

Fenglian Xu 

A thesis submitted to the Faculty of Graduate Studies and Research in partial fulfillment of the requirements for the degree of Doctor of Philosophy

Centre for Neuroscience

Edmonton, Alberta

Spring 2007

*Your file Votre référence*
*ISBN: 978-0-494-29772-8*
*Our file Notre référence*
*ISBN: 978-0-494-29772-8*

## Abstract

Type I (glomus) cells in the carotid body are the major peripheral chemoreceptors that respond to changes in $P_{O_2}$, $P_{CO_2}$ and pH level in blood vessels. The actions of three important transmitters (ATP, adenosine and PACAP) on enzymatically dissociated single type I cells of rat carotid bodies were studied with cytosolic $[Ca^{2+}]$ ($[Ca^{2+}]_i$) measurement in conjunction with perforated patch-clamp techniques.

ATP (a transmitter released by type I cells during hypoxia) did not affect the resting $[Ca^{2+}]_i$ but strongly inhibited hypoxia-induced membrane depolarization and $[Ca^{2+}]_i$ elevation in type I cells via activities of $P2Y_1$ receptors. ATP did not oppose the hypoxia-mediated inhibition of the oxygen ($O_2$)-sensitive TWIK-related acid-sensitive $K^+$ (TASK)-like $K^+$ current. Neither the inhibition of large-conductance $Ca^{2+}$-activated $K^+$ (BK) channels nor the removal of extracellular $Na^+$ could affect the inhibitory action of ATP. Under normoxic condition, ATP caused hyperpolarization and increase in cell input resistance. These results suggest that the inhibitory action of ATP is mediated via the closure of background conductance(s) other than the TASK-like $K^+$, BK or $Na^+$ conductance. In summary, ATP exerts strong negative feedback regulation on hypoxia signaling in rat type I cells.

Adenosine, the ATP metabolite, acting via $A_{2A}$ receptors coupled to adenylate cyclase and protein kinase A (PKA) pathway, inhibited the TASK-like $K^+$ channels. This led to depolarization and activation of $Ca^{2+}$ influx via voltage-gated $Ca^{2+}$

channels (VGCC). This excitatory action of adenosine on type I cells may help type I cells to recover from the negative feedback action of ATP.

PACAP, a circulating hormone, is also thought to play an important role in respiration. PACAP-deficient mice are prone to sudden neonatal death and have reduced respiratory response to hypoxia. My findings have shown that PACAP triggered a rise in $[Ca^{2+}]_i$ in type I cells, but not glial-like type II cells. In type I cells, PACAP, acting via the PACAP type I receptor ($PAC_1$)-coupled PKA pathway, inhibited a TASK-like $K^+$ current and caused depolarization and VGCC activation. This stimulatory action of PACAP in carotid type I cells may partly account for the role of PACAP in respiratory disorders.

In summary, chemotransduction in the carotid body is regulated by complex autocrine/paracrine actions of transmitters as well as circulating peptides.

## Dedication

This thesis is dedicated to my parents and my husband. Without their constant love and support, this body of work would never have been completed.

# Acknowledgments

First and foremost, I would like to thank my co-supervisors Dr. Amy Tse and Fred Tse for giving me the chance to come from China and study in their laboratory. With their enthusiasm, their inspiration and great efforts to explain things clearly and simply, they have helped me gain valuable knowledge and expertise in doing research. They provided kind encouragement, sound advice, and tremendous help not only in my study, but also in my personal life. Without their great supervision, generous help and good company, I would not have been able complete this body of work.

I wound especially like to thank the former postdoc in our lab, Dr. Jianhua Xu, who contributed to this thesis by collaborating with me on the ATP and adenosine projects. I thank him for teaching me the techniques for cell dissociation and culture, calcium imaging, and patch-clamp recording. With his encouragement and good teaching, I quickly picked up all the techniques and began work on my thesis projects.

I am grateful to my supervisory committee members, Drs. Peter Smith and Peter Nguyen, for their valuable suggestions, guidance, and kind help during my studies and all my committee meetings. I also thank Bill Dryden, Jeff Goldberg, and John Greer for sitting in my other committee meetings.

I wish to thank my external examiner, Dr. Kerry Delaney, for his suggestions and constructive criticism at my thesis defense. His comments greatly improved the quality of my thesis. I would also like to extend my thanks to Drs. Greg Funk and Keir Pearson for reading my thesis and participating my thesis defense.

I am indebted to the people in Drs. Tse's lab, Andy Lee for the wise suggestions and good experimental ideas, Valerie Yeung for the correction of my thesis writing and for all the encouragement and enjoyable company, and Nan Wang for the good friendship. Many thanks also go to the former members of Drs. Tse's lab: Cecilia Shiu, for her excellent technical assistance, and Elizabeth Hughes, for her friendship and help in the laboratory.

Other people also helped me in some of the experiments. Two summer students in the lab, Joanna Cheung and Justin Ma, helped me with the adenosine project. Woojung Cho, in Dr. Edwin Daniel's lab in the Department of Pharmacology, helped me with the immunostaining experiments and Honey Chan, in the Department of Cell Biology, helped me with the confocal microscope.

I thank the secretary in Centre for Neuroscience, Carol Ann Johnson, for providing all the information and good service that I needed in my study. Thank you also to the secretary in the Department of Pharmacology, Judy Deuel, for writing me various supporting letters.

My thesis work has been supported by the following funding agencies to whom I am very grateful: the Canadian Institutes for Health Research, the Alberta Heritage Foundation of Medical Research, and the Heart and Stroke Foundation of Canada, and the Faculty of Graduate Studies and Research at the University of Alberta.

Most importantly, I am forever indebted to my loving husband, Tiewei He, who was always there to provide endless support and encouragement during my ups and downs in the completion of this degree. His love, care, patience, understanding,

and support made all the work in this thesis possible. I am also grateful to my mother-in-law, Cailan Zhang, who took care of my son while I was completing my final project and writing my thesis. I also thank my son, Colin Weifeng He, for bringing me so much happiness and the motivation to achieve more in my career. Finally, I wish to thank my parents, Jinye Xu and Lizhen Jin, for raising me, teaching me, loving me, and especially supporting my studies in Canada. To my family, I dedicate this thesis.

# Table of Contents

# List of Figures

# List of Abbreviations

| | |
|---|---|
| $[Ca^{2+}]_i$ | intracellular $Ca^{2+}$ concentration |
| 2-MeSATP | 2-methylthioATP |
| 4-AP | 4-aminopyridine |
| 5-HT | 5-hydroxytryptamine |
| 9-AC | anthracene-9-carboxylic acid |
| α,β-meATP | α,β-methylene ATP |
| ACh | acetylcholine |
| AM | acetoxymethyl ester |
| Ang II | angiotensin II |
| ATP | adenosine 5'-triphosphate |
| BK | large-conductance $Ca^{2+}$-activated $K^+$ channels |
| cAMP | adenosine 3',5'-cyclic monophosphate |
| CCPA | 2-chloro-$N^6$-cyclopentyladenosine |
| CGS21680 | 2-p-(carboxyethyl)phen-ethylamino-5'-N-ethylcarbox-amidoadenosine |
| ChTx | charybdotoxin |
| CO | carbon monoxide |
| $CO_2$ | carbon dioxide |
| CSN | carotid sinus nerve |
| DA | dopamine |
| DIDS | 4,4'-diisothiocyanatostilbene-2,2'-disulphonic acid |

| | |
|---|---|
| DNase | deoxyribonuclease |
| DPI | diphenyliodonium |
| EGTA | ethylene glycol-bis (β-aminoethyl ether)-N,N,N',N'-tetraacetic acid |
| GABA | γ-amino-butyric acid |
| GPN | glossopharyngeal nerve |
| HO | heme oxygenases |
| IBMX | 3-isobtyl-1-methylxanthine |
| IbTx | iberiotoxin |
| $IP_3$ | inositol trisphosphate |
| NADPH | nicotinamide adenine dinucleotide phosphate |
| NE | norepinephrine |
| NO | nitric oxide |
| NOS | nitric oxide synthase |
| PACAP | pituitary adenylate cyclase-activating polypeptide |
| $PAC_1$ | PACAP type I receptors |
| PBS | phosphate-buffered saline |
| PKA | protein kinase A |
| $P_{O_2}$ | partial $O_2$ pressure or $O_2$ tension (similarly, $P_{CO_2}$) |
| ROS | reactive oxygen species |
| SIDS | sudden infant death syndrome |
| SP | substance P |
| TASK | TWIK-related acid sensitive $K^+$ channels |

| | |
|---|---|
| TEA | tetraethylammonium |
| TH | tyrosine hydroxylase |
| TWIK | the weak inward rectifier-like $K^+$ channels |
| UTP | uridine 5'-triphosphate |
| VGCC | voltage-gated calcium channel |
| VIP | vasoactive intestinal peptide |
| VPAC | PACAP type II receptors |
| ZM241385 | 4-(2-[7-amino-2-(2-furyl)[1,2,4]triazolo[2,3-a][1,3,5]triazin-5-ylamino]ethyl)phenol |

# Chapter 1

# General Introduction

The research projects for my thesis involve examining the actions of several transmitters on type I cells of rat carotid bodies. There are three projects in this thesis. The first two projects focus on the actions of a neurotransmitter, ATP, and its metabolite, adenosine, on type I cells. The third project focuses on the actions of a circulating peptide, PACAP, on type I cells.

This introductory chapter begins with a brief review of the background information for my thesis. Three major aspects will be discussed: (1) carotid body histology, physiology and dysfunction-related diseases; (2) the current status of type I cells as the $O_2$ sensor in the carotid body; (3) the neurotransmitters released by type I cells and their functional roles in the chemotransduction of the carotid body. Information relating to the above topics was drawn from several excellent reviews (Gonzalez et al. 1994; Nurse 2005; Peers and Buckler 1995; Prabhakar 2000; Prabhakar and Overholt 2000; Prabhakar and Peng 2004; Prabhakar and Jacono 2005; Prabhakar 2006). At the end of this chapter, I shall briefly describe my objectives for this thesis.

## 1.1 Carotid body histology, physiology and dysfunction-related diseases

An adequate supply of $O_2$ is essential for the survival of all mammals. $O_2$ is the electron acceptor in the mitochondrial respiratory chain, where ATP is produced by oxidative phosphorylation (Lopez-Barneo et al. 2004). A decrease in $O_2$ level in the blood (hypoxia) triggers a fast (within seconds) respiratory and cardiovascular compensatory reflex that ensures sufficient $O_2$ supply to the most critical organs, such

as the brain and the heart. The ventilatory adjustments during hypoxia are critically dependent on the $O_2$-sensing ability of the peripheral chemoreceptors, the carotid bodies (Gonzalez et al. 1994).

### *1.1.1 Carotid body*

The carotid body is a reddish-brown oval structure located at the bifurcation of the two branches of the carotid artery. The rat carotid body measures 0.3–0.6 mm in diameter (McDonald and Blewett 1981). As shown in Figure 1-1, there are four major components in the carotid body: type I cells, type II (sustentacular) cells, nerve terminals and blood vessels (Gonzalez et al. 1994; McDonald 1980; McDonald and Larue 1983). Type I cells are electrically excitable and contain secretory dense core granules (Gonzalez et al. 1994). Type I cell clusters are surrounded by the spindle-shaped type II cells. Type II cells resemble glial cells of the peripheral nervous system and express S-100 protein, which is a common marker for glial cells (Abramovici et al. 1991; Kondo et al. 1982; Xu et al. 2003). Unlike type I cells, type II cells do not contain any dense core granules and lack voltage-gated calcium channels (VGCC) (Xu et al. 2003). Type I cells receive both afferent innervation from the carotid sinus nerve (CSN) terminals whose somata are in the petrosal ganglion (McDonald 1983) and efferent innervation from neurons located along the glossopharyngeal nerve (GPN) (Campanucci et al. 2003; Campanucci and Nurse 2005; Kobayashi et al. 2000). The cell clusters in the carotid body are richly supplied by blood vessels (Gonzalez et al. 1994; McDonald and Larue 1983). Electron microscopic analysis reveals that synaptic contacts are formed between a sub-

population of type I cells and the nerve endings (McDonald 1977). Gap junctions are present between some type I cells in the cluster (Monti-Bloch et al. 1993; McDonald 1981). Stimulation by hypoxia, hypercapnia, and acidity was found to reduce the coupling between type I cells (Abudara and Eyzaguirre 1998; Monti-Bloch et al. 1993). A functional consequence of variable coupling between type I cells is the uncertainty as to whether in a physiological context these cells respond individually or as a coupling cluster.

### *1.1.2 $O_2$- sensing element(s) in the carotid body*

The literature has implicated both type I cells (Fidone et al. 1988; Prabhakar 2006) and the CSN (Sun and Reis 1994) as possible sites of $O_2$ sensing. The mitochondrial inhibitor cyanide was reported to stimulate petrosal neurons *in vitro* (Sun and Reis 1994) and neurons in the petrosal ganglion were postulated to be the site of $O_2$ sensing. However, a subsequent study by Alcayaga et al. (1999) found that hypoxia did not affect the discharge frequency of petrosal neurons *in vitro*. Thus, it is unlikely that CSN terminals are the primary site of $O_2$ sensing (Alcayaga et al. 1999). At present, most experimental evidence suggests that type I cells are the initial site of $O_2$ sensing. First, type I cells were found to be sensitive to changes in blood $O_2$ level and were found to secrete neurotransmitters in response to hypoxia (Gonzalez et al. 1994; Montoro et al. 1996). Second, hypoxia failed to trigger CSN discharge following removal of the carotid body or destruction of type I cells (Ponte and Sadler 1989; Verna et al. 1975). Third, hypoxia depolarized type I cells in culture, but had no effect on the membrane potential of petrosal neurons in culture (Zhong et al. 1997).

On the other hand, when petrosal neurons were co-cultured with type I cells, the neurons that developed close contacts with type I cells responded to hypoxia (Nurse and Zhang 1999). Thus, the literature suggests that type I cells are the primary $O_2$-sensing element in the carotid body.

### *1.1.3 Physiological roles of the carotid body and carotid body dysfunction-related diseases*

Since the original description of the peripheral arterial chemoreceptors by De Castro in 1926, most of the research has focused on understanding the physiological role of the carotid body. Type I cells in carotid bodies were found to be able to detect changes in blood levels of $O_2$, $CO_2$ and pH (Gonzalez et al. 1994). In addition, type I cells are also sensitive to changes in blood osmolarity (Carpenter and Peers 1997; Eyzaguirre and Zapata 1984; Gallego et al. 1979; Gallego and Belmonte 1979) and blood glucose level (Lopez-Barneo 2003). Hypoxia and hypercapnia (increase in blood $CO_2$ level) are known to cause membrane depolarization in type I cells and thus activate VGCC. The resultant elevation of $[Ca^{2+}]_i$ triggers the release of transmitters from type I cells (Buckler and Vaughan-Jones 1994b; Buckler and Vaughan-Jones 1994a; Gonzalez et al. 1994). Most importantly, the $[Ca^{2+}]_i$ rise in carotid body type I cells is accompanied by an increase in CSN discharge (Roy et al. 2000). As shown in Figure 1-1, both hypoxia and hypercapnia induce type I cells to release neurotransmitters including dopamine (DA) (Rigual et al. 1986), acetylcholine (ACh) (Fitzgerald et al. 1999), ATP (Buttigieg and Nurse 2004; Zhang et al. 2000) and histamine (Koerner et al. 2004). These transmitters then stimulate the activities of the

CSN whose somata are in the petrosal ganglion. The output of the petrosal ganglion in turn regulates the activities of cardiorespiratory centres in the brain stem, which ultimately mediate the respiratory and cardiovascular reflexes (Gonzalez et al. 1994).

Since the carotid body is essential for respiratory control, dysfunction of the carotid body has been implicated in various diseases (Prabhakar and Peng 2004), such as sleep apnea, sudden infant death syndrome (SIDS), and congenital central hypoventilation syndrome. Increased carotid body sensitivity to hypoxia was suggested to be associated with the early stage of sleep apneas (Peng et al. 2003) and desensitization of carotid body to hypoxia was associated with continued apneas for several years (Osanai et al. 1999; Prabhakar and Peng 2004; Redline et al. 1997). Deficient carotid body function has also been suggested to be one factor contributing to SIDS, because denervation of carotid bodies caused unexpected death in infant lambs (Fewell et al. 1990), rats (Hofer 1984) and piglets (Donnelly and Haddad 1990). Abnormalities in the content and function of neurotransmitters (especially DA) leading to an underdeveloped carotid body have also been suggested to contribute to SIDS (Perrin et al. 1984). Congenital central hypoventilation syndrome, which is characterized by failure of central respiratory control, has now been found to be associated with abnormalities of the carotid body, such as a smaller carotid body, fewer type I cells and fewer dense core granules in type I cells, but more type II cells in the carotid body (Cutz et al. 1997).

## 1.2 Current status of type I cells as $O_2$ sensors

It is generally accepted that type I cells are the major $O_2$ sensing elements in the carotid body. However, the primary site(s) in type I cells that initiate $O_2$ sensing remains uncertain. So far, there are two main hypotheses concerning the initial site of $O_2$ sensing in type I cells. One hypothesis proposes that a direct inhibition of ion channels (mainly the $O_2$-sensitive $K^+$ channels) leads to hypoxia-induced membrane depolarization and thus to neurotransmitter release. In this hypothesis, $O_2$-sensitive ion channel proteins are suggested to be the $O_2$ sensor (Lopez-Barneo 1994; Lopez-Barneo et al. 2001; Prabhakar and Overholt 2000). The second hypothesis proposes that heme-containing proteins are the primary $O_2$ sensors in type I cells (Cross et al. 1990; Prabhakar and Overholt 2000; Streller et al. 2002; Williams et al. 2004). In this section, the evidence supporting these two hypotheses will be discussed.

### *1.2.1 Ion channel proteins as primary $O_2$ sensors in type I cells*

With the development of the patch clamp technique, a lot of research has focused on the identification and understanding of the functions of the various ionic conductances in type I cells. It is now clear that a variety of ion channels are expressed on the plasma membrane of type I cells, and the activities of some ion channels can be regulated by $O_2$.

#### *1.2.1.1 Electrical properties of type I cells in the carotid body*

Studies published since the late 1980's have reported species differences in the expression of different types of channels in type I cells of the carotid body. Since the channels in both rat and rabbit type I cells are well characterized, in this section, I

will focus mainly on the channels expressed in rat and rabbit type I cells. These cells typically have inward currents, mainly $Na^+$ and $Ca^{2+}$ currents, and outward currents, mainly $K^+$ currents. Three types of $Cl^-$ currents have also been characterized in rat type I cells. These include: a pH-sensitive inwardly rectifying $Cl^-$ channel which is anthracene-9-carboxylic acid (9-AC)-sensitive (Petheo et al. 2001), a voltage-insensitive large conductance $Cl^-$ channel which is also 9-AC-sensitive (Stea and Nurse 1989), and a swelling and cAMP-activated $Cl^-$ current which is sensitive to niflumic acid and 4,4'-diisothiocyanatostilbene-2,2'-disulphonic acid (DIDS) (Carpenter and Peers 1997; Molnar et al. 2003). These $Cl^-$ currents are thought to be involved in cell volume and acid regulation (Petheo et al. 2001).

Voltage-gated $Na^+$ channels are found in rabbit type I cells (Biscoe and Duchen 1990;Rocher et al. 1988), while in rat type I cells, voltage-gated $Na^+$ channels are either absent, or only present at low density (Fieber and McCleskey 1993). However, a background $Na^+$ conductance was found to be present in rat type I cells (Carpenter and Peers 2001).

Rabbit type I cells express L- (Obeso et al. 1992;Overholt and Prabhakar 1997), N- (Overholt and Prabhakar 1997), and P/Q-type VGCC (Overholt and Prabhakar 1997). In rat type I cells, the $Ca^{2+}$ channels are mainly L-type (Fieber and McCleskey 1993; Peers et al. 1996). There are conflicting reports on the presence of N-type $Ca^{2+}$ channels in rat type I cells. For example, studies have reported that ω-conotoxin GIVA, the selective N-type channel blocker, did (Silva and Lewis 1995) or did not (Fieber and McCleskey 1993) block $Ca^{2+}$ current. In neonatal rats, ω-conotoxin GIVA blocked $Ca^{2+}$ current in some cells, but had no effect in the majority

of cells (Peers et al. 1996). There have been no reports on the expression of P/Q-type $Ca^{2+}$ current in rat type I cells. In both rat and rabbit type I cells, there is no evidence to support the presence of low-voltage-activated T-type $Ca^{2+}$ channels (Silva and Lewis 1995; Urena et al. 1989).

The expression of $K^+$ current in type I cells also shows species differences. So far, at least four types of $K^+$ currents have been identified in rat type I cells. They are the delayed rectifiers (Lopez-Lopez et al. 1993), BK channels (Lopez-Barneo et al. 1997; Wyatt and Peers 1995), the 4-aminopyridine (4-AP)-sensitive A-type $K^+$ channels (Vandier et al. 1999), and the TASK-like $K^+$ channels (Buckler 1997; Buckler 1999). Rabbit type I cells also express 4-AP-sensitive $K^+$ channels, delayed rectifiers (Lopez-Lopez et al. 1993), and BK channels (Ganfornina and Lopez-Barneo 1992). Also in rabbit type I cells, Overholt et al. (2000) identified a human-ether-a-go-go related gene (HERG)-like $K^+$ current . A recent study on rat carotid body suggested that a HERG-like $K^+$ current is highly expressed in carotid body type I cells of newborn rats (0- to 1-day old), but declines rapidly with age (2.5- fold less in 11- to 16-day-old rat). This HERG-like $K^+$ current is suggested to have a role in stabilizing the membrane potential in the neonatal rat (Kim et al. 2005).

In summary, type I cells, like other excitable cells, possess a variety of ionic conductances, including $K^+$, $Ca^{2+}$, $Na^+$ and $Cl^-$ channels. Expression of these channels shows species differences, suggesting that there may be functional differences in common animal models such as the rat and rabbit.

*1.2.1.2 Modulation of ion channels by hypoxia in type I cells*

The modulation of ion channels by hypoxia plays a major role in chemotransduction in type I cells. In the rat type I cells, the voltage-gated $Ca^{2+}$ current was not affected by hypoxia (Peers et al. 1996). In rabbit type I cells, there are opposite findings on the effect of hypoxia on $Ca^{2+}$ channel activity. Montoro et al. (1996) found that the whole-cell $Ca^{2+}$ current was inhibited by hypoxia. However, Summers et al. (2000) reported that hypoxia augmented $Ca^{2+}$ currents.

In terms of the $O_2$ sensitivity of $K^+$ channels, in rabbit type I cells, hypoxia inhibited a $K^+$ current that is sensitive to tetraethylammonium (TEA) and 4-AP, but insensitive to charybdotoxin (ChTx). Thus, this $O_2$-sensitive $K^+$ current in rabbit type I cells is like the delayed rectifier and/or an A-type $K^+$ current (Lopez-Barneo et al. 1988; Lopez-Lopez et al. 1993). In rat type I cells, an $O_2$-sensitive $K^+$ current was blocked by iberiotoxin (IbTx) and ChTx, suggesting that it is the BK current (Peers 1990; Wyatt and Peers 1995). Also in rat type I cells, Buckler (1997) identified a TASK-like background $K^+$ current that could be inhibited by hypoxia. TASK channels belong to the two-pore domain $K^+$ channel family. They are active at resting membrane potential, and show little voltage sensitivity. TASK-like $K^+$ channels are insensitive to 4-AP and TEA (Buckler 1997; Buckler et al. 2000). Immunostaining experiments have detected the expression of TASK-1, TASK-2 and TASK-3 channels in type I cells of rat carotid bodies (Yamamoto et al. 2002). Therefore, in rat type I cells, both BK channels and TASK-like $K^+$ channels may be modulated by hypoxia.

In a functional context, since hypoxia triggers depolarization via inhibition of $O_2$-sensitive $K^+$ channels (Prabhakar 2000b), one must consider whether the $O_2$-sensitive currents are active at resting membrane potential in type I cells. Among the

$O_2$-sensitive ion channels, VGCC, delayed rectifiers, and BK channels are significantly active only at depolarized potentials. Moreover, the activation of BK channels requires a significant elevation in $[Ca^{2+}]_i$. It is not clear whether inhibition of these channels can lead to significant depolarization from the resting membrane potentials of type I cells. Therefore, the TASK-like background $K^+$ channels appear to be the best candidate for initiation of the hypoxia response. Although BK channels are not expected to be significantly activated at the resting membrane potential and at basal $[Ca^{2+}]_i$ in type I cells, recent studies suggest that BK channels may undergo modulation during the hypoxia response via activities of heme-containing proteins (Kemp 2005; Williams et al. 2004). The BK channel pore-forming α-subunit was found to coimmunoprecipitate with the heme-containing protein, hemoxygenase-2 (HO-2), and a carbon monoxide (CO) donor was found to increase the activity of BK channels (Kemp 2005; Williams et al. 2004). During normoxia, the CO produced by the oxidative action of HO-2 was suggested to exert an excitatory regulation on the BK channels by promoting opening of these channels at resting membrane potential (Prabhakar and Overholt 2000; Riesco-Fagundo et al. 2001). Therefore, closure of BK channels by hypoxia may also contribute to the hypoxia-induced membrane depolarization in type I cells, and the co-localized heme-containing protein may act as an $O_2$ sensor. The theory of heme-containing proteins as $O_2$ sensors is described in detail below.

### *1.2.2 Heme-containing proteins as primary $O_2$ sensors in type I cells*

Some hemes can bind to $O_2$ with high affinity and are suggested to be possible sites for $O_2$ sensing. Candidates for possible $O_2$ sensors include mitochondrial cytochromes (Biscoe and Duchen 1989; Mulligan and Lahiri 1982), and several non-mitochondrial enzymes including nicotinamide adenine dinucleotide phosphate (NADPH) oxidases (Cross et al. 1990), hemoxygenase (HO) (Prabhakar 1999; Williams et al. 2004) and nitric oxide synthases (NOS) (Kline et al. 1998;Prabhakar 1999). Here, I will discuss the evidence supporting each of the candidates as $O_2$ sensor.

*1.2.2.1 Mitochondrial cytochromes as $O_2$ sensors*

In support of the involvement of mitochondrial cytochromes in $O_2$ sensing, hypoxia was reported to cause mitochondrial depolarization in type I cells (Biscoe and Duchen 1989). Furthermore, substances that interfere with mitochondrial respiration (e.g. cyanide, antimycin A) mimic the effects of hypoxia on CSN discharge (Mulligan and Lahiri 1982).

*1.2.2.2 Non-mitochondrial enzymes as $O_2$ sensors*

The NADPH oxidase complex was identified in type I cells of human carotid bodies and diphenyliodonium, a selective inhibitor of NADPH oxidase, increased the CSN discharge indicating an inhibitory action of NADPH oxidase on CSN (Cross et al. 1990). The NADPH oxidase complex can generate reactive $O_2$ species (ROS; especially superoxide, $O_2^-$, and/or $H_2O_2$) (Acker 1989; Acker et al. 1992). $H_2O_2$ and organic peroxides have been found to inhibit CSN discharge (Acker 1989; Acker et al.

1992). However, a recent study by He et al. (2002) found that in NADPH-oxidase-deficient (gene knockout) mice, carotid body functions, including hypoxia-induced suppression of $K^+$ current, increase in $[Ca^{2+}]$ in type I cells, and increase in CSN discharge, remained unchanged. These observations cast doubt on a crucial role of NADPH oxidase in carotid body chemotransduction.

HO-2-like immunoreactivity has been reported in rat type I cells (Prabhakar 1995; Prabhakar 1999). In normoxia, HO-2 can use $O_2$ to convert heme into biliverdin, iron and carbon monoxide (CO) (Shibahara et al. 1985). Inhibitors of HO-2 augmented CSN discharge and potentiated the ventilatory response to hypoxia, indicating an inhibitory action of HO-2 on the carotid body (Prabhakar 1999). In addition, HO-2 was found to coimmunoprecipate with heterologously expressed BK channels and the BK channel conductance was increased by a CO donor (Williams et al. 2004). This suggests that HO-2 may inhibit carotid body activity by producing CO, which binds to and keeps BK channels open, thus maintaining the resting membrane potential at a negative level. However, a recent study showed that HO-2-deficient (gene knockout) mice exhibited normal responsiveness of carotid body type I cells to hypoxia, which puts into question the role of HO-2 as an $O_2$ sensor (Ortega-Saenz et al. 2006).

The NOS are a family of heme-containing enzymes that catalyze the formation of nitric oxide (NO) from arginine (Adhikari et al. 2000). Two NOS isoforms, the neuronal NOS (NOS-1) and endothelial NOS (NOS-3), are expressed in the carotid body tissue (Prabhakar and Overholt, 2000). NOS-1 is primarily expressed in CSN endings (Prabhakar and Overholt 2000; Wang et al. 1995) and GPN endings

(Campanucci et al. 2003; Campanucci and Nurse 2005). NOS-3 is expressed in blood vessels in the carotid body (Chugh et al. 1994; Prabhakar et al. 1993). Mutant mice with a targeted deletion of the NOS-1 gene exhibited enhanced CSN activity and augmented ventilatory responses to hypoxia (Kline et al. 1998). NO donors were reported to cause inhibition of $Ca^{2+}$ currents (Prabhakar 1999; Summers et al. 1999) and to cause membrane hyperpolarization of type I cells (Campanucci et al. 2006). These data indicate that NO, released from nerve endings or endothelial cells, may act as an inhibitory chemical messenger in the carotid body.

Taken together, these studies suggest that chemosensory discharge is under tonic inhibitory influence from CO and ROS generated by type I cells, as well as NO produced by CSN or GPN fibers and blood vessels. Since $O_2$ is required for generation of these molecules, under normoxic condition, ROS, CO and NO are expected to be continuously produced to maintain a hyperpolarizing membrane potential in type I cells (probably by opening of BK channels in an intracellular $Ca^{2+}$-independent manner). Under hypoxic conditions, the production of ROS, CO and NO is hypothesized to be interrupted, thus relieving inhibition and causing depolarization and $[Ca^{2+}]_i$ rise in type I cells (Prabhakar 1999).

### *1.2.3 Multiple $O_2$ sensors in type I cells of the carotid body*

Based on the hypotheses that $O_2$-sensitive $K^+$ channels and/or heme-containing proteins initiate the hypoxic signaling transduction, Prabhakar (2006) proposed a theory about why multiple putative $O_2$ sensors exist in the carotid body. The theory suggests that the carotid body may need multiple $O_2$ sensors to fulfill its

physiological function of sensing diverse chemostimulants and a wide range of $P_{O2}$ levels rapidly (i.e. in seconds). The various heme-containing proteins expressed in type I cells allow type I cells to respond to a broad range of $P_{O_2}$, while direct inhibition of $O_2$-sensitive $K^+$ channels allows type I cells to respond rapidly to hypoxia. The interaction between these two kinds of sensors allows type I cells to respond rapidly, as well as in a graded manner, to chemostimuli and thus protect vital organs from hypoxia-induced damage (Prabhakar et al. 2004; Prabhakar 2006).

## 1.3 Transmitters and their functional roles in the chemotransduction of the carotid body

There is considerable evidence for the involvement of transmitters in the transmission of the hypoxic signal from type I cells to CSN. Type I cells contain a variety of neurotransmitters that are released during hypoxia challenge. These transmitters include catecholamines, mainly DA and norepinephrine (NE), serotonin (5-hydroxytryptamine, 5-HT), γ-amino-butyric acid (GABA), ACh, ATP, substance-P (SP)-like peptide (Gonzalez et al. 1994; Nurse 2005; Prabhakar 1994) and histamine (Koerner et al. 2004).

### *1.3.1 Transmitters released by type I cells*

Among the transmitters released from type I cells, DA was originally thought to be the most abundant neurotransmitter synthesized and stored in dense–core granules (Gonzalez et al. 1994). Receptors for DA have been found in both CSN

endings and type I cells (Gonzalez et al. 1994; Mir et al. 1984). Tyrosine hydroxylase (TH), the rate-limiting enzyme in catecholamine biosynthesis, is expressed in type I cells (Gonzalez et al. 1994). Interestingly, a recent study has demonstrated that type I cells of rat carotid body store about ten-fold more histamine than DA (Koerner et al. 2004). All the receptor subtypes for histamine, including $H_1$, $H_2$ and $H_3$, are expressed in type I cells (Koerner et al. 2004). However, the physiological role of histamine and its receptors has not been tested. The presence of other biogenic amines, including NE and 5-HT, has been observed in type I cells in situ (Oomori et al. 1994), although the presence of the biosynthetic enzyme for serotonin has yet to be confirmed. ACh is released from rat carotid body type I cells during hypoxia (Nurse and Zhang 1999; Zhang et al. 2000) and rat type I cells express both nicotinic and muscarinic receptors (Dasso et al. 1997). ATP is released along with catecholamines (Rigual et al. 1986) and ACh (Zhang et al. 2000) during hypoxia. Using a co-culture of type I cell clusters and petrosal neurons, Prasad et al. (2001)) found that $P2X_2$ and $P2X_3$ receptors were expressed on CSN endings. Studies in our laboratory have shown that $P2Y_2$ receptors are expressed in type II cells (Xu et al. 2003) and $P2Y_1$ receptors are expressed in type I cells (Xu et al. 2005) of rat carotid bodies. GABA is also co-localized with catecholamines and 5-HT in type I cells of the rat (Fearon et al. 2003) and mouse (Oomori et al. 1994) carotid bodies. Kumar et al. (2000) have recently shown that hypoxia releases SP-like peptides from rabbit carotid bodies and that SP-like immunoreactivity is localized to type I cells and nerve fibers. Collectively, these studies demonstrate that type I cells synthesize and store multiple transmitters that

can be released during hypoxia, and that they also express autoreceptors for these transmitters.

### *1.3.2 Actions of transmitters in the carotid body*

Since hypoxia triggers the release of multiple transmitters from type I cells, it is essential to investigate the function of various transmitters and their receptors in the carotid body. Although significant progress has been made, many controversial observations regarding the functional role of the various transmitters in the carotid body have been reported (Gonzalez et al. 1994; Nurse 2005).

DA, one of the best-studied carotid body neurotransmitters, was once suggested to be the major excitatory neurotransmitter mediating chemotransduction of the carotid body (Fidone et al. 1982; Rigual et al. 1986). Previous studies showed that hypoxia-induced DA release from type I cells was accompanied by an increase in CSN discharge (Fidone et al. 1982; Rigual et al. 1986). However, superfusion of intact cat carotid body with DA inhibited CSN activity (Monti-Bloch and Eyzaguirre 1980; Monti-Bloch and Eyzaguirre 1980). On the other hand, both inhibitory and excitatory effects of DA perfusion on CSN activity have been reported, and the excitatory effect was observed with a higher dose of DA (Zapata 1975). Since DA receptors are also present on type I cells, it is not clear whether the inhibitory action of DA is due to the activation of the autoreceptors on type I cells. It is also possible that the excitatory action of DA is due to the activation of receptors on CSN endings. It is suggested that only a high dose of DA is able to access the synaptic cleft and thus stimulate the CSN endings (Gonzalez et al. 1994). More importantly, Donnelly (1996)

reported that repetitive hypoxia resulted in progressively smaller catecholamine secretion, but did not affect the peak amplitude of CSN discharge. Critically, the depletion of DA (with reserpine) from carotid body had little or no effect on the hypoxia-induced increase in CSN discharge. This suggests that the increase in CSN discharge to hypoxia is not proportional to the amount of DA release (Donnelly 1996). Therefore, a role for DA as the major excitatory neurotransmitter in carotid body is questionable.

On the other hand, ACh was found to exert potent stimulatory effects on CSN discharge in the cat and was proposed to act as the excitatory neurotransmitter between type I cells and CSN endings (Gonzalez et al. 1994). Interpretation of ACh action is complicated by the presence of nicotinic and muscarinic receptors on type I cells (Dasso et al. 1997), because the excitatory action of ACh on CSN may be mediated indirectly via the cholinergic receptors on type I cells. Most importantly, blockers of both nicotinic and muscarinic ACh receptors could not completely inhibit CSN discharge in response to hypoxia (Fitzgerald 2000). Consistent with this, Zhang et al. (2000) found that hypoxia- or hypercapnia-induced CSN discharge was reversibly abolished by a combination of nicotinic and purinergic blockers, but not by the nicotinic receptor alone. These findings suggest that ACh partially contributes to chemotransduction.

Recently, ATP has been suggested to play multiple roles in the carotid body (Iturriaga and Alcayaga 2004; Nurse 2005; Xu et al. 2003; Xu et al. 2005). First, the hypoxia-mediated increase in CSN activity was partially inhibited by blockers of P2X receptors. P2X receptors have been shown to localize at CSN endings, suggesting that

ATP may exert stimulatory action on CSN endings via P2X receptors (Prasad et al. 2001). Studies in our laboratory have shown that ATP triggers intracellular $Ca^{2+}$ release from type II cells via $P2Y_2$ receptors (Xu et al. 2003). Since the glial-like type II cells are in close contact with type I cells and nerve endings, it is possible that the ATP-mediated $Ca^{2+}$ signal in type II cells may in turn generate additional signaling molecules to act on type I cells and CSN endings in a paracrine fashion. In rat carotid body type I cells, Mokashi et al. (2003) reported that ATP increased $[Ca^{2+}]_i$ in amine-containing (presumably type I) cells . In contrast, our studies (see Chapter 3) in rat type I cells (identified by their $Ca^{2+}$ response to hypoxia) have shown that ATP did not affect the resting $[Ca^{2+}]_i$, but dramatically suppressed both hypoxia-induced membrane depolarization, as well as the hypoxia-mediated $[Ca^{2+}]_i$ rise, via $P2Y_1$ receptors (Xu et al. 2005). Possible reasons for the discrepancy between our studies and Mokashi's studies will be discussed in Chapter 3. In rat type I cells, GABA, acting via its autoreceptors ($GABA_B$), inhibits hypoxia-induced chemosensory discharge by enhancing a TASK-1-like $K^+$ current through a PKA-dependent pathway (Fearon et al. 2003).

In summary, tremendous effort has been made to study the function of various neurotransmitters on the carotid body for more than a decade. However, the complex autocrine and paracrine actions of the individual transmitters obscure a precise definition of the functional role of each neurotransmitter.

## 1.4 Objectives of my thesis

As described in 1.3.2, there are many controversial findings in terms of the functional roles of individual transmitter released by type I cells. This is partially due to the presence of multiple autocrine/paracrine receptors on the type I cells, type II cells and CSN or GPN endings. Therefore, to understand the chemotransduction in carotid body, it is essential to first identify the actions of neurotransmitters and their receptors on each cell type. In this thesis, I focused on actions of three transmitters (ATP, adenosine and PACAP) on single type I cells isolated from the rat carotid body.

ATP, one of the many transmitters released from type I cells upon hypoxic challenge, has been found to increase CSN activity via P2X receptors (Prasad et al. 2001) and to trigger intracellular $Ca^{2+}$ store release from type II cells via $P2Y_2$ receptors (Xu et al. 2003). Therefore, I focused on examining the actions of ATP on type I cells of rat carotid body in my first project (Chapter 3).

ATP released during hypoxia can be broken down into adenosine by ecto-5-nucleotidase (Dunwiddie and Masino 2001). Adenosine that is generated by metabolism of ATP, as well as by the stimulation of adenosine efflux via the adenosine equilibrative transporter during hypoxia (Conde and Monteiro 2004), is expected to increase the extracelllular concentration of adenosine near type I cells. In addition, the adenosine receptors $A_{2A}$ have been shown to be localized in type I cells of rat carotid body (Kobayashi et al. 2000). Furthermore, exogenous adenosine has been shown to stimulate CSN endings in cats (McQueen and Ribeiro 1981) and rats (Monteiro and Ribeiro 1987). However, an inhibitory action of adenosine on VGCC was reported on rat (Kobayashi et al. 2000) and rabbit (Rocher et al. 1999) carotid

body type I cells. Therefore, in my second project, I focused on the actions of adenosine on type I cells of rat carotid body (Chapter 4).

In addition to the transmitters released from type I cells, some circulating hormones can also modulate chemotransduction in type I cells of the carotid body. For example, the systemic level of angiotensin II (Ang II) increased during hypoxia (Marshall and Metcalfe 1990) and Ang II modulated the CSN activity of the carotid body by causing an increase in $[Ca^{2+}]_i$ level via the $AT_1$ receptors on type I cells (Allen 1998;Fung et al. 2001). Recently, PACAP has been suggested by several studies to be involved in carotid body function. First, Cummings et al. (2004) found that PACAP-deficient (gene knockout) mice have reduced respiratory responses to hypoxia and are more prone to sudden neonatal death. This raises the possibility that PACAP may play a significant role in respiration. PACAP is thought to be involved at the level of the carotid body because it was shown that injection of PACAP in dogs caused an increase in ventilation, which could be abolished when the CSN was cut (Runcie et al. 1995). Based on this evidence, I investigated whether PACAP affected the type I cells of rat carotid body in my third project (Chapter 5).

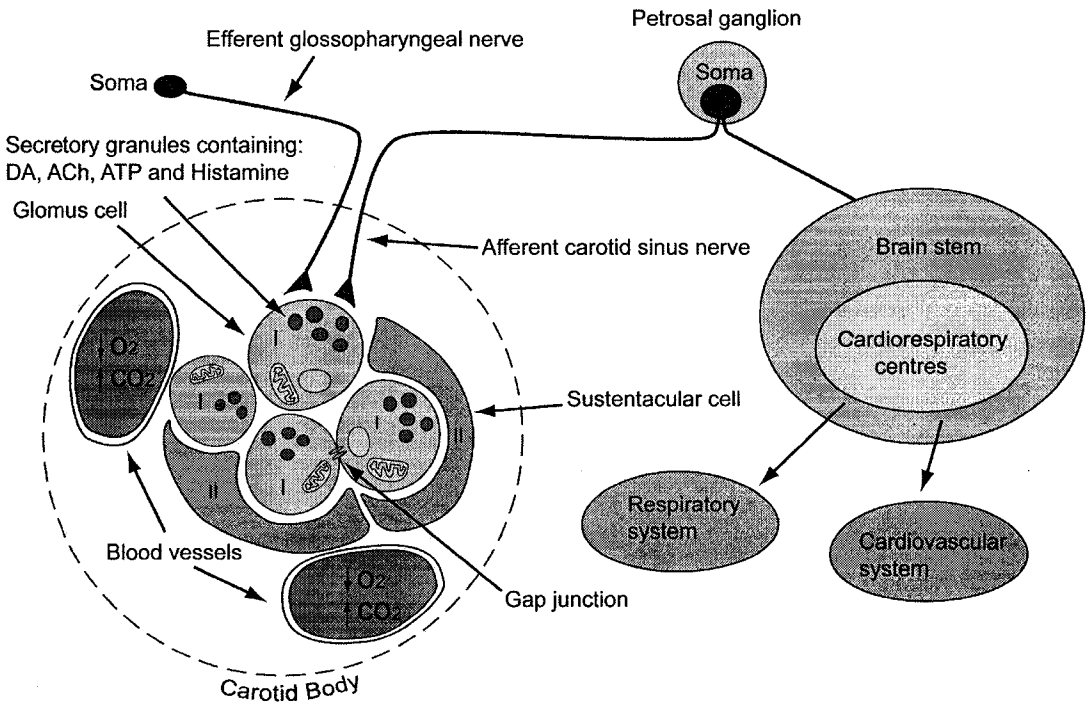


**Figure 1-1** Diagram of chemotransduction mediated by the carotid body. The carotid body comprises of type I (glomus) cells, type II (sustenticular) cells, nerve endings and blood vessels. Two types of nerve endings form close contact with type I cells: afferent endings of carotid sinus nerve and efferent endings of glossopharyngeal nerve. Gap junctions are present between type I cells. Decrease in $O_2$ level or increase in $CO_2$ level in the blood vessels stimulates type I cells in the carotid body to secrete neurotransmitters. These neurotransmitters then stimulate the carotid sinus nerve whose somata are in the petrosal ganglion. Output from the petrosal ganglion in turn regulates the activity of cardiorespiratory centres in the brain stem, which mediate the respiratory and cardiovascular reflexes.

## References


Abramovici A., Pallot D. J., and Polak J. M. (1991) Immunohistochemical approach to the study of the cat carotid body. *Acta Anat (Basel)* **140,** 70-74.

Abudara V. and Eyzaguirre C. (1998) Modulation of juctional conductance between rat cartoid body glomus cells by hypoxia, cAMP and acidity. *Brain Res* **792,** 114-125

Acker H. (1989) PO2 chemoreception in arterial chemoreceptors. *Annu Rev Physiol* **51,** 835-844.

Acker H., Bolling B., Delpiano M. A., Dufau E., Gorlach A., and Holtermann G. (1992) The meaning of H2O2 generation in carotid body cells for PO2 chemoreception. *J Auton Nerv Syst* **41,** 41-51.

Adhikari S., Ray S., and Gachhui R. (2000) Catalase activity of oxygenase domain of rat neuronal nitric oxide synthase. Evidence for product formation from L-arginine. *FEBS Lett* **475,** 35-38.

Alcayaga J., Varas R., Arroyo J., Iturriaga R., and Zapata P. (1999) Responses to hypoxia of petrosal ganglia in vitro. *Brain Res* **845,** 28-34.

Allen A. M. (1998) Angiotensin AT1 receptor-mediated excitation of rat carotid body chemoreceptor afferent activity. *J Physiol* **510 ( Pt 3),** 773-781.

Biscoe T. J. and Duchen M. R. (1989) Electrophysiological responses of dissociated type I cells of the rabbit carotid body to cyanide. *J Physiol* **413,** 447-468.

Biscoe T. J. and Duchen M. R. (1990) Responses of type I cells dissociated from the rabbit carotid body to hypoxia. *J Physiol* **428,** 39-59.

Buckler K. J. (1997) A novel oxygen-sensitive potassium current in rat carotid body type I cells. *J Physiol* **498 ( Pt 3),** 649-662.

Buckler K. J. (1999) Background leak K+-currents and oxygen sensing in carotid body type 1 cells. *Respir Physiol* **115,** 179-187.

Buckler K. J. and Vaughan-Jones R. D. (1994a) Effects of hypercapnia on membrane potential and intracellular calcium in rat carotid body type I cells. *J Physiol* **478 ( Pt 1),** 157-171.

Buckler K. J. and Vaughan-Jones R. D. (1994b) Effects of hypoxia on membrane potential and intracellular calcium in rat neonatal carotid body type I cells. *J Physiol* **476,** 423-428.

Buckler K. J., Williams B. A., and Honore E. (2000) An oxygen-, acid- and anaesthetic-sensitive TASK-like background potassium channel in rat arterial chemoreceptor cells. *J Physiol* **525 Pt 1,** 135-142.

Buttigieg J. and Nurse C. A. (2004) Detection of hypoxia-evoked ATP release from chemoreceptor cells of the rat carotid body. *Biochem Biophys Res Commun* **322,** 82-87.

Campanucci V. A., Fearon I. M., and Nurse C. A. (2003) A novel O2-sensing mechanism in rat glossopharyngeal neurones mediated by a halothane-inhibitable background K+ conductance. *J Physiol* **548,** 731-743.

Campanucci V. A. and Nurse C. A. (2005) Biophysical characterization of whole-cell currents in O2-sensitive neurons from the rat glossopharyngeal nerve. *Neuroscience* **132,** 437-451.

Campanucci V. A., Zhang M., Vollmer C., and Nurse C. A. (2006) Expression of multiple P2X receptors by glossopharyngeal neurons projecting to rat carotid body O2-chemoreceptors: role in nitric oxide-mediated efferent inhibition. *J Neurosci* **26,** 9482-9493.

Carpenter E. and Peers C. (1997) Swelling- and cAMP-activated Cl- currents in isolated rat carotid body type I cells. *J Physiol* **503 ( Pt 3),** 497-511.

Carpenter E. and Peers C. (2001) A standing Na+ conductance in rat carotid body type I cells. *Neuroreport* **12,** 1421-1425.

Chugh D. K., Katayama M., Mokashi A., Bebout D. E., Ray D. K., and Lahiri S. (1994) Nitric oxide-related inhibition of carotid chemosensory nerve activity in the cat. *Respir Physiol* **97,** 147-156.

Conde S. V. and Monteiro E. C. (2004) Hypoxia induces adenosine release from the rat carotid body. *J Neurochem* **89,** 1148-1156.

Cross A. R., Henderson L., Jones O. T., Delpiano M. A., Hentschel J., and Acker H. (1990) Involvement of an NAD(P)H oxidase as a pO2 sensor protein in the rat carotid body. *Biochem J* **272,** 743-747.

Cummings K. J., Pendlebury J. D., Sherwood N. M., and Wilson R. J. (2004) Sudden neonatal death in PACAP-deficient mice is associated with reduced respiratory chemoresponse and susceptibility to apnoea. *J Physiol* **555,** 15-26.

Cutz E., Ma T. K., Perrin D. G., Moore A. M., and Becker L. E. (1997) Peripheral chemoreceptors in congenital central hypoventilation syndrome. *Am J Respir Crit Care Med* **155,** 358-363.

Dasso L. L., Buckler K. J., and Vaughan-Jones R. D. (1997) Muscarinic and nicotinic receptors raise intracellular Ca2+ levels in rat carotid body type I cells. *J Physiol* **498 ( Pt 2),** 327-338.

De Castro F. (1926) On the structure and innervation of the carotid body (glomus caroticum) in humans and mammals. and its novel autonomic innervation, the carotid sinus nerve. *Trab Lab Invest Biol* **24,** 365-432

Donnelly D. F. (1996) Chemoreceptor nerve excitation may not be proportional to catecholamine secretion. *J Appl Physiol* **81,** 657-664.

Donnelly D. F. and Haddad G. G. (1990) Prolonged apnea and impaired survival in piglets after sinus and aortic nerve section. *J Appl Physiol* **68,** 1048-1052.

Dunwiddie T. V. and Masino S. A. (2001) The role and regulation of adenosine in the central nervous system. *Annu Rev Neurosci* **24,** 31-55.

Eyzaguirre C. and Zapata P. (1984) Perspectives in carotid body research. *J Appl Physiol* **57,** 931-957.

Fearon I. M., Zhang M., Vollmer C., and Nurse C. A. (2003) GABA mediates autoreceptor feedback inhibition in the rat carotid body via presynaptic GABAB receptors and TASK-1. *J Physiol* **553,** 83-94.

Fewell J. E., Taylor B. J., Kondo C. S., Dascalu V., and Filyk S. C. (1990) Influence of carotid denervation on the arousal and cardiopulmonary responses to upper airway obstruction in lambs. *Pediatr Res* **28,** 374-378.

Fidone S., Gonzalez C., and Yoshizaki K. (1982) Effects of low oxygen on the release of dopamine from the rabbit carotid body in vitro. *J Physiol* **333,** 93-110.

Fidone S. J., Gonzalez C., Dinger B. G., and Hanson G. R. (1988) Mechanisms of chemotransmission in the mammalian carotid body. *Prog Brain Res* **74,** 169-179.

Fieber L. A. and McCleskey E. W. (1993) L-type calcium channels in type I cells of the rat carotid body. *J Neurophysiol* **70,** 1378-1384.

Fitzgerald R. S. (2000) Oxygen and carotid body chemotransduction: the cholinergic hypothesis - a brief history and new evaluation. *Respir Physiol* **120,** 89-104.

Fitzgerald R. S., Shirahata M., and Wang H. Y. (1999) Acetylcholine release from cat carotid bodies. *Brain Res* **841,** 53-61.

Fung M. L., Lam S. Y., Chen Y., Dong X., and Leung P. S. (2001) Functional expression of angiotensin II receptors in type-I cells of the rat carotid body. *Pflugers Arch* **441,** 474-480.

Gallego R. and Belmonte C. (1979) The effects of blood osmolality changes on cat carotid body chemoreceptors in vivo. *Pflugers Arch* **380,** 53-58.

Gallego R., Eyzaguirre C., and Monti-Bloch L. (1979) Thermal and osmotic responses of arterial receptors. *J Neurophysiol* **42,** 665-680.

Ganfornina M. D. and Lopez-Barneo J. (1992) Potassium channel types in arterial chemoreceptor cells and their selective modulation by oxygen. *J Gen Physiol* **100,** 401-426.

Gonzalez C., Almaraz L., Obeso A., and Rigual R. (1994) Carotid body chemoreceptors: from natural stimuli to sensory discharges. *Physiol Rev* **74,** 829-898.

He L., Chen J., Dinger B., Sanders K., Sundar K., Hoidal J., and Fidone S. (2002) Characteristics of carotid body chemosensitivity in NADPH oxidase-deficient mice. *Am J Physiol Cell Physiol* **282,** C27-C33.

Hofer M. A. (1984) Lethal respiratory disturbance in neonatal rats after arterial chemoreceptor denervation. *Life Sci* **34,** 489-496.

Iturriaga R. and Alcayaga J. (2004) Neurotransmission in the carotid body: transmitters and modulators between glomus cells and petrosal ganglion nerve terminals. *Brain Res Brain Res Rev* **47,** 46-53.

Kemp P. J. (2005) Hemeoxygenase-2 as an O2 sensor in K+ channel-dependent chemotransduction. *Biochem Biophys Res Commun* **338,** 648-652.

Kim I., Boyle K. M., and Carroll J. L. (2005) Postnatal development of E-4031-sensitive potassium current in rat carotid chemoreceptor cells. *J Appl Physiol* **98,** 1469-1477.

Kline D. D., Yang T., Huang P. L., and Prabhakar N. R. (1998) Altered respiratory responses to hypoxia in mutant mice deficient in neuronal nitric oxide synthase. *J Physiol* **511 ( Pt 1),** 273-287.

Kobayashi S., Conforti L., and Millhorn D. E. (2000) Gene expression and function of adenosine A(2A) receptor in the rat carotid body. *Am J Physiol Lung Cell Mol Physiol* **279,** L273-L282.

Koerner P., Hesslinger C., Schaefermeyer A., Prinz C., and Gratzl M. (2004) Evidence for histamine as a transmitter in rat carotid body sensor cells. *J Neurochem* **91,** 493-500.

Kondo H., Iwanaga T., and Nakajima T. (1982) Immunocytochemical study on the localization of neuron-specific enolase and S-100 protein in the carotid body of rats. *Cell Tissue Res* **227,** 291-295.

Kumar G. K., Kou Y. R., Overholt J. L., and Prabhakar N. R. (2000) Involvement of substance P in neutral endopeptidase modulation of carotid body sensory responses to hypoxia. *J Appl Physiol* **88,** 195-202.

Lopez-Barneo J. (1994) Oxygen-sensitive ion channels: how ubiquitous are they? *Trends Neurosci* **17,** 133-135.

Lopez-Barneo J. (2003) Oxygen and glucose sensing by carotid body glomus cells. *Curr Opin Neurobiol* **13,** 493-499.

Lopez-Barneo J., del Toro R., Levitsky K. L., Chiara M. D., and Ortega-Saenz P. (2004) Regulation of oxygen sensing by ion channels. *J Appl Physiol* **96,** 1187-1195.

Lopez-Barneo J., Lopez-Lopez J. R., Urena J., and Gonzalez C. (1988) Chemotransduction in the carotid body: K+ current modulated by PO2 in type I chemoreceptor cells. *Science* **241,** 580-582.

Lopez-Barneo J., Ortega-Saenz P., Molina A., Franco-Obregon A., Urena J., and Castellano A. (1997) Oxygen sensing by ion channels. *Kidney Int* **51,** 454-461.

Lopez-Barneo J., Pardal R., and Ortega-Saenz P. (2001) Cellular mechanism of oxygen sensing. *Annu Rev Physiol* **63,** 259-287.

Lopez-Lopez J. R., De Luis D. A., and Gonzalez C. (1993) Properties of a transient K+ current in chemoreceptor cells of rabbit carotid body. *J Physiol* **460,** 15-32.

Marshall J. M. and Metcalfe J. D. (1990) Effects of systemic hypoxia on the distribution of cardiac output in the rat. *J Physiol* **426,** 335-353.

McDonald D. M. (1977) Structure-function relationships of chemoreceptive nerves in the carotid body. *Am Rev Respir Dis* **115,** 193-207.

McDonald D. M. (1980) Regulation of chemoreceptor sensitivity in the carotid body: the role of presynaptic sensory nerves. *Fed Proc* **39,** 2627-2635.

McDonald D.M. (1981) Peripheral chemoreceptors: structure-function relationships of the carotid body. *In: regulation of breathing* 105-320

McDonald D. M. (1983) Morphology of the rat carotid sinus nerve. I. Course, connections, dimensions and ultrastructure. *J Neurocytol* **12,** 345-372.

McDonald D. M. and Blewett R. W. (1981) Location and size of carotid body-like organs (paraganglia) revealed in rats by the permeability of blood vessels to Evans blue dye. *J Neurocytol* **10,** 607-643.

McDonald D. M. and Larue D. T. (1983) The ultrastructure and connections of blood vessels supplying the rat carotid body and carotid sinus. *J Neurocytol* **12,** 117-153.

McQueen D. S. and Ribeiro J. A. (1981) Effect of adenosine on carotid chemoreceptor activity in the cat. *Br J Pharmacol* **74,** 129-136.

Mir A. K., McQueen D. S., Pallot D. J., and Nahorski S. R. (1984) Direct biochemical and neuropharmacological identification of dopamine D2-receptors in the rabbit carotid body. *Brain Res* **291,** 273-283.

Mokashi A., Li J., Roy A., Baby S. M., and Lahiri S. (2003) ATP causes glomus cell [Ca2+]c increase without corresponding increases in CSN activity. *Respir Physiol Neurobiol* **138,** 1-18.

Molnar Z., Petheo G. L., Fulop C., and Spat A. (2003) Effects of osmotic changes on the chemoreceptor cell of rat carotid body. *J Physiol* **546,** 471-481.

Monteiro E. C. and Ribeiro J. A. (1987) Ventilatory effects of adenosine mediated by carotid body chemoreceptors in the rat. *Naunyn Schmiedebergs Arch Pharmacol* **335,** 143-148.

Monti-Bloch L. and Eyzaguirre C. (1980) A comparative physiological and pharmacological study of cat and rabbit carotid body chemoreceptors. *Brain Res* **193,** 449-470.

Monti-Block L., Abudara V., and Eyzaguirre C. (1993) Electrical communication between glomus cells of the rat carotid body. *Brain Res* **622,** 119-131

Montoro R. J., Urena J., Fernandez-Chacon R., Alvarez d. T., and Lopez-Barneo J. (1996) Oxygen sensing by ion channels and chemotransduction in single glomus cells. *J Gen Physiol* **107,** 133-143.

Mulligan E. and Lahiri S. (1982) Separation of carotid body chemoreceptor responses to O2 and CO2 by oligomycin and by antimycin A. *Am J Physiol* **242,** C200-C206.

Nurse C. A. (2005) Neurotransmission and neuromodulation in the chemosensory carotid body. *Auton Neurosci* **120,** 1-9.

Nurse C. A. and Zhang M. (1999) Acetylcholine contributes to hypoxic chemotransmission in co-cultures of rat type 1 cells and petrosal neurons. *Respir Physiol* **115,** 189-199.

Obeso A., Rocher A., Fidone S., and Gonzalez C. (1992) The role of dihydropyridine-sensitive Ca2+ channels in stimulus-evoked catecholamine release from chemoreceptor cells of the carotid body. *Neuroscience* **47,** 463-472.

Oomori Y., Nakaya K., Tanaka H., Iuchi H., Ishikawa K., Satoh Y., and Ono K. (1994) Immunohistochemical and histochemical evidence for the presence of noradrenaline, serotonin and gamma-aminobutyric acid in chief cells of the mouse carotid body. *Cell Tissue Res* **278,** 249-254.

Ortega-Saenz P., Pascual A., Gomez-Diaz R., and Lopez-Barneo J. (2006) Acute oxygen sensing in heme oxygenase-2 null mice. *J Gen Physiol* **128,** 405-411.

Osanai S., Akiba Y., Fujiuchi S., Nakano H., Matsumoto H., Ohsaki Y., and Kikuchi K. (1999) Depression of peripheral chemosensitivity by a dopaminergic mechanism in patients with obstructive sleep apnoea syndrome. *Eur Respir J* **13,** 418-423.

Overholt J. L., Ficker E., Yang T., Shams H., Bright G. R., and Prabhakar N. R. (2000) HERG-Like potassium current regulates the resting membrane potential in glomus cells of the rabbit carotid body. *J Neurophysiol* **83,** 1150-1157.

Overholt J. L. and Prabhakar N. R. (1997) Ca2+ current in rabbit carotid body glomus cells is conducted by multiple types of high-voltage-activated Ca2+ channels. *J Neurophysiol* **78,** 2467-2474.

Peers C. (1990) Hypoxic suppression of K+ currents in type I carotid body cells: selective effect on the Ca2(+)-activated K+ current. *Neurosci Lett* **119,** 253-256.

Peers C. and Buckler K. J. (1995) Transduction of chemostimuli by the type I carotid body cell. *J Membr Biol* **144,** 1-9.

Peers C., Carpenter E., Hatton C. J., Wyatt C. N., and Bee D. (1996) Ca2+ channel currents in type I carotid body cells of normoxic and chronically hypoxic neonatal rats. *Brain Res* **739,** 251-257.

Peng Y. J., Overholt J. L., Kline D., Kumar G. K., and Prabhakar N. R. (2003) Induction of sensory long-term facilitation in the carotid body by intermittent hypoxia: implications for recurrent apneas. *Proc Natl Acad Sci U S A* **100,** 10073-10078.

Perrin D. G., Cutz E., Becker L. E., Bryan A. C., Madapallimatum A., and Sole M. J. (1984) Sudden infant death syndrome: increased carotid-body dopamine and noradrenaline content. *Lancet* **2,** 535-537.

Petheo G. L., Molnar Z., Roka A., Makara J. K., and Spat A. (2001) A pH-sensitive chloride current in the chemoreceptor cell of rat carotid body. *J Physiol* **535,** 95-106.

Ponte J. and Sadler C. L. (1989) Studies on the regenerated carotid sinus nerve of the rabbit. *J Physiol* **410,** 411-424.

Prabhakar N. R. (1994) Neurotransmitters in the carotid body. *Adv Exp Med Biol* **360,** 57-69.

Prabhakar N. R. (1995) Gases as chemical messengers in the carotid body. Role of nitric oxide and carbon monoxide in chemoreception. *Adv Exp Med Biol* **393,** 309-312.

Prabhakar N. R. (1999) NO and CO as second messengers in oxygen sensing in the carotid body. *Respir Physiol* **115,** 161-168.

Prabhakar N. R. (2000) Oxygen sensing by the carotid body chemoreceptors. *J Appl Physiol* **88,** 2287-2295.

Prabhakar N. R. (2006) O2 sensing at the mammalian carotid body: why multiple O2 sensors and multiple transmitters? *Exp Physiol* **91,** 17-23.

Prabhakar N. R. and Jacono F. J. (2005) Cellular and molecular mechanisms associated with carotid body adaptations to chronic hypoxia. *High Alt Med Biol* **6,** 112-120.

Prabhakar N. R., Kumar G. K., Chang C. H., Agani F. H., and Haxhiu M. A. (1993) Nitric oxide in the sensory function of the carotid body. *Brain Res* **625,** 16-22.

Prabhakar N. R. and Overholt J. L. (2000) Cellular mechanisms of oxygen sensing at the carotid body: heme proteins and ion channels. *Respir Physiol* **122,** 209-221.

Prabhakar N. R. and Peng Y. J. (2004) Peripheral chemoreceptors in health and disease. *J Appl Physiol* **96,** 359-366.

Prabhakar N. R., Peng Y. J., Overholt J. L., and Kumar G. K. (2004) Detection of oxygen sensing during intermittent hypoxia. *Methods Enzymol* **381,** 107-120.

Prasad M., Fearon I. M., Zhang M., Laing M., Vollmer C., and Nurse C. A. (2001) Expression of P2X2 and P2X3 receptor subunits in rat carotid body afferent neurones: role in chemosensory signalling. *J Physiol* **537,** 667-677.

Redline S., Leitner J., Arnold J., Tishler P. V., and Altose M. D. (1997) Ventilatory-control abnormalities in familial sleep apnea. *Am J Respir Crit Care Med* **156,** 155-160.

Riesco-Fagundo A. M., Perez-Garcia M. T., Gonzalez C., and Lopez-Lopez J. R. (2001) O(2) modulates large-conductance Ca(2+)-dependent K(+) channels of rat chemoreceptor cells by a membrane-restricted and CO-sensitive mechanism. *Circ Res* **89,** 430-436.

Rigual R., Gonzalez E., Gonzalez C., and Fidone S. (1986) Synthesis and release of catecholamines by the cat carotid body in vitro: effects of hypoxic stimulation. *Brain Res* **374,** 101-109.

Rocher A., Gonzalez C., and Almaraz L. (1999) Adenosine inhibits L-type $Ca^{2+}$ current and catecholamine release in the rabbit carotid body chemoreceptor cells. *Eur J Neurosci* **11,** 673-681.

Rocher A., Obeso A., Herreros B., and Gonzalez C. (1988) Activation of the release of dopamine in the carotid body by veratridine. Evidence for the presence of voltage-dependent Na+ channels in type I cells. *Neurosci Lett* **94,** 274-278.

Roy A., Rozanov C., Mokashi A., and Lahiri S. (2000) P(O(2))-P(CO(2)) stimulus interaction in [Ca(2+)](i) and CSN activity in the adult rat carotid body. *Respir Physiol* **122,** 15-26.

Runcie M. J., Ulman L. G., and Potter E. K. (1995) Effects of pituitary adenylate cyclase-activating polypeptide on cardiovascular and respiratory responses in anaesthetised dogs. *Regul Pept* **60,** 193-200.

Shibahara S., Muller R., Taguchi H., and Yoshida T. (1985) Cloning and expression of cDNA for rat heme oxygenase. *Proc Natl Acad Sci U S A* **82,** 7865-7869.

Silva M. J. and Lewis D. L. (1995) L- and N-type Ca2+ channels in adult rat carotid body chemoreceptor type I cells. *J Physiol* **489 ( Pt 3),** 689-699.

Stea A. and Nurse C. A. (1989) Chloride channels in cultured glomus cells of the rat carotid body. *Am J Physiol* **257,** C174-C181.

Streller T., Huckstorf C., Pfeiffer C., and Acker H. (2002) Unusual cytochrome a592 with low PO2 affinity correlates as putative oxygen sensor with rat carotid body chemoreceptor discharge. *FASEB J* **16,** 1277-1279.

Summers B. A., Overholt J. L., and Prabhakar N. R. (1999) Nitric oxide inhibits L-type Ca2+ current in glomus cells of the rabbit carotid body via a cGMP-independent mechanism. *J Neurophysiol* **81,** 1449-1457.

Summers B. A., Overholt J. L., and Prabhakar N. R. (2000) Augmentation of L-type calcium current by hypoxia in rabbit carotid body glomus cells: evidence for a PKC-sensitive pathway. *J Neurophysiol* **84,** 1636-1644.

Sun M. K. and Reis D. J. (1994) Dopamine or transmitter release from rat carotid body may not be essential to hypoxic chemoreception. *Am J Physiol* **267,** R1632-R1639.

Urena J., Lopez-Lopez J., Gonzalez C., and Lopez-Barneo J. (1989) Ionic currents in dispersed chemoreceptor cells of the mammalian carotid body. *J Gen Physiol* **93,** 979-999.

Vandier C., Conway A. F., Landauer R. C., and Kumar P. (1999) Presynaptic action of adenosine on a 4-aminopyridine-sensitive current in the rat carotid body. *J Physiol* **515 ( Pt 2),** 419-429.

Verna A., Roumy M., and Leitner L. M. (1975) Loss of chemoreceptive properties of the rabbit carotid body after destruction of the glomus cells. *Brain Res* **100,** 13-23.

Wang Z. Z., Stensaas L. J., Dinger B. G., and Fidone S. J. (1995) Nitric oxide mediates chemoreceptor inhibition in the cat carotid body. *Neuroscience* **65,** 217-229.

Williams S. E., Wootton P., Mason H. S., Bould J., Iles D. E., Riccardi D., Peers C., and Kemp P. J. (2004) Hemoxygenase-2 is an oxygen sensor for a calcium-sensitive potassium channel. *Science* **306,** 2093-2097.

Wyatt C. N. and Peers C. (1995) Ca(2+)-activated K+ channels in isolated type I cells of the neonatal rat carotid body. *J Physiol* **483 ( Pt 3),** 559-565.

Xu J., Tse F. W., and Tse A. (2003) ATP triggers intracellular Ca2+ release in type II cells of the rat carotid body. *J Physiol* **549,** 739-747.

Xu J., Xu F., Tse F. W., and Tse A. (2005) ATP inhibits the hypoxia response in type I cells of rat carotid bodies. *J Neurochem* **92,** 1419-1430.

Yamamoto Y., Kummer W., Atoji Y., and Suzuki Y. (2002) TASK-1, TASK-2, TASK-3 and TRAAK immunoreactivities in the rat carotid body. *Brain Res* **950,** 304-307.

Zapata P. (1975) Effects of dopamine on carotid chemo- and baroreceptors in vitro. *J Physiol* **244,** 235-251.

Zhang M., Zhong H., Vollmer C., and Nurse C. A. (2000) Co-release of ATP and ACh mediates hypoxic signalling at rat carotid body chemoreceptors. *J Physiol* **525 Pt 1,** 143-158.

Zhong H., Zhang M., and Nurse C. A. (1997) Synapse formation and hypoxic signalling in co-cultures of rat petrosal neurones and carotid body type 1 cells. *J Physiol* **503 ( Pt 3),** 599-612.

# Chapter 2

# Materials and Methods

## 2.1 Chemicals

Fura-2 acetoxymethyl ester (AM) and indo-1 AM were obtained from Teflabs (Austin, TX, USA). ATP, 2-methylthioATP (2-MeSATP), α,β-methylene ATP (α,β-meATP), uridine 5-triphosphate (UTP), 4-AP, IbTx, TEA-Cl, adenosine, 2-p-(carboxyethyl)phen-ethylamino-5'-N-ethylcarbox-amidoadenosine (CGS21680), 2-chloro-$N^6$-cyclopentyladenosine (CCPA), forskolin, 1,9-dideoxyforskolin, H-89, N-methyl-glucamine, ethylene glycol-bis (β-aminoethyl ether)-N,N,N',N'-tetraacetic acid (EGTA), amphotericin B, bovine serum albumin (BSA), and all the enzymes, including collagenase type IV, deoxyribonuclease (DNase) type V, and trypsin type VIII, were purchased from Sigma-Aldrich Ltd. (Oakville, ON, Canada). 4-(2-[7-amino-2-(2-furyl)[1,2,4]triazolo[2,3-a][1,3,5]triazin-5-ylamino]ethyl)phenol (ZM241385) is from Tocris (Ellisville, MO, USA). PACAP, PACAP 6-38, and vasoactive intestinal poly-peptide (VIP) were purchased from Peptide Institute, INC. (Minoh-shi Osaka, Japan). Anandamide was from Calbiochem (San Diego, CA, USA). Fetal bovine serum, Dulbecco's modified Eagle's medium (DMEM) F-12, insulin-transferrin-selenium-A, penicillin G, and streptomycin were obtained from Gibco (Grand Island, NY, USA).

## 2.2 Cell preparation and short-term culture

Male Sprague-Dawley rats (age 6-7 weeks) were first euthanized with an overdose of halothane and were then decapitated in accordance with the standards of the Canadian Council on Animal Care. The carotid bifurcation was removed and placed in ice-cold 100% $O_2$-equilibrated Tyrode solution (mM): 140 NaCl, 5 KCl, 2 $CaCl_2$, 1.1 $MgCl_2$, 5 glucose and 10 Hepes, pH 7.4. Following the dissection of the carotid bodies from the surrounding tissue under a dissecting microscope, the carotid bodies were incubated with a $Ca^{2+}$- and $Mg^{2+}$-free Tyrode solution containing collagenase (Type IV, 2 mg/ml), DNase (type V, 0.5 mg/ml) and trypsin (type XIII; 0.4 mg/ml) for 25 min at 37°C. The carotid bodies were then triturated with a fire-polished glass pipette and incubated at 37°C for another 5-10 mins. Further triturations yielded single cells. DMEM containing 0.1% BSA was then added and the cell suspension was centrifuged (2000 rpm for 5 mins). The cell pellet was dissolved in DMEM and cell suspension (around 5-10 μl) were plated on the center of glass coverslips and allowed to attach for ~45 mins in the incubator. A medium containing F-12/Dulbecco's modified Eagle's medium (1:1), supplemented with 5% fetal bovine serum, 50 U/ml penicillin G and 50 μg/ml streptomycin, was then added to the culture dish. Cells were cultured at 37°C in an incubator circulated with air and 5% $CO_2$ for 2-6 hours before recording. For experiments on type II cells, cells were cultured for 24 hours in the incubator.

## 2.3 Solutions

The standard bath solution contained (in mM): 117 NaCl, 4.5 KCl, 23 $NaHCO_3$, 5 sucrose, 5 glucose, 2.5 $CaCl_2$ and 1 $MgCl_2$ (pH 7.4 when bubbled with 5% $CO_2$). For experiments with $Ca^{2+}$-free extracellular solution, $Ca^{2+}$ was omitted from the standard bath solution and 2.5 mM $MgCl_2$ and 1mM Na-EGTA were added. In experiments where the cells were depolarized with KCl, the NaCl in the standard bath solution was reduced to 101.5 mM and KCl was increased to 20 mM. In experiments where extracellular $Na^+$ was omitted, the bath solution contained (in mM): 140 N-methyl-glucamine, 4.5 KCl, 5 sucrose, 5 glucose, 2.5 $CaCl_2$, 1 $MgCl_2$ and 117 HCl (pH 7.4 when bubbled with 5% $CO_2$). For recording background TASK-like $K^+$ currents, the bath solution contained (in mM): 58.5 $K_2SO_4$, 23 $KHCO_3$, 21 NaCl, 2.5 $CaCl_2$, 10 glucose and 1 $MgCl_2$ (pH 7.4 when bubbled with 5% $O_2$). In addition, 5 mM 4-AP, 10 mM TEA-Cl, and 2.5 mM $NiCl_2$ were included in the bath solution to block respectively the A-type $K^+$ current, the delayed rectifier $K^+$ current, the voltage-gated $Ca^{2+}$ current and any other $Ca^{2+}$-activated currents. The pipette solution contained (in mM): 140 K-gluconate, 10 K-Hepes, 5 $MgCl_2$, 1 EGTA (pH 7.2). For recording of voltage-gated $Ca^{2+}$ current, the standard bath solution (containing 2.5 mM $Ca^{2+}$) was employed and the pipette solution contained (in mM): 120 Cs-Asp, 20 TEA-Cl, 20 Cs-Hepes, 10 EGTA, 2 $MgCl_2$, 2 $Na_2ATP$, 0.1 $Na_4GTP$ (pH 7.4). Amphotericin B (250

μg/ml) was included in the pipette solution for perforated patch recording. For experiments involving normoxic conditions, cells were perfused with bath solution, with or without drugs added, bubbled continuously with 5% $CO_2$-95% air. In experiments involving only $[Ca^{2+}]_i$ measurement, the flow rate was around 3-4 ml/min, while in experiments involving patch-clamp recording, the flow rate was reduced to 1-2 ml/min to avoid disturbing the patched cell. Bars shown in the figures in Chapters 3, 4 and 5 indicate the time when the distribution valve was switched from one solution reservoir to another. The response to each change of solution was delayed due to the time it takes for the solution to reach the chamber (from the valve) and to the time it takes for the solution to exchange in the chamber. Hypoxia was induced by perfusing the cells with bath solution bubbled with 5% $CO_2$-95% $N_2$. Under the hypoxic condition, the $P_{O_2}$ of the bath solution was ~40 mm Hg (measured with a blood gas analyzer, RapidLab 348 CHIRON Diagonostics, Toronto, ON, Canada). Hypercapnia was induced by perfusing the cells with bath solution bubbled with 20% $CO_2$-80% air.

## 2.4 Electrophysiology

In all experiments involving electrophysiology, single cells were patch-clamped with the perforated patch-clamp technique. Membrane potentials or currents were recorded using an EPC-7 patch-clamp amplifier that was controlled by an IBM-compatible PC and the data acquisition program pCLAMP version 6 (Axon

Instruments, Foster City, CA, USA). The pipettes were made from hematocrit glass (VWR Scientific Canada, London, ON, Canada). The pipette resistance was 2-4 MΩ after filling with internal solution and was 20-30 MΩ during perforated patch recording. No correction for junction potential was applied in any of the experiments described in this thesis.

All recordings were performed at room temperature (20–23°C). Values given in the text are mean ± S.E.M. Statistical difference was determined by a paired Student's t-test or by an independent Student's t-test for two populations (when comparing between two different groups of cells). A difference with $p < 0.05$ was considered statistically significant.

## 2.5 $[Ca^{2+}]_i$ measurement

All $[Ca^{2+}]_i$ measurements were performed at room temperature (20–23°C). In experiments involving only measurements of the $Ca^{2+}$ signal, $[Ca^{2+}]_i$ was monitored with imaging using a Tillvision imaging system equipped with Polychrome II high speed monochromator (Applied Scientific Instrument, OR, USA). Details were as described previously (Xu et al. 2003; Xu et al. 2005). Cells were loaded with fura-2 AM (2.5 μM) in standard bath solution at 37°C for 10 min and then washed with standard bath solution at 20–23°C for 15 min before recording. Fura-2 was excited sequentially by 340 and 380 nm light delivered from a Xenon lamp via a 40X, 1.3 NA

UV fluor oil objective (Olympus, Carsen Group, Markham, ON, Canada). Fluorescent images were collected at 510 nm every 10 s by a Peltier-cooled CCD camera. Since the cells were loaded with AM dyes, there was no correction for cell autofluorescence in this study. The ratio of fluorescence, R (340nm /380 nm) from individual cell was analyzed with Tillvision Software 3.02 (Till Photonics, Applied Scientific Instrument) on an IBM-compatible computer, according to the equation (Grynkiewicz et al. 1985): $[Ca^{2+}]_i = K^* (R - R_{min})/(R_{max} - R)$. $R_{min}$ is the fluorescence ratio of $Ca^{2+}$-free indicator and $R_{max}$ is the ratio of $Ca^{2+}$-bound indicator. $K^*$ is the dissociation constant of the indicator for $Ca^{2+}$ which was determined empirically. Calibrations for indo-1 or fura-2 measurements were determined from single cells dialyzed (via the whole-cell pipette) with one of the three pipette solutions as described previously (Tse and Tse 1998). $R_{min}$ was measured in cells loaded with (mM): 52 K-aspartate, 10 KCl, 50 K-EGTA, 50 K-Hepes and 0.1 fura-2, pH 7.4; and $R_{max}$ was measured in cells loaded with (mM): 136 K-aspartate, 15 $CaCl_2$, 50 K-Hepes and 0.1 fura-2, pH 7.4. $K^*$ was calculated from the equation above using R values obtained from cells loaded with (mM): 60 K-aspartate, 50 K-Hepes, 20 K-EGTA, 15 $CaCl_2$, 0.1 fura-2, pH 7.4, which had a calculated free $Ca^{2+}$ concentration of 212 nM at 22°C (Blinks et al. 1982). For all fura-2 measurements shown in chapter 3, 4, and 5, the values for $R_{min}$, $R_{max}$ and $K^*$ were 0.13, 3.4, and 2.72 μM, respectively.

In experiments involving simultaneous measurement of $[Ca^{2+}]_i$ and membrane potential or current, the electrophysiology rig was equipped with indo-1 fluorescence

measurement. Therefore, cells were incubated with indo-1 AM (2.5 μM) instead of fura-2. The incubation procedure was similar to that described above for fura-2 AM. Details of the instrumentation and procedures of $[Ca^{2+}]_i$ measurement with indo-1 were as described previously (Lee and Tse 1997; Tse and Tse 1998). Briefly, indo-1 was excited by 365 nm light from a HBO 100 W mercury lamp via a 40X, 1.3 NA UV fluor oil objective lens (Nikon). Emission fluorescence at 405 ± 35 nm and 495 ± 45 nm was collected with two photomultiplier tubes (Hamamatsu H3460-04). The output of the photomultiplier tubes were converted to TTL pulses and counted by a CYCTM-10 counter card (Cyber Research Inc., Branford CT, USA) installed in an IBM-compatible PC. The ratio R (400 nm/500 nm) was used to calculate $[Ca^{2+}]_i$, as described above for fura-2. The values for $R_{min}$, $R_{max}$ and $K^*$ for indo-1 were obtained as described above for fura-2. For all indo-1 measurements shown in chapter 3, 4 and 5, the values for $R_{min}$, $R_{max}$ and K were 0.26, 3.17, and 2.37 μM, respectively.

## 2.6 Immunocytochemistry of $P2Y_1$ receptors on carotid body sections

Rat carotid bodies were fixed with phosphate-buffered saline (PBS) containing 4% paraformaldehyde for 8 hours at room temperature and then incubated in PBS containing 25% sucrose for 15 hours. The tissue was immersed in Optimal Temperature Cutting Compound (OCT; TissueTek, Sakura Finetek, Torrance CA, USA) and frozen at -20°C. Sections (~20 μm thickness) were cut in a cryostat and

collected on glass slides. After drying, the sections were rinsed twice with PBS containing 0.3% Triton-X-100 (15 min each) and then once with PBS (15 min) before incubated at room temperature for 2 hours with a blocking, permeabilizing solution containing 7.5% horse serum and 0.3% Triton X-100 in PBS. The sections were then incubated overnight at 4°C with a primary antibody which was a rabbit polyclonal antibody raised against the 3rd intracellular loop of the $P2Y_1$ receptors (1:100; Alomone Labs, Jerusalem, Israel). After 2 washes (15 min each) with 0.3% Triton X-100 (in PBS) and 1 wash with PBS, the sections were incubated at room temperature for ~1.5 hours with a fluorescent-tagged secondary antibody, a donkey anti-rabbit IgG conjugated to Cy5 (1:80; Novus Biological, Littleton, CO, USA). The sections were rinsed 2 times with 0.3% TritonX-100 (15 min each) and then washed with PBS for 15 min before viewing with a 63X oil immersion objective (Zeiss) in a confocal microscope (Zeiss LSM 510). The specimen was excited with a HeNe laser at 633 nm and the emission was collected via a long-pass filter at 680 nm. For controls, sections were incubated with the primary antibody premixed with the antigen peptide (1 μg peptide/1 μg antibody; Alamone Labs, Jerusalem, Israel).

## References


Blinks J. R., Wier W. G., Hess P., and Prendergast F. G. (1982) Measurement of $Ca^{2+}$ concentrations in living cells. *Prog Biophys Mol Biol* **40,** 1-114.

Grynkiewicz G., Poenie M., and Tsien R. Y. (1985) A new generation of $Ca^{2+}$ indicators with greatly improved fluorescence properties. *J Biol Chem* **260,** 3440-3450.

Lee A. K. and Tse A. (1997) Mechanism underlying corticotropin-releasing hormone (CRH) triggered cytosolic Ca2+ rise in identified rat corticotrophs. *J Physiol* **504 ( Pt 2),** 367-378.

Tse A. and Tse F. W. (1998) alpha-adrenergic stimulation of cytosolic $Ca^{2+}$ oscillations and exocytosis in identified rat corticotrophs. *J Physiol* **512 ( Pt 2),** 385-393.

Xu J., Tse F. W., and Tse A. (2003) ATP triggers intracellular Ca2+ release in type II cells of the rat carotid body. *J Physiol* **549,** 739-747.

Xu J., Xu F., Tse F. W., and Tse A. (2005) ATP inhibits the hypoxia response in type I cells of rat carotid bodies. *J Neurochem* **92,** 1419-1430.

# Chapter 3

# ATP Inhibits the Hypoxia Response in Type I Cells of Rat Carotid Bodies

## 3.1 Introduction

Hypoxia depolarizes type I cells in the carotid body by inhibition of $O_2$-sensitive $K^+$ channels. This inhibition leads to depolarization and extracellular $Ca^{2+}$ entry via VGCC. The rise in $[Ca^{2+}]_i$ in turn triggers the release of multiple neurotransmitters from type I cells (Gonzalez et al. 1994; Prabhakar 2000). As mentioned in Chapter 1.3, the precise functional roles of the different neurotransmitters in carotid body remain controversial. Recently, ATP has been suggested to have an important role in hypoxic signaling (Zhang et al. 2000; Prasad et al. 2001). P2X receptors were found to be expressed in rat petrosal neurons which were co-cultured with type I cells (Prasad et al. 2001) and hypoxic chemotransmission could be partially inhibited by blockers of P2X receptors (Zhang et al. 2000). Thus, ATP released from type I cells during hypoxia may stimulate chemosensory discharge on the nerve terminals via P2X receptors. The actions of ATP in carotid body, however, are complex. Our previous study (Xu et al. 2003) has shown that ATP, acting via $P2Y_2$ receptors, triggered $Ca^{2+}$ release from the intracellular stores of the glial-like type II cells. Since type II cells are in close contact with type I cells as well as nerve endings, the ATP-induced $Ca^{2+}$ signal in type II cells may mediate paracrine interactions within the carotid body. In the present study, we found that ATP also exerted autocrine action on type I cells. Using a combination of $[Ca^{2+}]_i$ measurement and electrophysiological techniques, we found that ATP strongly suppressed the hypoxia-induced $Ca^{2+}$ signal in type I cells. This inhibitory action of ATP was mediated via the $P2Y_1$ receptors and was associated with a reduction in cell electrical

excitability. Thus, ATP may act as a negative feedback regulator of the hypoxic response in type I cells.

## 3.2 Results

### *3.2.1 Hypoxia triggered $[Ca^{2+}]_i$ elevation in type I cells isolated from adult rat carotid bodies*

Hypoxia has been shown to elevate $[Ca^{2+}]_i$ in type I cells isolated from adult rabbit (Ureña et al. 1994) as well as neonatal rat carotid bodies (Buckler and Vaughan-Jones 1994a). In type I cells isolated from adult rat carotid bodies, however, hypoxia has been reported to elevate (Bright et al. 1996) or decrease $[Ca^{2+}]_i$ (Donnelly and Kholwadwala 1992). To clarify how hypoxia affects $[Ca^{2+}]_i$ in type I cells isolated from adult rat carotid bodies, we employed $Ca^{2+}$ imaging to measure $[Ca^{2+}]_i$ in carotid body cell mixtures loaded with the $Ca^{2+}$ fluorescent dye fura-2 AM. In our previous study, we found that the catecholamine-secreting type I (but not type II) cells in rat carotid body possessed VGCC, and KCl depolarization triggered robust $[Ca^{2+}]_i$ elevation in type I cells (Xu et al. 2003). Figure 3-1A shows an example of a type I cell in which both hypoxia and KCl depolarization caused $[Ca^{2+}]_i$ elevation. In 30 cells that responded to KCl-depolarization with an elevation of $[Ca^{2+}]_i$, hypoxia triggered a rise in $[Ca^{2+}]_i$ in 26 cells. In these cells, the mean $[Ca^{2+}]_i$ elevation stimulated by hypoxia and KCl depolarization was 246 ± 32 nM and 539 ± 56 nM respectively. Thus, hypoxia could trigger $[Ca^{2+}]_i$ rise in almost 90% of type I cells isolated from adult rat carotid bodies. In the remaining 4 cells, hypoxia did not affect

the resting $[Ca^{2+}]_i$. The lack of hypoxia-induced $Ca^{2+}$ signal in these 4 cells may be related to a lower density of VGCC as the mean $[Ca^{2+}]_i$ rise induced by KCl depolarization in these cells was smaller (230 ± 24 nM versus 539 ± 56 nM in hypoxia responding cells). Consistent with the involvement of VGCC in the hypoxia response (Ureña et al. 1994; Buckler and Vaughan-Jones 1994a), Figure 3-1B shows that the hypoxia-induced $[Ca^{2+}]_i$ rise in type I cells could be abolished by the VGCC blocker, $Ni^{2+}$ (2.5mM; n = 8). In the following experiments, each individual type I cell was identified by its $Ca^{2+}$ response to hypoxia (e.g. Figure 3-1) or the presence of voltage-gated $Ca^{2+}$ current (e.g. Figure 3-5).

### *3.2.2 ATP, acting via $P2Y_1$ receptors, strongly suppressed the hypoxia-induced $[Ca^{2+}]_i$ rise in type I cells*

In our previous study (Xu et al. 2003), we showed that ATP did not affect the basal $[Ca^{2+}]_i$ of type I cells. Interestingly, we found here that the hypoxia-induced $[Ca^{2+}]_i$ rise in type I cell was strongly suppressed by ATP. In the example shown in Figure 3-2A, a hypoxia challenge to a type I cell raised $[Ca^{2+}]_i$ to ~0.3 μM. When the same cell was subjected to a second hypoxia challenge in the presence of ATP (100 μM), there was no appreciable increase in $[Ca^{2+}]_i$. This lack of response to the second hypoxia challenge was not due to rundown, as a third hypoxia challenge after the removal of ATP could elicit a robust $[Ca^{2+}]_i$ rise. Similar experiments were performed in 18 type I cells and ATP (100 μM) reversibly reduced the hypoxia-triggered $[Ca^{2+}]_i$ elevation by 97.8 ± 0.8% ( n = 18). Figure3-2B shows that in a type I cell with ongoing $Ca^{2+}$ response to hypoxia, ATP could also reversibly suppress the

hypoxia-induced $[Ca^{2+}]_i$ rise. In this example, $[Ca^{2+}]_i$ rose to ~0.3 μM under hypoxic condition. During the two applications of ATP (100 μM) under hypoxic condition, $[Ca^{2+}]_i$ returned to the resting level. Upon removal of ATP (under hypoxic condition), $[Ca^{2+}]_i$ rose to ~0.3 μM again. Similar experiments were performed in 12 type I cells and ATP reduced the hypoxia-triggered $[Ca^{2+}]_i$ rise by 88.9 ± 3 %. To examine the receptor involved in the inhibitory action of ATP, we tested the ability of different purinoreceptor agonists to suppress the hypoxia-induced $Ca^{2+}$ signals in type I cells (Figure 3-3). In these experiments, cells were first subjected to a brief hypoxic challenge under control condition. Following the recovery of the hypoxia-induced $[Ca^{2+}]_i$ rise, a second hypoxia challenge was applied in the continued presence of the purinoreceptor agonist. Figure 3-3A & B show that both 2-MeSATP (10 μM; Figure 3-3A) and ADP (100 μM; Figure 3-3B) prevented the elevation of $[Ca^{2+}]_i$ by hypoxia in type I cells. On the other hand, α,β -MeATP (100 μM, Figure 3-3C) or UTP (100 μM, Figure 3-3D) had little or no effect on the amplitude of the hypoxia-induced $[Ca^{2+}]_i$ rise. Similar experiments were also repeated with different concentrations of 2- MeSATP, ATP, and ADP. In each experiment, the amplitude of the hypoxia-induced $[Ca^{2+}]_i$ elevation in the presence of the purinoreceptor agonist was compared to that elicited in the same cell under control condition. The fractional inhibition of the hypoxia-induced $[Ca^{2+}]_i$ rise was plotted against the log concentration of different purinoreceptor agonists in Figure 3-4A. The potency order for inhibition of the hypoxia-induced $[Ca^{2+}]_i$ rise was 2-MeSATP > ATP > ADP >> α,β-MeATP > UTP. This result suggests that the inhibitory action of ATP involved $P2Y_1$ receptors (Ralevic and Burnstock 1998). Figure 3-4A also shows that the physiological agonist,

ATP, at 1 μM, already suppressed the amplitude of the hypoxia-induced $[Ca^{2+}]_i$ rise by ~60%. To examine whether $P2Y_1$ receptors are indeed present in type I cells of rat carotid bodies, we immunostained cryostat sections of rat carotid body with an antibody against $P2Y_1$ receptors. The confocal fluorescence image shown in Figure 3-4B shows that the $P2Y_1$ receptors were localized on the clusters of ovoid type 1 cells but not on the spindle shaped type II cells. Note that although some fluorescence was found on the periphery as well as throughout the cytoplasm of the ovoid cells, the most intense fluorescence was punctate and inside the individual cells. Since our immunostaining procedures involved cell fixation and permeabilization (see Chapter 2) and the primary antibody was raised against the 3rd intracellular loop of the $P2Y_1$ receptors, all $P2Y_1$ receptors (on the cell membrane and trafficking compartments) would be labeled. Thus, it is likely that a significant fraction of $P2Y_1$ receptors was indeed located in the intracellular compartments. Note also that in the control section, which was processed with the primary antibody that was premixed with the antigen peptide, the fluorescence in the ovoid type I cells was absent (Figure 3-4C). These findings indicate that $P2Y_1$ receptors are selectively localized in type I carotid cells.

### *3.2.3 ATP caused a small reduction of voltage-gated $Ca^{2+}$ current*

Since the hypoxia-elicited rise in $[Ca^{2+}]_i$ in type I cell is dependent on activation of VGCC (Figure 3-1B), one possible mechanism underlying the inhibitory action of ATP may be an ATP-mediated inhibition of VGCC. Indeed, feedback inhibition of VGCC by DA has been shown in rabbit type I cells (Benot and López-Barneo 1990). To examine this possibility, single type I cells were voltage-clamped

at -60 mV using the perforated whole-cell patch clamp technique. Voltage steps (25 ms in duration) to potentials between -50 and +80 mV were applied to elicit voltage-gated $Ca^{2+}$ current before and following the application of ATP (100 μM). Figure 3-5A shows that ATP partially inhibited the $Ca^{2+}$ current elicited during a voltage step to +10 mV. The current-voltage relationship of the ATP effect on $Ca^{2+}$ current was shown in Figure 3-5B. The inhibitory effect of ATP (100 μM) was maximal at the peak of the I-V curve and the mean reduction of $Ca^{2+}$ current at this potential (+10 mV) was 35 ± 4 % (n = 6). Note that at more negative potentials, ATP has much smaller fractional effect on the $Ca^{2+}$ current than that at more positive potentials. For example, ATP reduced the amplitude of the $Ca^{2+}$ elicited at -20 mV by ~ 6%. At more positive potentials (from +10 to +40 mV), ATP reduced the $Ca^{2+}$ by ~35%. Under our experimental conditions, hypoxia typically depolarized the type I cells to ~-35 mV (see Figure 3-6C), therefore, we examined in detail whether ATP had any significant effect on $Ca^{2+}$ current near this potential. In this series of experiments, single type I cells were voltage-stepped (25 ms in duration) alternatively to -30 or +10 mV every 10 s before and following the application of ATP (100 μM). An example of such experiment is shown in Figure 3-5C. In this cell, ATP reversibly reduced the $Ca^{2+}$ current elicited at +10 mV by ~38%, similar to that described in Figure 3-5B. Note that however, ATP had no appreciable effect on the amplitude of the $Ca^{2+}$ current elicited at -30 mV. In 4 cells examined with this experimental protocol, ATP significantly reduced the peak amplitude of the $Ca^{2+}$ current elicited at +10 mV by 37.4 ± 4% (paired t-test, $p < 0.05$). In contrast, at -30 mV, the reduction of $Ca^{2+}$ current by ATP was not statistically significant (7. 8 ± 3%; paired t-test, $p > 0.05$). The

small and insignificant reduction of voltage-gated $Ca^{2+}$ current at -30 mV by ATP raised the question of whether this mechanism can account for the robust inhibitory action of ATP on the hypoxia-induced $[Ca^{2+}]_i$ rise. To further examine this, we bypassed the hypoxia-mediated signaling and directly triggered $[Ca^{2+}]_i$ elevation in type I cells with KCl depolarization (Figure 3-5D). In order to identify type I cells, cells were first exposed to hypoxia. Following the recovery of the hypoxia-induced $Ca^{2+}$ signal, $[Ca^{2+}]_i$ was elevated to a similar level by exposing the cells to 20 mM KCl. A second KCl challenge was then applied in the presence of ATP (100 μM). Note that ATP caused only a small reduction in the amplitude of the $[Ca^{2+}]_i$ rise triggered by the KCl depolarization. In 27 cells examined, the KCl depolarization triggered $[Ca^{2+}]_i$ rise in the presence of ATP (100 μM) was 0.49 ± 0.05 μM, only slightly smaller than that recorded in control condition (0.53 ± 0.06 μM). In contrast, ATP at this concentration (100 μM) completely abolished the hypoxia-induced $[Ca^{2+}]_i$ rise (Figure 3-4). Overall, our results suggest that the small reduction of the voltage-gated $Ca^{2+}$ current is not a major mechanism in the potent inhibitory action of ATP on the hypoxic response.

### *3.2.4 The hypoxia-induced depolarization was reversed by ATP*

In rat neonatal type I cells, hypoxia has been shown to cause membrane depolarization (Buckler and Vaughan-Jones 1994a). This raises the possibility that the inhibitory action of ATP may involve a reduction in cell excitability. To investigate this, we examined whether ATP could inhibit the hypoxia-induced depolarization. Figure 3-6A shows the simultaneous measurement of membrane

potential and $[Ca^{2+}]_i$ from a type I cell. Note that hypoxia caused membrane depolarization and it was accompanied by a rise in $[Ca^{2+}]_i$. Application of ATP (100 μM) under hypoxic condition reversed both the hypoxia-induced depolarization and rise in $[Ca^{2+}]_i$ (n = 5). Thus, ATP opposed the hypoxia-mediated depolarization and prevented the subsequent activation of VGCC. To further elucidate the underlying mechanisms, we injected current pulses (-1 to -3 pA in different cells; 800 ms duration) periodically to monitor the apparent input resistance of the cell during measurement of membrane potential. Figure 3-6B shows that the hypoxia-induced depolarization was accompanied by an increase in the cell apparent input resistance, suggesting that closure of a background conductance underlined the hypoxia-induced depolarization. Note that, however, ATP (100 μM) reversed the hypoxia-induced depolarization without a concomitant reduction in the cell apparent input resistance (see below). In 5 cells examined, hypoxia depolarized the membrane potential by 9 mV (from -46 ± 3 to -37 ± 2 mV; Fig. 6C; paired t test, $p < 0.05$) and increased the cell apparent input resistance to 1.3-fold the initial resting value (from 6.5 ± 1.1 to 8.3 ± 2.1 GΩ, Figure 3-6D). In the presence of ATP and hypoxia, the membrane potential returned to around the resting level (from -37 ± 2 mV to -48 ± 2 mV; paired t test, $p < 0.05$) but the cell input resistance remained near the elevated level (8.9 ± 1.7 GΩ versus 6.5 ± 1.1 GΩ in control; Figure 3-6D, paired t test, $p < 0.05$).

Our observation that the hypoxia-mediated increase in cell input resistance remained elevated in the presence of ATP, suggested that ATP did not prevent a hypoxia-mediated closure of background conductance. Nevertheless, multiple types of channels may be involved during the ATP inhibition of hypoxia response. Thus, the

possibility that our observations of cell apparent input resistance are obscured by opposite changes in membrane conductance cannot be completely ruled out here. For instance, if ATP activates an inwardly rectifying $K^+$ current, this current may indeed cause a larger negative voltage deflection in our constant (negative) current injections (Weight and Padjen, 1973; Selyanko et al. 1990). However, there has been no report of inwardly rectifying $K^+$ current in carotid type I cells. Therefore, we further examined whether ATP affected the background currents that have been implicated in the hypoxic response.

In rat type I cells, the closure of a background TASK-like $K^+$ conductance has been suggested to mediate the hypoxia-induced depolarization (Buckler 1997). The same conductance has also been implicated in GABA-mediated autoreceptor feedback regulation in rat carotid body (Fearon et al. 2003). To investigate whether ATP affects the $O_2$-sensitive TASK-like $K^+$ current, we recorded from type I cells bathed in an extracellular solution containing 140 mM $K^+$. TEA, 4-AP and $Ni^{2+}$ were also included in the bath solution (see chapter 2) to inhibit the delayed rectifier $K^+$ current, the A-type $K^+$ current, the $Ca^{2+}$ current and the $Ca^{2+}$-activated currents. Cells were voltage clamped at -60 mV and voltage steps (20 ms in duration) were applied to various potentials (-80 to +60 mV in 20 mV increments) in control (Figure 3-7A), hypoxia (Figure 3-7B) and in the presence of ATP (100 μM) and hypoxia (Figure 3-7C). A comparison between Figure 3-7A & B shows that there was a reduction in the amplitude of elicited current during hypoxia. The current-voltage relation of the $O_2$-sensitive TASK-like $K^+$ currents was determined by the difference in the currents elicited under hypoxic condition and that of the control and was plotted in Figure 3-

7D. Figure 3-7D also shows the current-voltage relation of the background current that was inhibited by the presence of both ATP and hypoxia (difference in currents between Figure 3-7A & C). Note that the inhibition of background current by hypoxia and ATP was identical to that by hypoxia alone. In 4 out of 4 cells examined, ATP did not affect the inhibition of background current by hypoxia. Thus, in the presence of ATP, hypoxia could still inhibit the background TASK-like $K^+$ current. The above results also indicate that ATP did not interfere with the $O_2$-sensing mechanism in type I cells mediated by the background TASK-like $K^+$ current. Application of ATP alone also failed to affect the background $K^+$ current elicited under similar experimental conditions (140 mM extracellular $K^+$ and in the presence of TEA, 4-AP and $Ni^{2+}$; n = 3). Thus, in contrast to the action of GABA on type I cells, ATP did not cause any activation of TASK-like $K^+$ current (Fearon et al. 2003).

In rat type I cells, the BK channels have also been shown to be sensitive to hypoxia (Peers and Carpenter 1998; Riesco-Fagundo et al 2001). This raises the possibility that the inhibitory action of ATP may involve an increase in the openings of the BK channels, thus reversing the hypoxia-induced depolarization. To test this, we examined whether the inhibition of BK channels could abolish the inhibitory action of ATP on hypoxia. In this experiment, BK channels were inhibited with IbTx, a highly selective and potent blocker of BK channels ($IC_{50}$ = 250 pM). In the presence of IbTx (20 nM), ATP (100 μM) could still reversibly inhibit the hypoxia-induced $Ca^{2+}$ signal in type I cells (Figure 3-8). Thus, the involvement of BK channels in the inhibitory action of ATP is unlikely.

Since ATP had no effect on the two $K^+$ conductances (TASK-like and BK) that have been reported to be modulated by hypoxia, we examined the effect of ATP on the membrane potential and input resistance of the type I cells under normoxic condition. Figure 3-9A shows that under normoxic condition, ATP could cause hyperpolarization. In this example, the cell resting membrane potential was -50 mV, and the cell was identified as a type I cell because it depolarized to ~-30 mV during hypoxia. A subsequent exposure to ATP (100 μM) hyperpolarized the membrane potential to ~-60 mV. As shown in Figure 3-9B, the ATP-mediated hyperpolarization was accompanied by an increase in cell input resistance. For 4 cells recorded in normoxic conditions, ATP hyperpolarized the resting membrane potential by ~ 5 mV (from -45 ± 4 to -50 ± 5 mV; Figure 3-9C, paired t test, $p < 0.05$) and increased the cell input resistance by 1.2 fold (from 5.0 ± 0.6 to 5.8 ± 0.8 GΩ; Figure 3-9D, paired t-test, $p < 0.05$). Thus, under normoxic conditions, the membrane hyperpolarization caused by ATP might involve either the activity of an inwardly rectifying $K^+$ current (as discussed earlier) or the closure of some background conductance.

In rat type I cells, removal of extracellular $Na^+$ has been shown to cause membrane hyperpolarization and this effect has been attributed to the inhibition of a background $Na^+$ conductance (Buckler and Vaughan-Jones 1994b; Carpenter and Peers 2001). Thus, it is possible that the inhibitory action of ATP on hypoxia may involve an inhibition of the background $Na^+$ conductance. To test this possibility, we examined whether elimination of the background $Na^+$ conductance could occlude the action of ATP. An example of this experiment is shown in Figure 3-10. The cell was first challenged with hypoxia under control condition. Following the recovery from

hypoxia, the cell membrane potential was ~-47 mV. When extracellular $Na^+$ was removed, the cell membrane potential was hyperpolarized to ~-70 mV. Since this potential is near the equilibrium potential of $K^+$, and the hypoxia-induced depolarization is mediated significantly by the closure of TASK-like $K^+$ channels, hypoxia caused only very small depolarization under such conditions (data not shown). In order to elicit a more robust hypoxia response in the absence of extracellular $Na^+$, we injected current (2.6 pA) into the cell to bring the cell membrane potential near its initial value. Under this condition, a second hypoxia challenge (in the absence of extracellular $Na^+$) depolarized the cell from ~-48 mV to ~-40 mV. Note that upon application of ATP (100 μM; in the continued presence of hypoxia), the cell membrane potential returned to ~-46 mV. In 8 out of 8 cells examined, ATP reversed the hypoxia-induced depolarization in the absence of extracellular $Na^+$. This finding indicates that the inhibitory action of ATP on hypoxia does not involve the background $Na^+$ conductance.

## 3.3 Discussion

Here we show that in type I cells isolated from adult rat carotid bodies, hypoxia triggered robust $[Ca^{2+}]_i$ elevation even at room temperature (20-23 °C). Similar to that reported in neonatal rat carotid bodies (Buckler and Vaughan-Jones, 1994a), the hypoxia-induced $[Ca^{2+}]_i$ rise was accompanied by membrane depolarization (Figure 3-6) and activation of VGCC (Figure 3-1B). Under our experimental condition, hypoxia ($P_{O_2}$ of ~40 mm Hg) typically depolarized the type I

cells by ~9 mV. Although the depolarization was small, it was sufficient to activate VGCC and elevate $[Ca^{2+}]_i$ to ~0.3 μM. Interestingly, ATP, one of the major neurotransmitters released from type I cells during hypoxia, did not affect the resting $[Ca^{2+}]_i$ of type I cells (Xu et al. 2003) but strongly suppressed the hypoxia-induced $[Ca^{2+}]_i$ rise (Figure 3-2). Our results contrast with a recent study that showed that ATP caused $[Ca^{2+}]_i$ rise in dissociated rat type I cells via $P_2$ receptors (Mokashi et al. 2003). The opposite findings in the two studies may be related to the criteria for identification of type I cells. In an acutely dissociated cell preparation of rat carotid bodies, the cell mixture comprises type I and type II cells, as well as white blood cells. Although the glial-like sustentacular type II cells typically become spindle-shaped after ~ 24 hours in culture (see Fig. 1 in Xu et al. 2003), these cells are initially ovoid for at least 12 hours after the cell isolation procedure. Since all three types of cells are initially similar in size and shape, both type II cells and white blood cells can be easily mistaken for type I cells in the overnight culture of Mokashi et al. (2003). In our previous study, individual type I cells were identified by their catecholamine secretion (detected by carbon fiber amperometry) during KCl challenge (see Fig. 2B in Xu et al. 2003). In the current study, we identified individual type I cells based on their $Ca^{2+}$ response to hypoxia (see for example, Figure 3-2, 3-3 & 3-6). Thus, in this study, every type I cell that was challenged with ATP had previously exhibited a hypoxic response. In contrast, Mokashi et al. (2003) only confirmed the presence of TH containing cells in the cell mixture with immunofluorescence staining. Their study did not examine whether individual ATP-responding cells in the same study indeed expressed TH. Moreover, some white blood cells are known to express TH (Marino

et al. 1999; Reguzzoni et al. 2002). Thus, identification of type I cells based solely on the presence of TH immunofluorescence may not be reliable. Interestingly, P2 receptors are expressed by many white blood cells, including macrophages and lymphocytes (Di Virgilio et al. 2001). In our $Ca^{2+}$ imaging experiments on cell populations isolated from rat carotid bodies, ATP did elicit $[Ca^{2+}]_i$ rise in some ovoid shaped cells (unpublished observations). However, neither hypoxia nor KCl depolarization could trigger any $[Ca^{2+}]_i$ rise in these cells, indicating that these ATP-responding cells were not type I cells. We speculate that these ATP-responding cells may be white blood cells or type II cells that became spherical after the cell dissociation procedure and did not resume their spindle shape. As shown in our previous study (Xu et al. 2003), ATP triggered intracellular $Ca^{2+}$ release in type II cells via activation of $P2Y_2$ receptors.

In this study, we show that the hypoxia-induced $Ca^{2+}$ signal in type I cells could be completely abolished by 10 or 100 μM ATP (Figure 3-4). At a lower concentration, such as, 0.5 μM, ATP reduced the amplitude of the hypoxia-induced $Ca^{2+}$ signal by ~40% (Figure 3-4). A recent study in rat carotid body slices showed that the concentration of ATP reached ~0.5 μM during hypoxia (Buttigieg and Nurse, 2004). Thus, the inhibitory action of ATP on hypoxia-induced $Ca^{2+}$ signal reported here may have important physiological implications. Among the different purinoreceptor agonists, 2-MeSATP was slightly more potent than ATP in abolishing the hypoxia-induced $Ca^{2+}$ signal. ADP was slightly less potent than ATP but α, β-MeATP and UTP (even at 100 μM) were ineffective in reducing the hypoxia-induced $Ca^{2+}$ signal (Figure 3-3 & 3-4). The agonist potency profile is consistent with the

activation of $P2Y_1$ receptors (Ralevic and Burnstock 1998). Our immuohistochemistry experiments have also detected the presence of $P2Y_1$ receptors on the type I cell clusters in the carotid body section (Figure 3-4B). We found that a significant fraction of $P2Y_1$ receptors were located in the intracellular compartment of type I cells. Since the receptors are synthesized in the endoplasmic reticulum (ER)-Golgi compartment before being transported to the plasma membrane, some of the immunofluorescence probably arose from $P2Y_1$ receptors in the ER compartment. The presence of a major pool of $P2Y_1$ receptors in intracellular compartments (membranes of α-granules and the open canalicular system) has also been reported in platelets (Nurden et al. 2003). However, a previous electron microscopic study on type I cells had not reported the presence of any canalicular system (McDonald 1981). P2Y receptors are typically coupled to $G_{q/11}$ or $G_{i/o}$. Since ATP did not affect the basal $[Ca^{2+}]_i$ in type I cells (Figure 3-2), the involvement of the $G_{q/11}$ and the phosphoinositide pathway is unlikely. In bovine chromaffin cells (Currie and Fox 1996), ATP, acting via P2Y receptors, mediated an autocrine inhibition of voltage-gated $Ca^{2+}$ current. Similar to the finding in chromaffin cells, we found that ATP partially suppressed the voltage-gated $Ca^{2+}$ current in type I cells (Figure 3-5). However, the maximal inhibition of voltage-gated $Ca^{2+}$ current (at +10 mV) by 100 μM ATP was only ~35%. At potentials near the hypoxia-induced depolarization (e.g. ~-30 mV), the fraction of $Ca^{2+}$ current inhibited by ATP was negligible (Figure 3-5C). The different percentage of inhibition of $Ca^{2+}$ current by ATP at negative or positive potentials might be due to the presence of different components of voltage-gated $Ca^{2+}$ current at different potentials. L-type $Ca^{2+}$ current may contribute more at +10 mV

than at -30 mV. Regardless, the small inhibition of $Ca^{2+}$ current indicates that the voltage-gated $Ca^{2+}$ current can not be the major contributor for the robust suppression of the hypoxia-induced $Ca^{2+}$ signal by ATP. Consistent with this, the $[Ca^{2+}]_i$ rise evoked by KCl depolarization was only slightly reduced by 100 μM ATP (Figure 3-5D).

Our results show that a reversal of the hypoxia-mediated depolarization by ATP is the major contributing factor for the inhibition of hypoxia induced $[Ca^{2+}]_i$ elevation (Figure 3-6A). Depolarization of type I cells during hypoxia has been suggested to involve the inhibition of several $O_2$-sensitive $K^+$ currents, including a 4-AP-sensitive $K^+$ current (López-López et al. 1993), a TEA-sensitive $Ca^{2+}$-activated $K^+$ current (Peers 1990; Pardal et al. 2000) and a TEA- and 4-AP-insensitive TASK-like $K^+$ current (Buckler 1997; Buckler et al. 2000). Therefore, it is possible that the inhibitory action of ATP might involve enhancement of some of these $O_2$-sensitive $K^+$ currents. Alternatively, ATP might reduce the $O_2$ sensitivity of some of these $K^+$ currents, thus opposing their closure during hypoxia. For both possibilities, ATP should cause a reduction in cell input resistance. However, we found that ATP did not reduce the hypoxia mediated increase in cellular input resistance. The cellular input resistance in the presence of ATP and hypoxia was not statistically different from that in hypoxia. Instead, application of ATP in the continued presence of hypoxia caused a small further increase (not statistically significant) in cellular input resistance (Figure 3-6D). This result raises the possibility that the inhibitory effect of ATP may be independent of the $O_2$-sensitive $K^+$ currents. Most importantly, we found that the $O_2$-sensitive TASK-like $K^+$ current (a major background conductance

at the resting membrane potential of rat type I cells) was not affected by ATP (Figure 3-7). In addition, inhibition of the BK channels also failed to ablate the inhibitory action of ATP on the hypoxia-induced $[Ca^{2+}]_i$ elevation (Figure 3-8). Under normoxic condition, ATP caused a membrane hyperpolarization (Figure 3-9). Although the amplitude of the hyperpolarization was small, it may be sufficient to bring the membrane potential to a level below the activation threshold of the voltage-gated $Ca^{2+}$ current. An ATP-mediated membrane hyperpolarization was also reported by Mokashi et al. (2003). Interestingly, we found that the ATP-mediated hyperpolarization was accompanied by an increase in cell input resistance (Figure 3-9D), which may indicate the closure of a background conductance. Under our experimental conditions, the major ions present are $K^+$, $Na^+$ and $Cl^-$. The involvement of a background non-rectifying $K^+$ conductance is unlikely because the closure of background $K^+$ conductance should cause depolarization. The involvement of background $Na^+$ is also ruled out here as the inhibitory action of ATP can be observed even in the absence of extracellular $Na^+$ (Figure 3-10). The role of $Cl^-$ channels is unclear because the reversal potential of $Cl^-$ ion in intact type I cells is not known. Thus, ATP, acting via $P2Y_1$ receptors, closes some unknown background conductance and causes membrane hyperpolarization (Figure 3-11). The hyperpolarization in turn opposes hypoxia-induced membrane depolarization and $[Ca^{2+}]_i$ rise (Figure 3-11).

We speculated that in type I cells of rat carotid body, the suppression of ATP on hypoxia-induced $[Ca^{2+}]_i$ rise would in turn reduce neurotransmitter release from the type I cells. In view of the role of ATP as an excitatory neurotransmitter released from type I cells to stimulate the CSN (via P2X receptors; Zhang et al. 2000), our data

suggests that the released ATP also acts as a negative regulator on type I cells to prevent excessive chemotransduction in the carotid body. Consistent with this, exogenous application of ATP (100 μM) has been shown to suppress hypoxia-induced afferent CSN activities in rat (Mokashi et al. 2003). Other neurotransmitters, including DA and GABA, have also been implicated in autoreceptor feedback inhibition in carotid bodies (Benot and López-Barneo 1990; Fearon et al. 2003). Negative feedback regulation of catecholamine release via activation of autoreceptors for co-released ATP has also been reported in other cells (Currie and Fox, 1996).

## 3.4 Acknowledgements

This work was done in collaboration with Dr. Jianhua Xu. I performed the experiments including the ATP inhibition of the ongoing hypoxia response, the dose-response relationships of the different purinergic agonists, the immunostaining of $P2Y_1$ receptors, the effect of ATP on $I_{Ca}$ at -30 & +10 mV and on KCl depolarization-triggered $[Ca^{2+}]_i$ rise, and the role of the background $Na^+$ conductance and BK channels in the action of ATP. The findings in this chapter have been published in J Neurochem 92: 1419-1430, 2005.

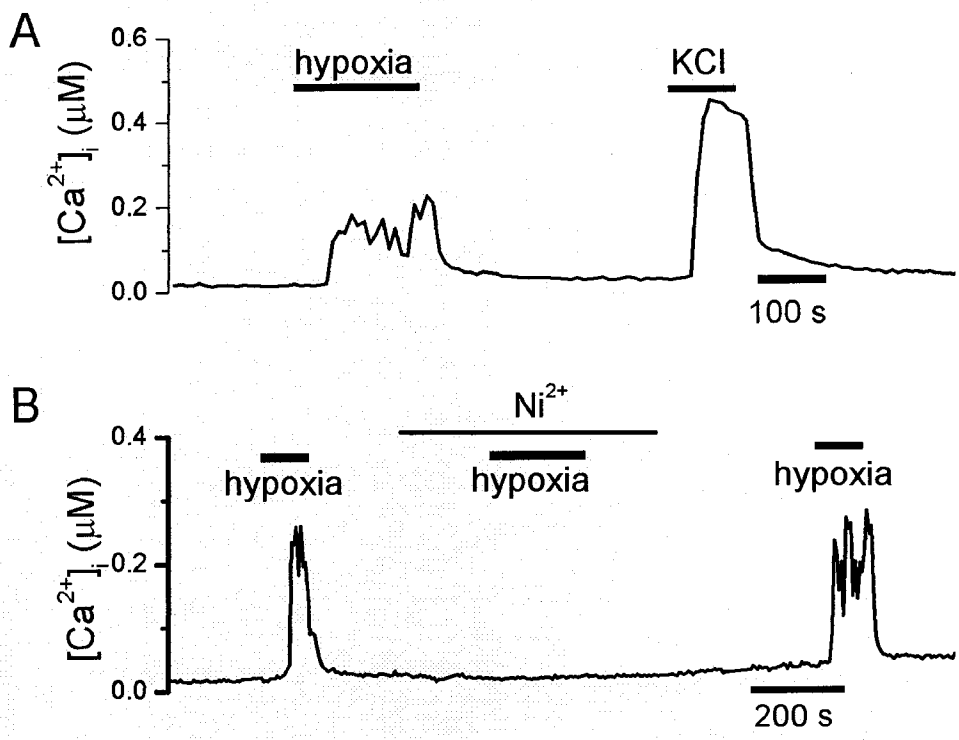


**Figure 3-1** Hypoxia triggered $[Ca^{2+}]_i$ rise in type I cells via activation of VGCC. *A*, Hypoxia and KCl-depolarization triggered $[Ca^{2+}]_i$ rise in the same cell. Under hypoxic condition, $[Ca^{2+}]_i$ rose to ~0.2 μM and remained elevated until the cell was returned to normoxic conditions. Subsequent application of KCl (20 mM) raised $[Ca^{2+}]_i$ to ~0.45 μM. *B*, Inhibition of VGCC prevented hypoxia from eliciting any $[Ca^{2+}]_i$ elevation. In the presence of $Ni^{2+}$ (2.5 mM), a blocker of VGCC, hypoxia failed to trigger any $[Ca^{2+}]_i$ rise. After the removal of $Ni^{2+}$, a subsequent hypoxia challenge could still elicit robust $[Ca^{2+}]_i$ rise. Cells were loaded with fura-2AM and $[Ca^{2+}]_i$ was monitored with $Ca^{2+}$ imaging.

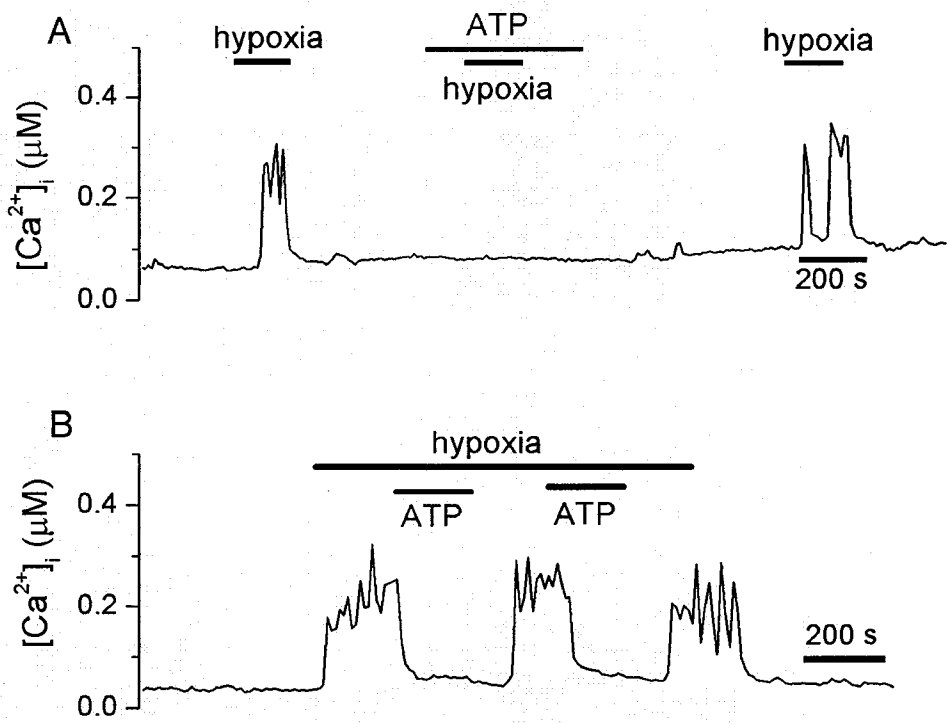


**Figure 3-2** ATP inhibited the hypoxia-induced $[Ca^{2+}]_i$ rise in type I cells. *A*, ATP prevented the triggering of $Ca^{2+}$ response by hypoxia. ATP (100 μM) did not affect the resting $[Ca^{2+}]_i$ in type I cells. In the continued presence of ATP, however, hypoxia failed to trigger any $[Ca^{2+}]_i$ rise. Following the removal of ATP, the hypoxia response was restored. *B*, the ongoing hypoxia response was inhibited by ATP. Continuous hypoxia caused a sustained $[Ca^{2+}]_i$ elevation in type I cells. In the presence of hypoxia, ATP (100 μM) reversibly suppressed the $[Ca^{2+}]_i$ elevation. Cells were loaded with fura-2 AM and $[Ca^{2+}]_i$ was monitored with $Ca^{2+}$ imaging.

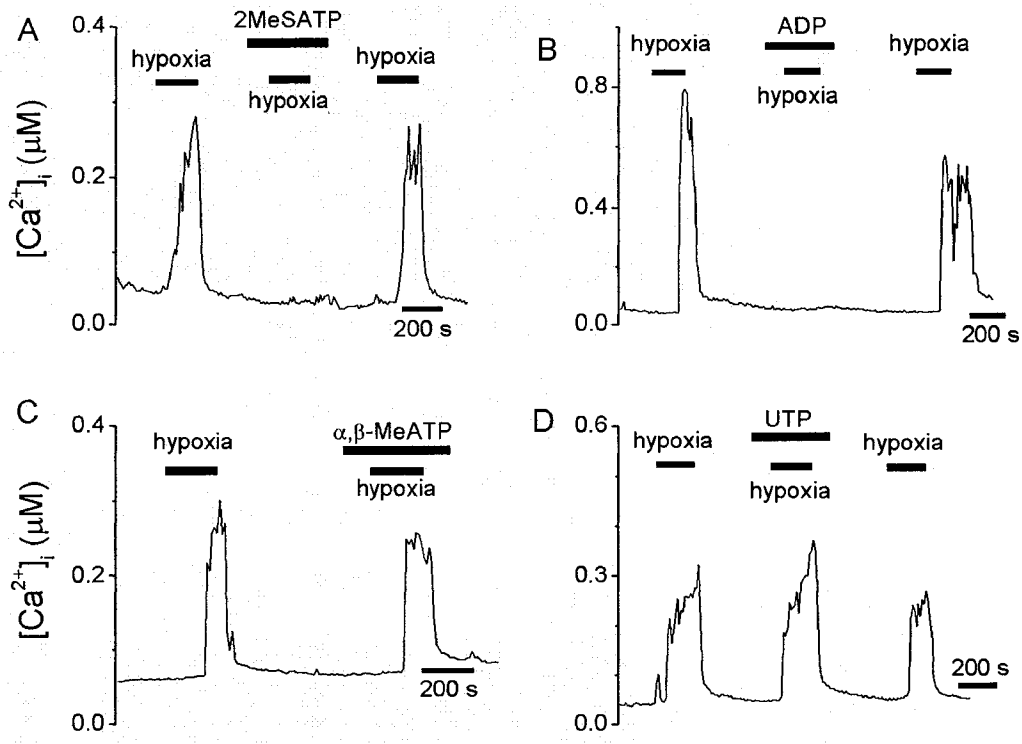


**Figure 3-3** Actions of different purinoreceptor agonists on hypoxia induced $Ca^{2+}$ signal. *A,* the hypoxia-induced $[Ca^{2+}]_i$ rise could be prevented by 2-MeSATP (10 μM). *B*, ADP (100 μM) also inhibited the hypoxia-induced $Ca^{2+}$ signal. *C,* α,β-MeATP (100 μM) caused only a slight reduction of the hypoxia-induced $[Ca^{2+}]_i$ rise. *D,* UTP (100 μM) did not affect the hypoxia-induced $Ca^{2+}$ signal. $[Ca^{2+}]_i$ was measured with fura-2 $Ca^{2+}$ imaging.

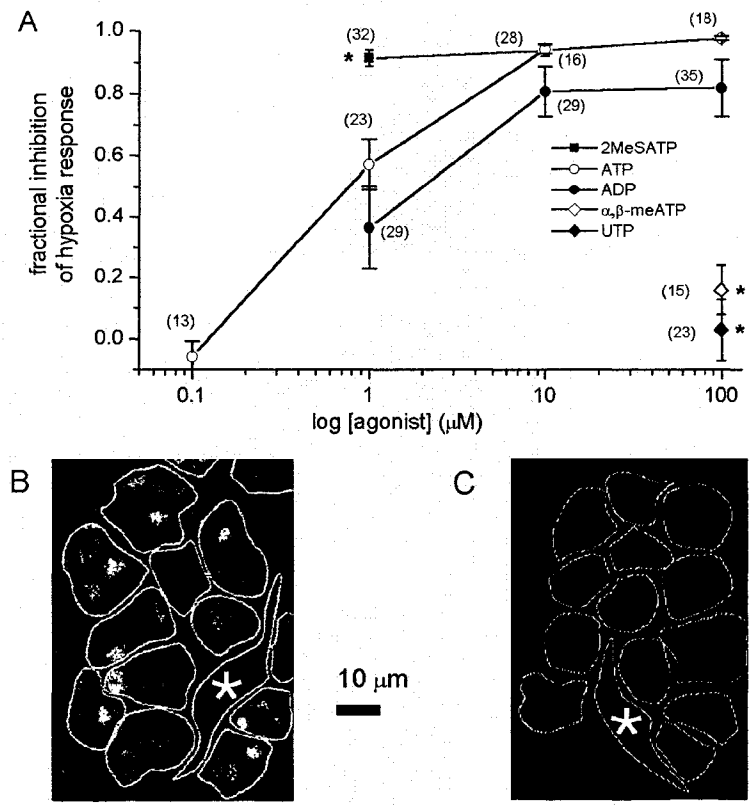


**Figure 3-4** The inhibitory action of ATP on hypoxia response is mediated via $P2Y_1$ receptors. *A,* Dose relation of different purinoreceptor agonists on hypoxia response. Plot of the fractional inhibition of the hypoxia-induced $[Ca^{2+}]_i$ rise *versus* log concentrations of different purinoreceptor agonists. The potency order for inhibition was 2-MeSATP > ATP > ADP >> α,β-meATP and UTP, implicating the involvement of $P2Y_1$ receptors. Each cell was subjected first to a hypoxia challenge in standard bath solutions. Following the recovery of $[Ca^{2+}]_i$, a second hypoxia challenge in the presence of a purinoreceptor agonist was applied. The protocol was similar to that described in Figure 3-3. The amplitude of the hypoxia-induced $Ca^{2+}$ signal in the presence of the purinoreceptor agonist was compared to that of the first hypoxia challenge. The number of cells included in each data point is shown in parentheses and values of statistical significance (when compared to same concentrations of ATP) are denoted with *. *B,* Confocal image of a carotid body section immunostained with a fluorescently labelled antibody against an epitope on the 3rd intracellular loop of the $P2Y_1$ receptors. Note that the fluorescence was localized in the clusters of ovoid type I cells. *C,* Confocal image of a carotid body section immunostained with the $P2Y_1$ antibody together with the antigen peptide. In both *B & C,* the outlines of individual cells were estimated by comparing bright-field and fluorescent images. A spindle-shaped type II cell is marked with an asterisk.

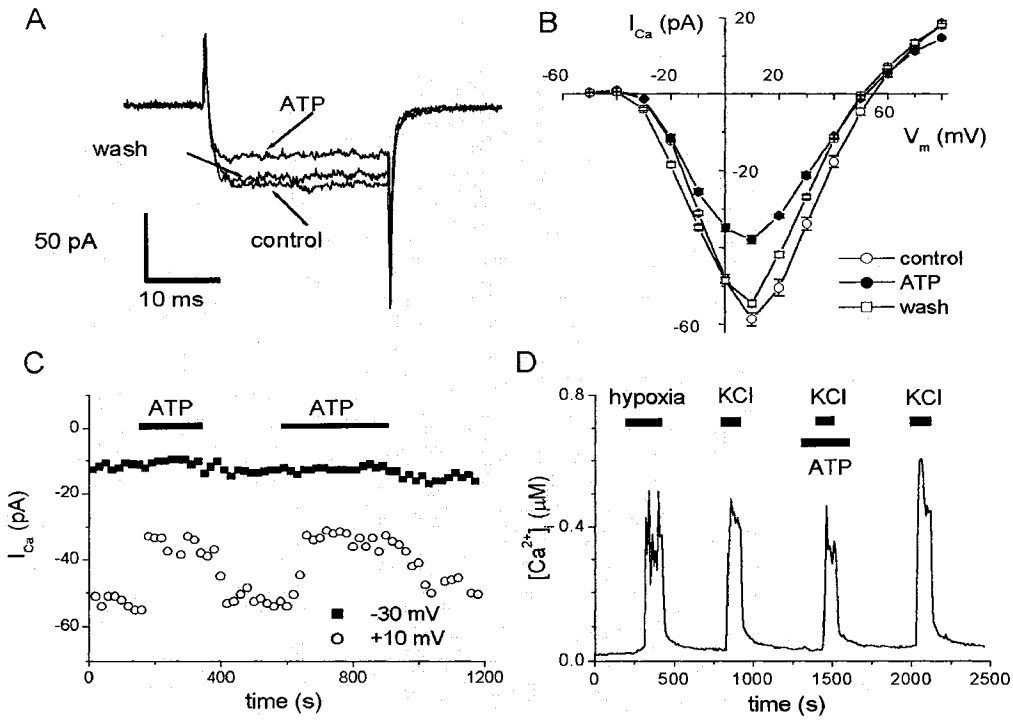


**Figure 3-5** ATP partially inhibited the voltage-gated $Ca^{2+}$ current but only slightly reduced the KCl-triggered $[Ca^{2+}]_i$ rise. *A*, ATP reversibly reduced a small fraction of the $Ca^{2+}$ current. Superimposed records of $Ca^{2+}$ current elicited during a test step to +10 mV from a holding potential of -60 mV in control, in the presence of ATP (100 μM) and following the removal of ATP (wash). *B*, the current-voltage relation of the inhibitory action of ATP on $Ca^{2+}$ current. On average, ATP reduced the peak $Ca^{2+}$ current elicited at +10 mV by ~ 35%. The holding potential was -60 mV and 25 ms voltage steps to various potentials were applied. The data shown in *B* was averaged from 6 cells. *C*, ATP had negligible effect on the $Ca^{2+}$ current elicited at -30 mV. Plot of the amplitudes of the $Ca^{2+}$ current elicited by voltage steps (25 ms in duration) to -30 mV or +10 mV (delivered every 10s). The holding potential was -60 mV. Note that ATP (100 μM) did not affect the $Ca^{2+}$ current elicited at -30 mV (closed squares) but reversibly reduced the $Ca^{2+}$ current elicited at +10 mV (open circles) by ~38%. In *A*, *B* & *C*, individual type I cells were recorded with perforated whole-cell patch recording. *D*, ATP caused only a small reduction of the KCl-triggered $[Ca^{2+}]_i$ rise. To mimic the hypoxia-induced $Ca^{2+}$ signal, $[Ca^{2+}]_i$ in type I cell was elevated to ~0.5 μM via exposure to a standard bath solution that contained 20 mM KCl. Note that in the continued presence of ATP (100 μM), the KCl depolarization-triggered $[Ca^{2+}]_i$ rise was only slightly smaller than elicited before ATP application. In this cell, KCl elicited a larger $[Ca^{2+}]_i$ rise following the removal of ATP. $[Ca^{2+}]_i$ was measured with fura-2 $Ca^{2+}$ imaging.

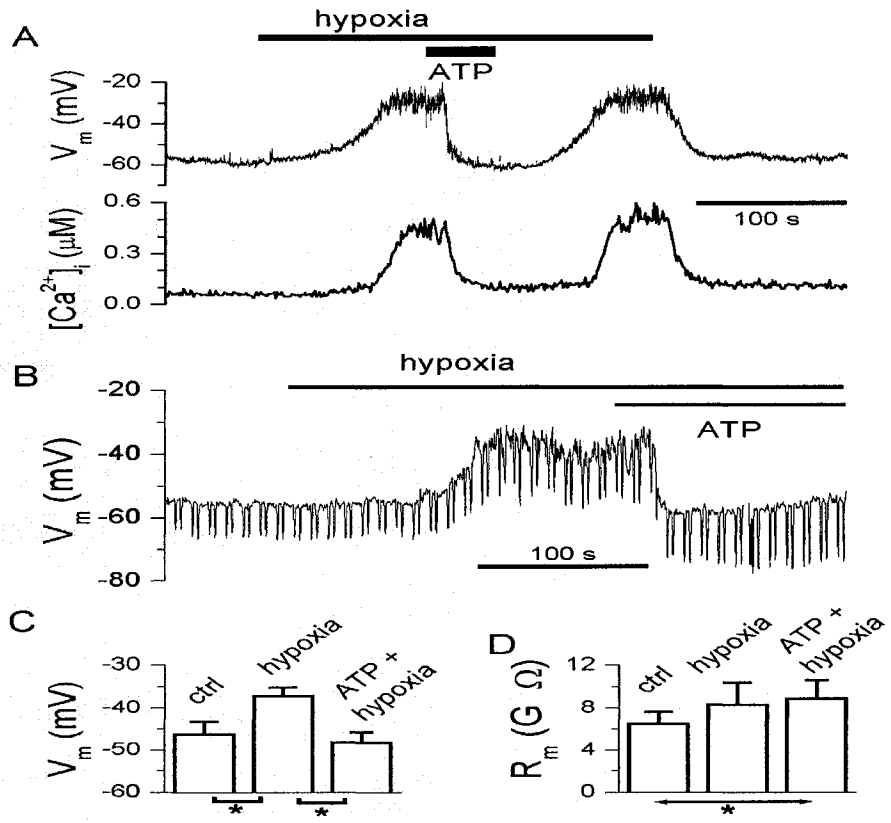


**Figure 3-6** The hypoxia-induced depolarization was reversed by ATP. *A*, Hypoxia caused a membrane depolarization which was accompanied by $[Ca^{2+}]_i$ rise. Application of ATP (100 μM) in hypoxia caused hyperpolarization which was accompanied by a decay in $[Ca^{2+}]_i$ to resting level. Following ATP removal, both the hypoxia-induced depolarization and $[Ca^{2+}]_i$ rise were restored. Membrane potential (perforated whole-cell patch clamp recording) was monitored simultaneously with $[Ca^{2+}]_i$ (indo-1 fluorometry). *B*, the hypoxia-mediated increase in cell apparent input resistance was not reversed by ATP. Current pulses of -2 pA (800 ms in duration) were injected periodically to monitor the cell apparent input resistance (downward deflections on $V_m$ trace) during measurement of membrane potential. The hypoxia-induced depolarization was accompanied by an increase in cell apparent input resistance, implicating the reduction of a background conductance. Application of ATP (in hypoxia) hyperpolarized the cell but did not cause any reduction in cell apparent input resistance. *C*, Summary of the effect of hypoxia and ATP on membrane potential. Hypoxia depolarized the membrane potential by ~9 mV (from -46 ± 3 to -37 ± 2 mV; n = 5). Application of ATP (in hypoxia) returned the membrane potential to resting level (-48 ± 2 mV). * denotes values of significant difference. *D*, Summary of the effect of ATP and hypoxia on cell apparent input resistance. In cells challenged with hypoxia (n = 5), the cell apparent input resistance increased by ~1.8 GΩ (from 6.5 ± 1.1 to 8.3 ± 2.1 GΩ). Application of ATP (in the continued presence of hypoxia) caused a further increase in cell apparent input resistance (to 8.9 ± 1.7 GΩ).

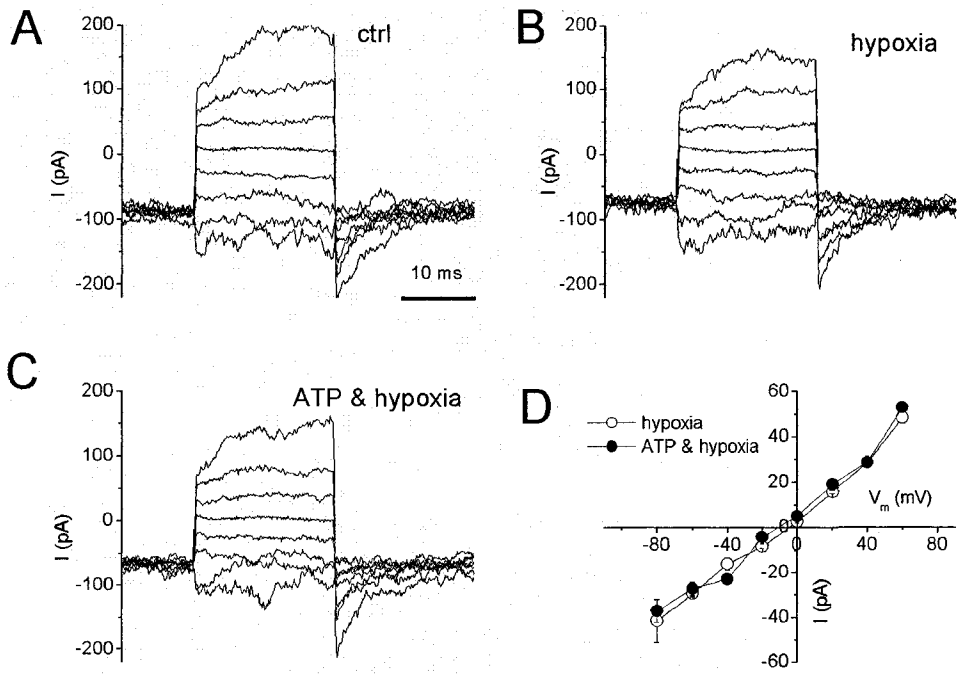


**Figure 3-7** The $O_2$-sensitive TASK-like background $K^+$ current was not affected by ATP. *A*, *B* & *C*, superimposed current records elicited by 20 ms voltage steps from -80 to +60 mV in 20 mV increments under normoxic (*A*), hypoxic (*B*) and hypoxic conditions in the presence of ATP (*C*). The cell was bathed in a solution containing 140 mM $K^+$, 10 mM TEA-Cl, 5 mM 4-AP and 2.5 mM $Ni^{2+}$. *D*, ATP had no effect on the $O_2$-sensitive TASK-like $K^+$ current at the potentials examined. The plot of the current-voltage relation of the $O_2$-sensitive TASK-like $K^+$ current (open circle) was determined by the subtraction of I-V (averaged from 3 records) obtained under hypoxic conditions from that obtained under normoxic conditions. The plot of effect of ATP on the $O_2$-sensitive $K^+$ current (closed circle) was determined by the subtraction of I-V obtained in the presence of ATP & hypoxia from that obtained under normoxic conditions.

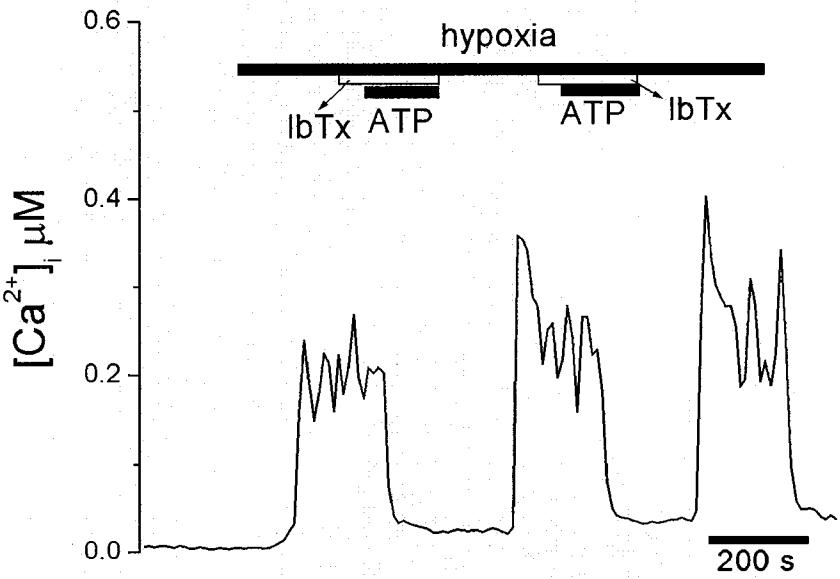


**Figure 3-8** The inhibitory action of ATP on hypoxia-induced $[Ca^{2+}]_i$ rise was not occluded by IbTx, a blocker of BK channels. Hypoxia triggered a robust $[Ca^{2+}]_i$ rise in type I cell. Application of IbTx (20 nM) did not significantly affect the hypoxia response. In the presence of IbTx, ATP (100 µM) could still reversibly suppress the hypoxia-induced $Ca^{2+}$ signal. $[Ca^{2+}]_i$ was measured with fura-2 $Ca^{2+}$ imaging

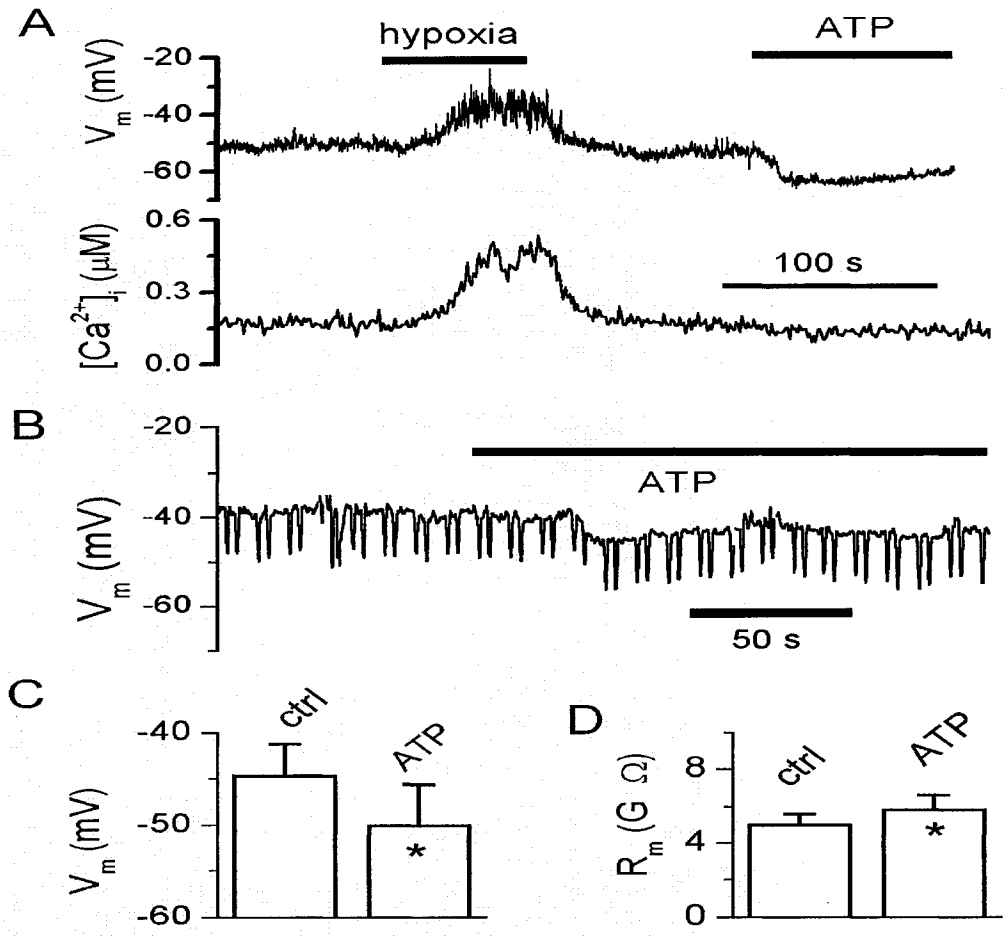


**Figure 3-9** ATP caused hyperpolarization and increase in cell input resistance. *A*, in the absence of hypoxia, application of ATP (100 μM) caused hyperpolarization. Simultaneous measurement of membrane potential (perforated whole-cell patch clamp recording) and $[Ca^{2+}]_i$ (indo-1 fluorometry). *B*, The ATP-mediated hyperpolarization was accompanied by an increase in cell input resistance, implicating the closure of a background conductance. Current pulses of -3 pA (800 ms in duration) were injected periodically to monitor the cell input resistance (downward deflections on $V_m$ trace) during measurement of membrane potential. *C*, Summary of the effect of ATP on resting membrane potential. In 4 cells challenged with ATP (100 μM), the mean resting membrane potential hyperpolarized by ~ 5 mV (from -45 ± 4 to -50 ± 5 mV). *D*, in cells challenged with ATP alone (n = 4), ATP increased the cell input resistance by ~ 0.8 GΩ (from 5.0 ± 0.6 to 65.8 ± 0.8 GΩ). * denotes value significantly different from control.

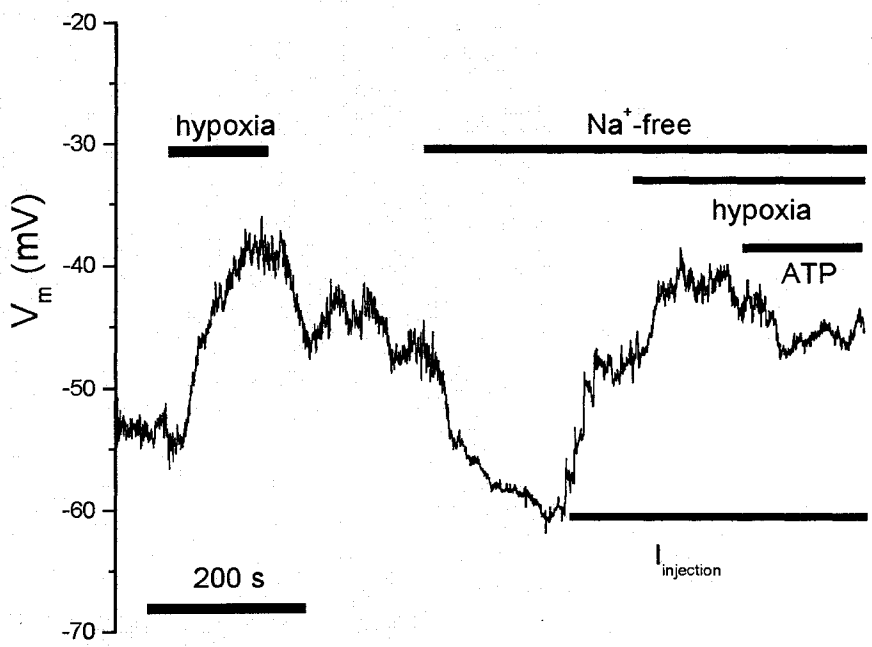


**Figure 3-10** The inhibitory action of ATP on hypoxia-mediated depolarization was independent of the background $Na^+$ conductance. The initial resting membrane potential of this type I cell was ~-53 mV. A brief hypoxia challenge under control condition depolarized the cell to ~-38 mV. Following the removal of hypoxia, the membrane potential returned to ~-47 mV. When the background $Na^+$ conductance was inhibited by the removal of extracellular $Na^+$, the cell hyperpolarized to ~-70 mV. To bring the cell membrane potential back near the basal level, we injected current (2.6 pA) into the cell to keep the cell membrane potential near ~-48 mV. A second hypoxia challenge resulted in membrane depolarization (to ~-40 mV) and this depolarization was reversed by the application of ATP (100 μM).

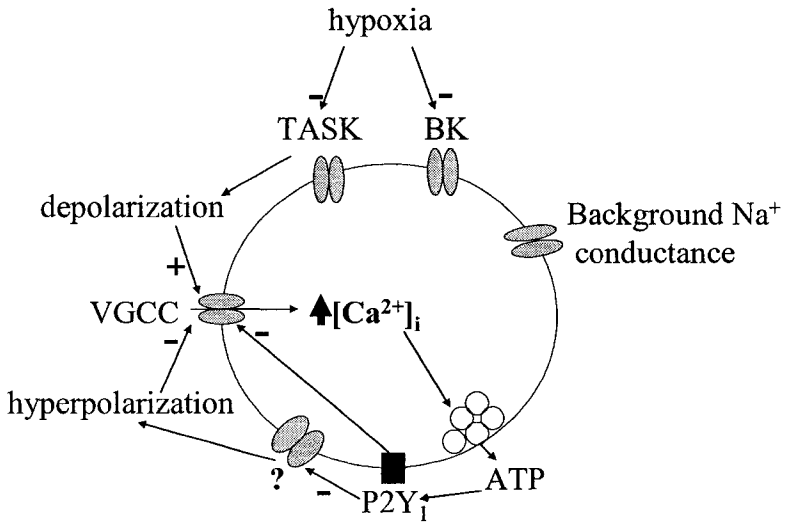


**Figure 3-11** Summary of actions of ATP on rat type I cells. Hypoxia inhibits TASK-like $K^+$ channels and BK channels, and thus causes membrane depolarization in type I cells. This depolarization leads to activation of VGCC and $Ca^{2+}$ influx via these channels. The rise in $[Ca^{2+}]_i$ in turn triggers the release of ATP from type I cells. ATP can in turn suppress hypoxia-mediated $[Ca^{2+}]_i$ rise. The negative feedback action of ATP on type I cell does not involve TASK-like $K^+$ channels, BK channels or background $Na^+$ conductance. The inhibition of voltage-gated $Ca^{2+}$ current is small, and thus may not be the major contributor either. Our data suggested that ATP, acting via $P2Y_1$ receptors, causes hyperpolarization in type I cells via closure of some unknown background conductance. The hyperpolarization in turn opposes the hypoxia-mediated membrane depolarization and $[Ca^{2+}]_i$ rise.

## References


Benot A. R. and López-Barneo J. (1990) Feedback inhibition of $Ca^{2+}$ currents by dopamine in glomus cells of the carotid body. *Eur. J. Neurosci.* **2**, 809-812.

Bright G. R., Agani F. H., Haque U., Overholt J. L. and Prabhakar N. R. (1996) Heterogeneity in cytosolic calcium responses to hypoxia in carotid body cells. *Brain Res.* **706**, 297-302.

Buckler K. J. (1997) A novel oxygen-sensitive potassium current in rat carotid body type I cells. *J. Physiol.* **498**, 649-662.

Buckler K. J. and Vaughan-Jones R. D. (1994a) Effects of hypoxia on membrane potential and intracellular calcium in rat neonatal carotid body type I cells. *J. Physiol.* **476**, 423-428.

Buckler K. J. and Vaughan-Jones R. D. (1994b) Effects of hypercapnia on membrane potential and intracellular calcium in rat carotid body type I cells. *J. Physiol.* **478**, 157-171.

Buckler K. J., Williams B. A. and Honore E. (2000) An oxygen-, acid- and anaesthetic-sensitive TASK-like background potassium channel in rat arterial chemoreceptor cells. *J. Physiol.* **525**, 135-142.

Buttigieg J. and Nurse C. A. (2004) Detection of hypoxia-evoked ATP release from chemoreceptor cells of the rat carotid body. *Biochem. & Biophy. Res. Comm.* **322**, 82-87.

Carpenter E. and Peers C. (1997) Swelling- and cAMP-activated $Cl^-$ currents in isolated rat carotid body type I cells. *J. Physiol.* **503**, 497-511.

Carpenter E. and Peers C. (2001) A standing $Na^+$ conductance in rat carotid body type I cells. *NeuroReport* **12**, 1421-1425.

Currie K. P. M. and Fox A. P. (1996) ATP serves as a negative feedback inhibitor of voltage-gated $Ca^{2+}$ channel currents in bovine adrenal chromaffin cells. *Neuron* **16**, 1027-1036.

Di Virgilio F., Chiozzi P., Ferrari D., Falzoni S., Sanz J. M., Morelli A., Torboli M., Bolognesi F. and Baricordi R. (2001) Nucleotide receptors: an emerging family of regulatory molecules in blood cells. *Blood* **97**, 587-600.

Donnelly D. F. and Kholwadwala D. (1992) Hypoxia decreases intracellular calcium in adult rat carotid body glomus cells. *J. Neurophysiol.* **67**, 1543-1551.

Fearon I. M., Zhang M., Vollmer C. and Nurse C. A. (2003) GABA mediates autoreceptor feedback inhibition in the rat carotid body via presynaptic $GABA_A$ receptors and TASK-1. *J. Physiol.* **553**, 83-94.

Fitzgerald R. S. (2000). Oxygen and carotid body chemotransduction: the cholinergic hypothesis – a brief history and new evaluation. *Respir. Physiol.* **120**, 89-104.

Gonalez C., Almaraz L., Obeso A. and Rigual R. (1994) Carotid body chemoreceptors: from natural stimuli to sensory discharges. *Physiol. Rev.* **74**, 829-897.

Grönblad M. (1983). Function and structure of the carotid body. *Med. Biol.* **61**, 229-248.

Grynkiewicz G., Poenie M. and Tsien R. Y. (1985) A new generation of Ca indicators with greatly improved fluorescence properties. *J. Biol. Chem.* **260**, 3440-3450.

López-Barneo J. (1996) Oxygen-sensing by ion channels and the regulation of cellular functions. *Trends in Neuroscience* **19**, 43-440.

López-López J. R., De Luis D. A. and Gonzale C. (1993) Properties of a transient $K^+$ current in chemoreceptor cells of rabbit carotid body. *J. Physiol.* **460**, 15-32.

López-López J. R., Gonzale C. and Pérez-García M. T. (1997) Properties of ionic currents from isolated adult rat carotid body chemoreceptor cells: effect of hypoxia. *J. Physiol.* **499**, 429-441.

McDonald D. M. (1981) Peripheral chemoreceptors: structure-function relationships of the carotid body. in Regulation of Breathing (Hornbein T.F. ed), pp.105-319. Dellker, New York.

Marino F., Cosentino M., Bombelli R., Ferrari M., Lecchini S. and Frigo G. (1999) Endogenous catecholamine synthesis, metabolism storage, and uptake in human peripheral blood mononuclear cells. *Exp. Hematology* **27**, 489-495.

Mokashi A., Li J., Roy A., Baby S. M. and Lahiri S. (2003) ATP causes glomus cell $[Ca^{2+}]_c$ increase without corresponding increases in CNS activity. *Resp. Physiol. & Neurobiol.* **138**, 1-18.

Nurden P., Poujol C., Winckler J., Combrié R., Pousseau N., Conley P. B., Levy-Toledano S., Habib A. and Nurden A. T. (2003) Immunolocalization of $P2Y_1$ receptors and TP□ receptors in platelets showed a major pool associated with membranes of □-granules and the open canalicular system. *Blood* **101**, 1400-1408.

Pardal R., Ludewig U., García-Hirschfeld J. and López-Barneo J. (2000). Secretory responses of intact glomus cells in thin slices of rat carotid body to hypoxia and tetraethylammonium. *Proc. Natl. Acad. Sci. USA* **97**, 2361-2366.

Peers C. (1990) Hypoxic suppression of $K^+$ currents in type I carotid body cells – selective effect on the $Ca^{2+}$-activated $K^+$ current. *Neurosci. Lett.* **119**, 253-256.

Peers C. and Carpenter E. (1998). Inhibition of $Ca^{2+}$-activated $K^+$ channels in rat carotid body type I cells by protein kinase C. *J. Physiol.* 512, 743-750.

Prabhakar N.R. (2000) Oxygen sensing by the carotid body chemoreceptors. *J. Appl. Physiol.* **88**, 2287-2295.

Prasad M., Fearon I. M., Zhang M., Laing M., Vollmer C. and Nurse C. A. (2001) Expression of P2X2 and P2X3 receptor subunits in rat carotid body afferent neurones: role in chemosensory signalling. *J. Physiol.* **537**, 667-677.

Ralevic V. and Burnstock G. (1998) Receptors for purines and pyrimidines. *Pharmacological Reviews* **50**, 415-492.

Reguzzoni M., Cosentino M., Rasini E., Marino F., Ferrari M., Bombelli R., Congiu T., Protasoni M., Quacci D., Lecchini S., Raspanti M. and Frigo G. (2002) Ultrastructural localization of tyrosine hydroxylase in human peripheral blood mononuclear cells: effect of stimulation with phytohaemagglutinin. *Cell & Tissue Res.* **310**, 297-304.

Riesco-Fagundo A. M., Pérez-García M.T., González C. and López-López J. R. (2001) $O_2$ modulates large-conductance $Ca^{2+}$-dependent $K^+$ channels of rat chemoreceptor cells by a membrane restricted and CO-sensitive mechanism. *Circ Res* **89**, 430-436.

Selyanko A. A., Smith P. A. and Zidichouski J. A. (1990) Effects of muscarine and adrenaline on neurons from rana pipiens sympathetic ganglia. *J of Physiol* **425,** 471-500

Tse A. and Tse F. W. (1998) □-adrenergic stimulation of cytosolic $Ca^{2+}$ oscillations and exocytosis in identified rat corticotrophs. *J. Physiol.* **512,** 385-393.

Ureña J., Fernandez-chacon R., Benot A. R., De Toledo A. and López-Barneo J. (1994) Hypoxia induces voltage-dependent $Ca^{2+}$ entry and quantal dopamine secretion in carotid body glomus cells. *Proc. Natl. Acad. Sci. USA* **91**, 10308-10211.

Weight F.F. and Padjen A. (1973) Acetylcholine and slow synaptic inhibition in frog sympathetic ganglion cells. *Brain Res* **55,** 225-228

Xu J., Tse F. W. and Tse A. (2003) ATP triggers intracellular $Ca^{2+}$ release in type II cells of the rat carotid body. *J. Physiol.* **549**, 739-747.

Zhang M., Zhong H., Vollmer C. and Nurse C. A. (2000) Co-release of ATP and ACh mediates hypoxic signaling at rat carotid body chemoreceptors. *J. Physiol.* **525,** 143-158.

# Chapter 4

# Adenosine Stimulates Depolarization and Rise in $[Ca^{2+}]_i$ in Type I Cells of Rat Carotid Bodies

## 4.1 Introduction

Following its release from type I cells, ATP may be metabolized to adenosine in the extracellular space by ecto-nucleotidases (Dunwiddie and Masino 2001). Hypoxia is also known to elevate the extracellular level of adenosine in most tissues (Dunwiddie and Masino 2001). A recent study suggests that carotid bodies may be particularly sensitive to the hypoxia-mediated adenosine release (Conde and Monteiro 2004). A moderate hypoxia challenge to rat carotid body increased adenosine release by ~40% but failed to evoke any adenosine release in superior cervical ganglia and carotid arteries (Conde and Monteiro 2004). About 40% of the increase in adenosine level in carotid body during hypoxia arises from the catabolism of ATP released from type I cells (Conde and Monteiro 2004). In addition, hypoxia also stimulates adenosine efflux from carotid cells and arteries via the adenosine equilibrative transporters (Conde and Monteiro 2004). Thus, during hypoxia, the local concentration of adenosine near type I cells is indeed elevated.

It has been well documented that exogenous administration of adenosine to carotid body increases CSN discharge in cats (McQueen and Ribeiro 1981; McQueen and Ribeiro 1983; Runold et al. 1990) and rats (Monteiro and Ribeiro 1987; Vandier et al. 1999). This action has been suggested to involve an excitatory action of adenosine on the $A_{2A}$ receptors of type I cells (McQueen and Ribeiro 1986; Monteiro and Ribeiro 1987; Vandier et al. 1999). Consistent with this, $A_{2A}$ receptors have been detected on type I cells of rat carotid body (Gauda 2000; Kobayashi et al. 2000) whereas $A_1$ receptors are found to be expressed predominantly in the postsynaptic

sites of the petrosal ganglia (Gauda 2000). However, inhibitory instead of excitatory action of adenosine on type I cells has been reported. Adenosine has been shown to inhibit VGCC in rat (via $A_{2A}$ receptors; (Kobayashi et al. 2000)) and rabbit (via $A_1$ receptors; (Rocher et al. 1999)) type 1 cells. Adenosine has also been shown to inhibit a 4-AP sensitive $K^+$ current in rat type I cells, but the membrane potential of type I cells was not affected by adenosine (Vandier et al. 1999). This issue is further complicated by the observation that in cat carotid body, adenosine increased the release of ACh but decreased the hypoxia-mediated release of DA (Fitzgerald et al. 2004). Thus, the mechanism underlying the excitatory action of adenosine on the carotid body remains elusive. In the current study, we found that adenosine, acting via $A_{2A}$ receptors coupled to adenylate cyclase and PKA pathway, reduced the background TASK-like $K^+$ current to trigger depolarization and $[Ca^{2+}]_i$ rise in rat carotid type I cells. This action of adenosine on type I cells may underlie the excitatory effect of adenosine on CSN discharge.

## 4.2 Results

### *4.2.1 Adenosine triggered $[Ca^{2+}]_i$ elevation in type I cells via activation of $A_{2A}$ receptors*

Using the $Ca^{2+}$ imaging technique, we examined the action of adenosine on $[Ca^{2+}]_i$ of type I cells isolated from adult rat carotid bodies. The acutely dissociated cell preparation of rat carotid bodies comprised type I, type II and occasionally white blood cells. All three cell types are ovoid. However, only type I cells contain

catecholamines (Xu et al. 2003) and have $Ca^{2+}$ response to hypoxia or hypercapnia challenge (Buckler and Vaughan-Jones 1994a; Buckler and Vaughan-Jones 1994b; Xu et al. 2005). Therefore, in the current study, we identified individual type I cells based on their $Ca^{2+}$ response to hypoxia or hypercapnia challenge. As shown in our previous study (Xu et al. 2005), such a hypoxia challenge could repetitively elicit $[Ca^{2+}]_i$ rise in type I cells. Figure 4-1A shows that application of adenosine (100 μM) to a hypoxia-sensitive type I cell also triggered a rise in $[Ca^{2+}]_i$. Note that in the example shown in Figure 4-1A, the peak amplitude of the adenosine-mediated $[Ca^{2+}]_i$ rise was slightly smaller than the hypoxia challenge but the duration of the $Ca^{2+}$ signal was longer than those triggered by hypoxia. As shown later (Figure 4-3), the longer duration of the adenosine-mediated $Ca^{2+}$ signal was due to the activation of the adenylate cyclase pathway. The adenosine-mediated $[Ca^{2+}]_i$ rise could be observed in 23 out of the 29 cells that also exhibited a $[Ca^{2+}]_i$ rise when challenged with hypoxia. In these 23 cells, the mean amplitude of the peak $[Ca^{2+}]_i$ rise triggered by adenosine (100 μM) was 156 ± 19 nM, similar to the peak amplitude of $Ca^{2+}$ signal triggered by moderate hypoxia in the same cells (184 ± 72 nM; n = 23). As described later in the Discussion (Chapter 4.3), the physiological concentration of adenosine in carotid body is at the micromolar range. Therefore, we examined whether the $Ca^{2+}$ response could be triggered by lower concentrations of adenosine. Figure4-1B shows that adenosine at 1 μM, but not 10 nM, could elicit $[Ca^{2+}]_i$ rise. In 15 cells that responded to 100 μM adenosine, only 3 cells responded to 10 nM adenosine, but adenosine at 1 μM could elicit $[Ca^{2+}]_i$ rise in 14 cells. In these 14 cells, the mean peak amplitude of the $[Ca^{2+}]_i$ rise triggered by 1 μM adenosine was 130 ± 19 nM, similar to that

triggered by 100 μM adenosine in the same batch of cells (134 ± 17 nM; n = 15). Thus, adenosine at 1 μM was sufficient to trigger the maximum response in type I cells. We also examined whether the effect of adenosine and hypoxia on $[Ca^{2+}]_i$ in type I cell was additive by comparing the $Ca^{2+}$ response mediated by hypoxia alone and that evoked by a combination of adenosine and hypoxia in the same cell. In 9 of the 11 cells examined, the peak amplitude of the $Ca^{2+}$ signal evoked by the combination of hypoxia and adenosine was slightly smaller than that triggered by hypoxia alone (mean decrease = 35 ± 3 nM) but larger than that triggered by adenosine alone (mean increase = 28 ± 2 nM).

Since $A_{2A}$ receptors were reported to be present on type I cells of rat carotid body (Gauda 2000; Kobayashi et al. 2000), we examined the involvement of the $A_{2A}$ receptors in the adenosine-mediated $Ca^{2+}$ signal with ZM241385, a selective antagonist of $A_{2A}$ receptors (Poucher et al. 1995). Figure 4-2A shows that applications of adenosine (100 μM) were able to trigger repetitively $[Ca^{2+}]_i$ rises in control condition but failed to evoke any $Ca^{2+}$ signal in the presence of ZM241385 (10 μM). Following the removal of ZM241385, adenosine was able to trigger a robust $Ca^{2+}$ signal in the same cell. In 34 out of 38 cells examined, the adenosine (100 μM)-mediated $Ca^{2+}$ signal was either reduced or abolished by ZM241385 (10 μM). In these 34 cells, the peak amplitude of the $[Ca^{2+}]_i$ rise elicited by adenosine alone was 153 ± 13 nM but was reduced to 45 ± 6 nM in the presence of ZM241385. Consistent with the involvement of $A_{2A}$ receptors, Figure 4-2B shows that the adenosine response could be mimicked by the selective $A_{2A}$ receptor agonist, CGS21680, but not by the $A_1$ receptor agonist, CCPA (Klotz 2000). In 13 cells examined, CGS21680 (10 nM)

evoked a $[Ca^{2+}]_i$ rise in every cell (mean increase = 162 ± 14 nM) but CCPA (10 nM) failed to evoke any response. $A_{2A}$ receptors were reported to be coupled to the adenylate cyclase pathway (Ralevic and Burnstock 1998) and $A_{2A}$ receptor activation has been shown to increase the adenosine 3',5'-cyclic monophosphate (cAMP) content in rabbit (Chen et al. 1997) and rat carotid body (Monteiro et al. 1996). Therefore, we examined whether the activation of the adenylate cyclase by forskolin could mimic the adenosine response in type I cells. Figure 4-3A shows that application of forskolin (10 μM) triggered a $[Ca^{2+}]_i$ rise which was similar to that triggered by adenosine (100 μM) in the same cell. In 15 cells which exhibited adenosine response, forskolin triggered $[Ca^{2+}]_i$ elevation in 14 cells and the mean peak $[Ca^{2+}]_i$ rise triggered by forskolin (178 ± 23 nM) was similar to that triggered by adenosine in the same cells (179 ± 21 nM). In contrast, the inactive analog of forskolin, 1,9-dideoxyforskolin (10 μM), failed to elicit any $[Ca^{2+}]_i$ rise in the adenosine responsive cells (n = 17; Figure 4-3B). Consistent with the involvement of the adenylate cyclase/PKA pathway, Figure 4-3C shows that the adenosine response was abolished by H89 (10 μM), a selective inhibitor of PKA. A similarly robust inhibition by H89 was observed in 15 out of 17 cells examined.

### *4.2.2 The adenosine response was mediated via membrane depolarization and inhibition of TASK-like $K^+$ channels*

To examine whether the adenosine-mediated $[Ca^{2+}]_i$ rise involves changes in membrane excitability, we simultaneously monitored $[Ca^{2+}]_i$ and membrane potential (perforated patch recording) in type I cells. An example of one such experiment is

shown in Figure 4-4A. In control condition, the resting membrane potential of this cell was ~-38 mV. Following the application of adenosine, the membrane potential depolarized to a plateau of ~-20 mV and there was some firing of action potentials. Note that the membrane depolarization was accompanied by $[Ca^{2+}]_i$ rise (Figure 4-4A). In 6 cells examined, the resting membrane potential before adenosine application was -40 ± 2 mV (range -36 to -44 mV at 20 - 23°C). These values of resting membrane potential are comparable to those reported previously in adult rat type I cells [-32 ± 4 mV, n= 12, at room temperature (Fieber and McCleskey 1993)] and neonatal rat type I cells [range -39 to -63 mV at 35 -37°C; (Buckler and Vaughan-Jones 1994b)]. In the presence of adenosine, the membrane potential depolarized by 16 ± 2 mV (to a plateau) and the mean increase in peak $[Ca^{2+}]_i$ in these cells was 311 ± 70 nM. Application of the $A_{2A}$ receptor, CGS21680 (10 nM) also caused membrane depolarization in type I cells (by 12 ± 3 mV; n = 7). Treatment with the PKA inhibitor H89 (10 μM) did not affect the membrane potential of type I cells (n = 3) but inhibited the CGS21680-mediated depolarization (n = 4). Consistent with the notion that the $A_{2A}$ receptor-mediated membrane depolarization in turn leads to activation of voltage-gated $Ca^{2+}$ entry, Fig 4B shows that the CGS21680-triggered $[Ca^{2+}]_i$ rise could be reversibly inhibited by the VGCC blocker, $Ni^{2+}$ (3 mM; n = 6). Note that we did not employ $Cd^{2+}$, another common VGCC blocker in this experiment, because $Cd^{2+}$ (but not $Ni^{2+}$) was reported to enter cells and cause quenching of the fluorescence of the $Ca^{2+}$ indicator (Shibuya and Douglas 1992). In separate experiments, we also confirmed that $Ni^{2+}$ did not affect the membrane potential of type I cells (n = 5).

Since a previous study (Vandier et al. 1999) has shown that adenosine inhibited a 4-AP sensitive $K^+$ current in rat type I cells, we examined whether the inhibition of 4-AP sensitive $K^+$ current was involved in the adenosine-mediated $[Ca^{2+}]_i$ rise. Figure 4-5A shows that the application of 4-AP (5 mM) to type I cell did not trigger any $[Ca^{2+}]_i$ rise, and adenosine (100 μM) was still able to trigger a rise in $[Ca^{2+}]_i$ in the continued presence of 4-AP. In 31 cells examined, 4-AP (5 mM) could not trigger a $[Ca^{2+}]_i$ rise in any of the cells but adenosine (100 μM) or CGS21680 (20 nM) was still able to trigger a $[Ca^{2+}]_i$ rise in the presence of 4-AP. In these cells, the mean $[Ca^{2+}]_i$ rise evoked by adenosine or CGS21680 in the presence of 4-AP was 187 ± 35 nM. Consistent with the previous studies (Buckler 1997; Vandier et al. 1999), we also found that application of 4-AP (5 mM) did not affect the membrane potential of type I cells (n = 5). These results suggest that the 4-AP sensitive $K^+$ current did not contribute significantly to the adenosine-mediated $Ca^{2+}$ signal.

Hypoxia has been shown to inhibit the activities of BK channels in type I cells (Riesco-Fagundo et al. 2001; Williams et al. 2004; Wyatt and Peers 1995). To investigate the involvement of BK channels in the adenosine response, we examined whether the adenosine response could be affected by TEA, which is a blocker of a number of voltage-dependent $K^+$ channels, including BK channels (Pardal et al. 2000). In neonatal rat type I cells, TEA (10 mM) was reported to have no effect on the membrane potential or $[Ca^{2+}]_i$. In 4 out of 7 adult rat type I cells examined, we found that TEA (10 mM) caused membrane depolarization (11 ± 2 mV; n = 4). When the $Ca^{2+}$ response of the adult rat type I cells was examined (n = 35), TEA (10 mM) triggered $[Ca^{2+}]_i$ elevations (e.g. Figure 4-5B) in ~60% of the cells. In ~75% of the

cells that responded to TEA, application of adenosine in the continued presence of TEA evoked a larger and more sustained $[Ca^{2+}]_i$ rise (Figure 4-5B). The time integral (for 200 s) of the $Ca^{2+}$ signal (see Figure 4-5B for example) triggered in the presence of a combination of TEA and adenosine (23 ± 3 μM s; n = 14) was almost 2-fold larger than that triggered by TEA alone (12 ± 1 μM s; n = 14). For type I cells which did not exhibit any rise in $[Ca^{2+}]_i$ when challenged with TEA, application of adenosine could still trigger $[Ca^{2+}]_i$ elevations (Figure 4-5C; n = 15). Overall, this result suggests that the adenosine response did not involve any major contribution from TEA-sensitive $K^+$ currents.

In rat type I cells, a TEA-insensitive background TASK-like $K^+$ current has been shown to be an important mechanism underlying the hypoxia-mediated membrane depolarization and $[Ca^{2+}]_i$ rise (Buckler 1997). Immunohistochemical study has revealed the presence of multiple TASK-like channels (including TASK-1, TASK-2, TASK-3) in rat type I cells (Yamamoto et al. 2002). Therefore, we examined whether anandamide, a selective TASK-1 $K^+$ channel blocker (Maingret et al. 2001), could affect the adenosine response. Anandamide at 3 μM was reported to inhibit ~90% of the TASK-1 $K^+$ channels but had no significant effect on the TASK-2 or TASK-3 channels (Maingret et al. 2001). We found that application of anandamide (5 μM) resulted in robust $[Ca^{2+}]_i$ rise in type I cells (Figure 4-6A). Note that in the continued presence of anandamide, adenosine did not cause any further increase in $[Ca^{2+}]_i$ (Figure 4-6A; n = 27). Figure 4-6B shows that the anandamide mediated $[Ca^{2+}]_i$ rise in type I cells was accompanied by membrane depolarization and firing of action potentials. Application of adenosine did not cause any further increase in

depolarization (Figure 4-6B; n = 5). Thus, the action of adenosine was blunted by anandamide. This result is consistent with the notion that reduction of the TASK-1 background $K^+$ current is the major mechanism underlying the adenosine-mediated $Ca^{2+}$ signal in type I cells.

## 4.3 Discussion

The findings here demonstrate that in the majority of rat carotid type I cells (identified by their $Ca^{2+}$ response to hypoxia or hypercapnia), adenosine triggered a rise in $[Ca^{2+}]_i$. In ~20% of the hypoxia-responding cells, adenosine failed to elicit any $[Ca^{2+}]_i$ rise. Since the adenosine-mediated $[Ca^{2+}]_i$ rise was dependent on depolarization and activation of VGCC (Figure 4-4), it is possible that the adenosine-mediated depolarization in some type I cells may be insufficient to trigger significant VGCC activation and $Ca^{2+}$ entry. We also found that the adenosine at 1 or 100 μM triggered a similar increase in $[Ca^{2+}]_i$, suggesting that a maximal response could be achieved by 1 μM adenosine. The amount of adenosine released from the carotid body was estimated to be ~100 pmol per carotid body during normoxia, and increased by ~34% during 10 min of moderate hypoxia (Conde and Monteiro 2004). Although the concentration of adenosine in the carotid body has not been measured, the level of adenosine in rat hippocampal slices during hypoxia was found to reach ~5 μM (Dale et al. 2000). Thus, it is likely that the local concentration of adenosine near type I cells during hypoxia may also reach the micromolar range. Adenosine, at concentrations of 1 to 100 μM, has been reported to increase chemoreceptor discharge

in rat carotid body as well as inhibiting a 4-AP sensitive $K^+$ current in type I cells (Vandier et al. 1999). Interestingly, the same study showed that adenosine did not affect the membrane potential of type I cells (Vandier et al. 1999). In contrast, our current findings show that the adenosine-mediated $[Ca^{2+}]_i$ rise was accompanied by depolarization and firing of action potentials (Figure 4-4A). One possible explanation for this discrepancy is that perforated patch-clamp recording was employed in our current study. Since the adenosine response involved inhibition of TASK-like $K^+$ channels (Figure 4-6) and these $K^+$ channels were reported to be regulated by cytosolic factors (Williams and Buckler 2004), it is possible that these modulations might be lost during whole-cell recording (Vandier et al. 1999). Our experiments also show that the 4-AP sensitive $K^+$ current has no significant contribution to the adenosine-triggered $Ca^{2+}$ signal as application of 4-AP did not trigger any $[Ca^{2+}]_i$ rise in type I cells and the mean peak $[Ca^{2+}]_i$ rise evoked by adenosine in the presence of 4-AP was similar to that in the control cells (Figure 4-5A).

Consistent with the presence of $A_{2A}$ receptors on type I cells of rat carotid bodies (Gauda 2000;Kobayashi et al. 2000), we found that the adenosine-triggered $[Ca^{2+}]_i$ rise in type I cells was mediated via $A_{2A}$ receptors as the response could be mimicked by the $A_{2A}$ receptor agonist, CGS21680 (Figure 4-2B), and inhibited by ZM241385, an $A_{2A}$ receptor antagonist (Figure 4-2A). $A_{2A}$ receptors are known to stimulate PKA activity via $G_s$ protein and adenylate cyclase (Ralevic and Burnstock 1998). Inhibition of PKA by H89 abolished the adenosine-mediated $Ca^{2+}$ signal (Fig. 3C). H89 has been reported to have PKA-independent actions such as inhibition of

sarcoplasmic reticulum $Ca^{2+}$-ATPase and L-type $Ca^{2+}$ current (Hussain et al. 1999), inhibition of Kv1.3 channels (Choi et al. 2001) and translocation of epithelial $Na^{+}$ channels (Marunaka and Niisato 2003). Nevertheless, our finding that forskolin, an activator of adenylate cyclase, but not the inactive analog of forskolin, could mimic the adenosine-mediated $[Ca^{2+}]_i$ rise in type I cells (Figure 4-3A & B) further implicated the involvement of PKA in the adenosine response. Overall, our results suggest that stimulation of $A_{2A}$ receptor in rat type I cell activates PKA, which in turn inhibits the TASK-like $K^{+}$ channels and leads to depolarization. Consistent with an inhibitory effect of PKA on TASK-like $K^{+}$ channels, activation of PKA by forskolin and 3-isobtyl-1-methylxanthine (IBMX) has been shown to reduce TASK-like $K^{+}$ current by ~40% (Leonoudakis et al. 1998; Lopes et al. 2000). Inhibition of PKA via $GABA_B$ receptor activation in rat type I cells has been shown to activate TASK-like $K^{+}$ channels and cause hyperpolarization (Fearon et al. 2003).

Activation of $A_{2A}$ receptors has been reported to decrease the voltage-gated $Ca^{2+}$ current in rat type I cells (Kobayashi et al. 2000) and PC-12 cells (Kobayashi et al. 1998). Note that our observation that adenosine triggered $[Ca^{2+}]_i$ rise in type I cells does not necessarily contradict an inhibitory action of adenosine on voltage-gated $Ca^{2+}$ current. Application of adenosine typically depolarized the membrane potential of type I cells by ~15 mV (e.g. from ~-38 to -23 mV in Figure 4-4A). At -20 mV, the inhibition of voltage-gated $Ca^{2+}$ current by adenosine was very small (Kobayashi et al. 2000). Thus, adenosine could still trigger a robust $[Ca^{2+}]_i$ rise at this potential. Our result also suggests that adenosine does not cause additional increase in the peak amplitude of the hypoxia-induced $Ca^{2+}$ signal. At least two factors may

contribute to this observation. First, the TASK-like channel is a common target for both hypoxia and adenosine. If hypoxia already inhibited most of the TASK-like $K^+$ channels, the effects of adenosine and hypoxia would not be additive. Second, with increasing depolarization during the combined challenge, the inhibitory action of adenosine on voltage-gated $Ca^{2+}$ current would become more prominent and thus prevent a further increase in the amplitude of the $Ca^{2+}$ signal.

Our result contradicts a previous study by Kobayashi et al. (2000) which reported that adenosine did not evoke any $[Ca^{2+}]_i$ rise in rat type I cells. Two experimental conditions may contribute to this discrepancy. First, there may be a difference in the sensitivity of type I cells. In the study of Kobayashi et al. (2000), cells cultured overnight were employed and severe hypoxia (evoked by the $O_2$ scavenger, sodium dithionate) was required to evoke $Ca^{2+}$ signal in type I cells. We found that a large percentage of type I cells became unresponsive to hypoxia after 24 hrs of culture. Therefore, in our study, only cells cultured for 2-6 hrs were employed. Under this condition, even moderate hypoxia (~40 mm Hg) can evoke $[Ca^{2+}]_i$ rise in type I cells. Second, $Ca^{2+}$ indicators such as fura-2 act as $Ca^{2+}$ buffer. Thus, excessive loading of fura-2 will increase the cytosolic $Ca^{2+}$ buffering capacity and can lead to a decrease in the amplitude of the $Ca^{2+}$ signal. In our study, we loaded the cells with 2.5 μM fura-2 AM at 37°C for 10 min. In contrast, in the study by Kobayashi et al. (2000), cells were loaded with 5 μM fura-2 AM at 37° C for 40 min. Since the amplitude of the adenosine-mediated $Ca^{2+}$ signal in their study is small (~150 nM), it is possible that a reduction in the sensitivity of type I cells, in

conjunction with an increase in cytosolic $Ca^{2+}$ buffer, may mask the $[Ca^{2+}]_i$ rise triggered by adenosine in the latter study.

It has been suggested that adenosine may contribute to the carotid body chemosensitivity to modest hypoxia (Conde and Monteiro 2004). In this study, we found that adenosine triggered depolarization and $[Ca^{2+}]_i$ rise in type I cells and the $Ca^{2+}$ response was comparable to that triggered by moderate hypoxia (~40 mm Hg). This raises the possibility that, near the threshold level of tissue $P_{O_2}$ required for activation of CSN discharge, the rise in adenosine level may play a significant role in the stimulation of type I cells and thus in turn increase the CSN discharge. We have shown previously that ATP (released from type I cells) acts as a negative regulator to inhibit the hypoxia-mediated $Ca^{2+}$ signal in type I cells by causing membrane hyperpolarization (Xu et al. 2005). As shown in Figure 4-7, the catabolism of extracellular ATP into adenosine, in conjunction with the hypoxia-mediated adenosine efflux, may activate the $A_{2A}$ receptors and trigger membrane depolarization and $[Ca^{2+}]_i$ rise, thus opposing the inhibitory action of ATP on type I cells. In view of this, adenosine may be important in helping type I cells to recover from the negative feedback action of ATP.

## 4.4 Acknowledgements

This work was done in collaboration with Dr. Jianhua Xu. I performed the experiments including the inhibition of adenosine response by H89, the role of 4-AP- and TEA-sensitive current in the adenosine response, the effect of adenosine on

membrane depolarization and $[Ca^{2+}]_i$ rise, and all the experiments involving TASK-like channels. The findings in this chapter have been published in Am J Physiol Cell Physiol 290:C1592-C1598,2006.

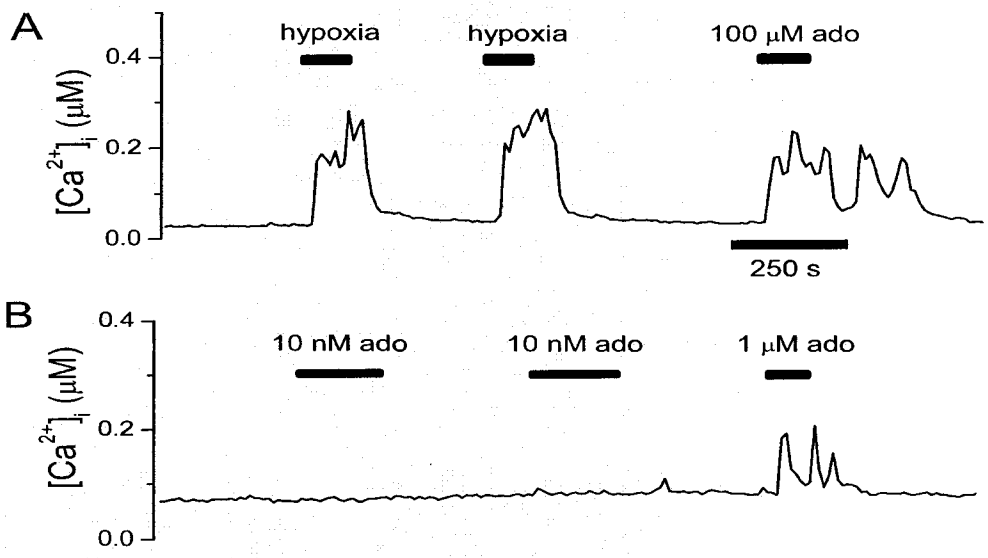


**Figure 4-1** Adenosine induced $[Ca^{2+}]_i$ rise in hypoxia-sensitive type I carotid cells in a concentration-dependent manner. *A*, adenosine (100 μM) triggered $[Ca^{2+}]_i$ rise in a type I cell (identified by its hypoxia-mediated $[Ca^{2+}]_i$ rise). *B*, $[Ca^{2+}]_i$ rise could be triggered by 1 μM but not by 10 nM adenosine. $[Ca^{2+}]_i$ was measured with fura-2 $Ca^{2+}$ imaging.

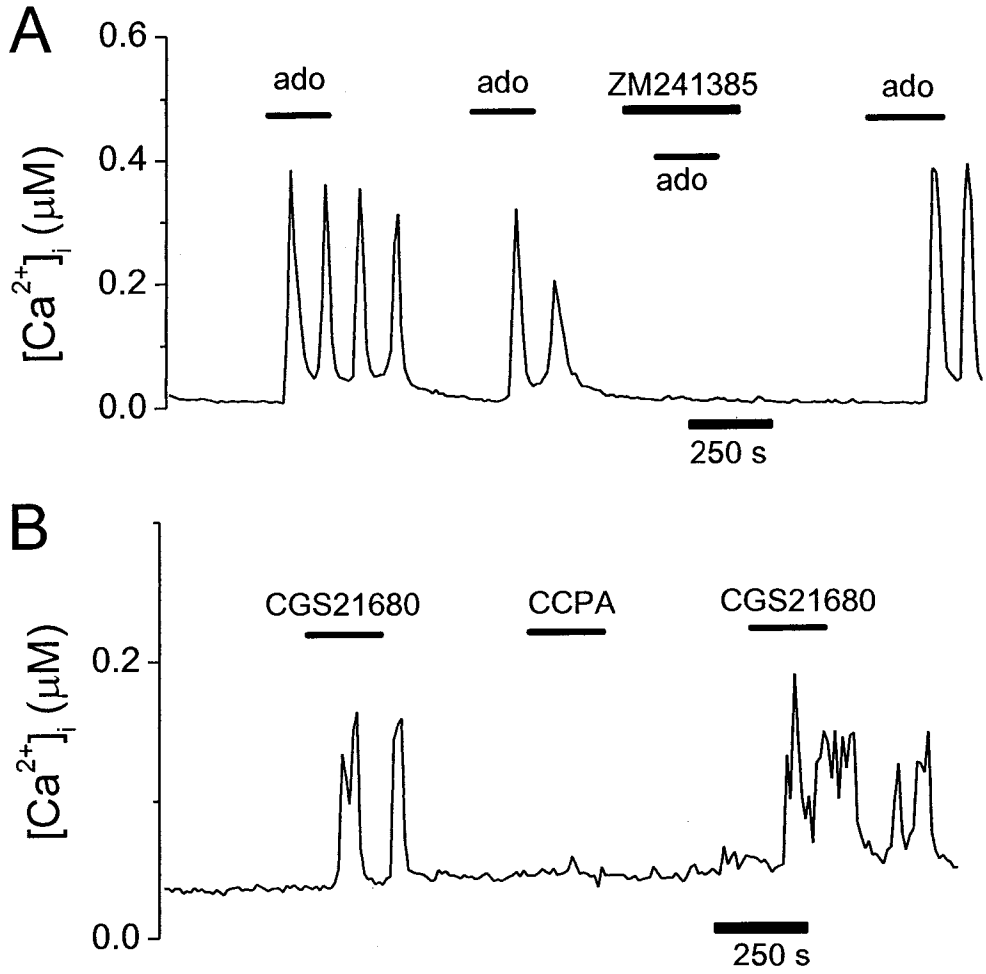


**Figure 4-2** The action of adenosine on $[Ca^{2+}]_i$ was mediated via $A_{2A}$ receptors. *A*, the $A_{2A}$ receptor antagonist ZM241385 (10 μM) reversibly inhibited the adenosine (100 μM) mediated $[Ca^{2+}]_i$ rise. *B*, the $A_{2A}$ receptor agonist, CGS21680 (10 nM), but not the $A_1$ receptor agonist, CCPA (10 nM), elicited $[Ca^{2+}]_i$ rise in type I cells. $[Ca^{2+}]_i$ was measured with fura-2 $Ca^{2+}$ imaging.

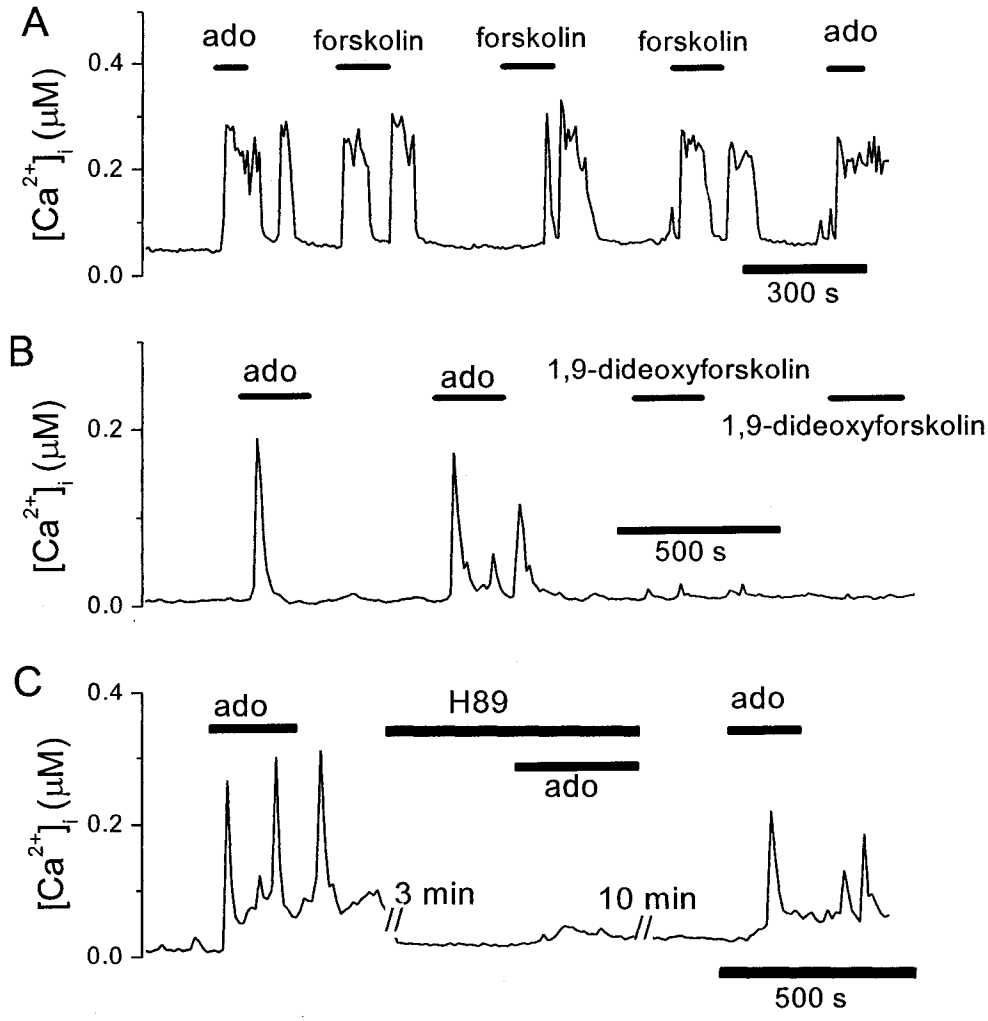


**Figure 4-3** The adenosine response was mediated via the adenylate cyclase/PKA pathway. *A*, the adenosine mediated $[Ca^{2+}]_i$ rise could be mimicked by forskolin (10 μM), an activator of the adenylate cyclase. *B*, the inactive analog of forskolin, 1,9-dideoxy forskolin (10 μM) failed to evoke $[Ca^{2+}]_i$ rise in type I cells. Note that adenosine (100 μM) could evoke $[Ca^{2+}]_i$ rise in the same cell. *C*, incubation with the PKA inhibitor, H89 (10 μM) inhibited the response of adenosine (100 μM). Following a long wash (~15 min), the adenosine response could be partially recovered following removal of H89. $[Ca^{2+}]_i$ was measured with fura-2 $Ca^{2+}$ imaging.

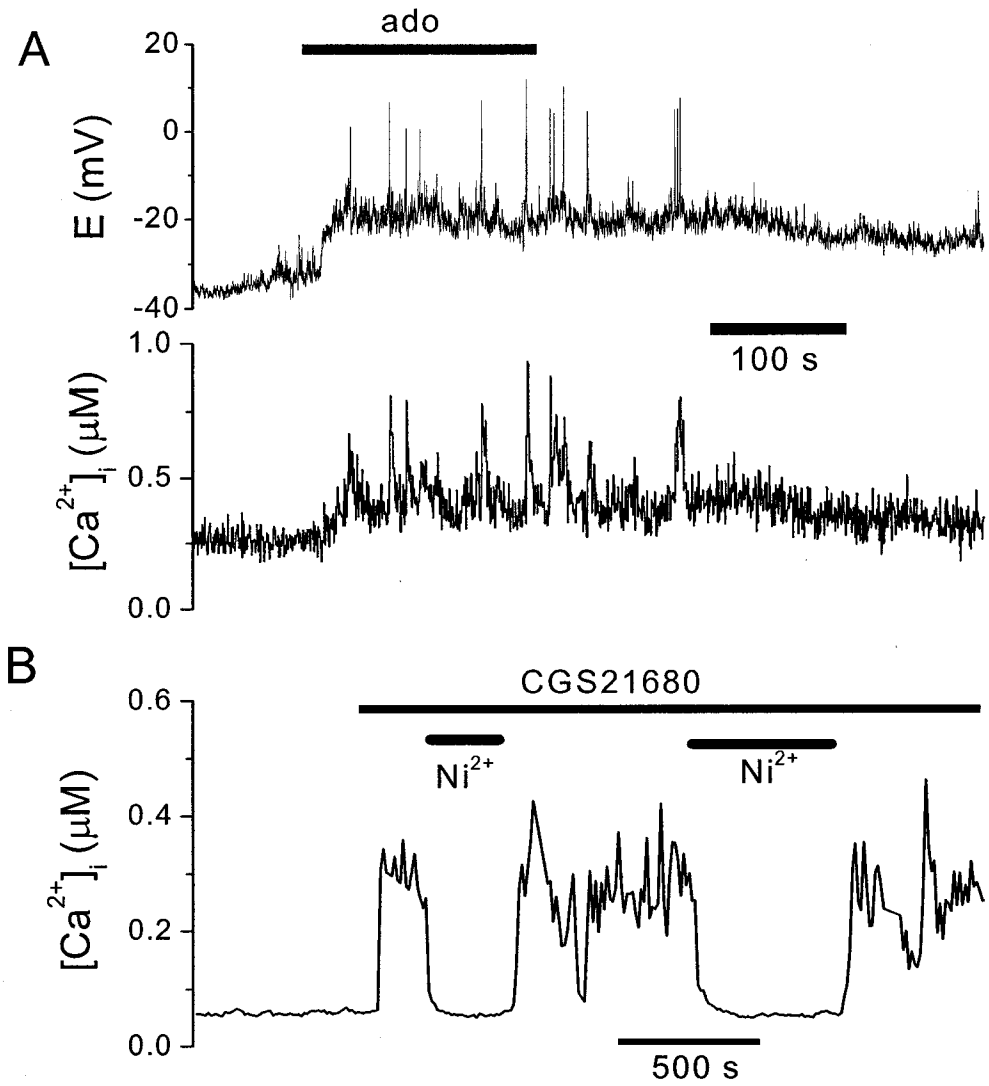


**Figure 4-4** The adenosine-mediated $[Ca^{2+}]_i$ rise was accompanied by membrane depolarization and activation of VGCC. *A*, simultaneous measurement of membrane potential (perforated patch recording) with $[Ca^{2+}]_i$ (indo-1 fluorometry). Adenosine (100 μM) caused depolarization and firing of action potentials. Note that the bursts of actions potentials were accompanied by transient increases in $[Ca^{2+}]_i$. *B*, the $A_{2A}$ receptor-mediated $[Ca^{2+}]_i$ rise was reversibly inhibited by the VGCC blocker, $Ni^{2+}$ (3mM). $[Ca^{2+}]_i$ was measured with fura-2 $Ca^{2+}$ imaging.

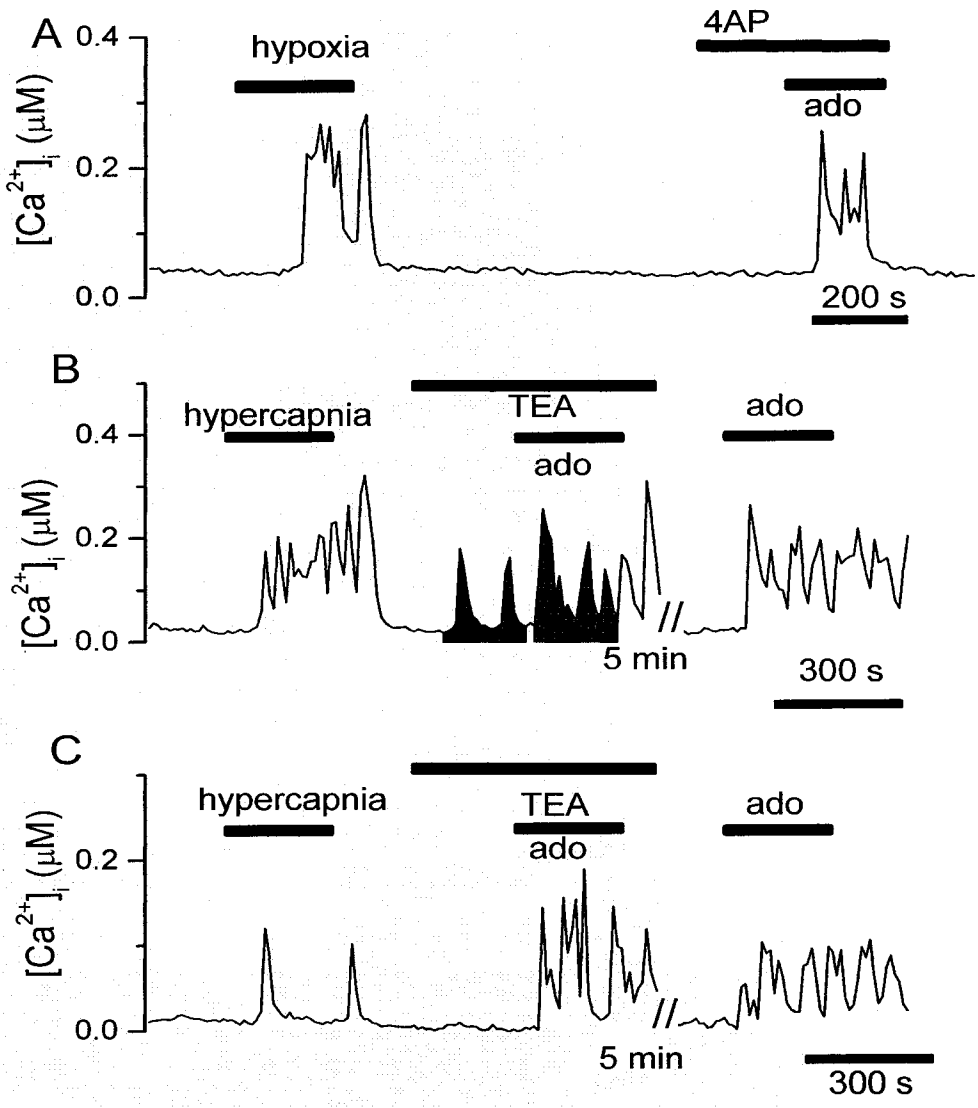


**Figure 4-5** The adenosine response could not be attenuated by 4-AP or TEA. *A*, in the presence of 4-AP (5 mM), adenosine (100 μM) could still trigger $[Ca^{2+}]_i$ rise, indicating that the 4-AP-sensitive $K^+$ current had little contribution to the adenosine mediated $[Ca^{2+}]_i$ rise. *B*, example of a type I cell in which TEA (10 mM) triggered $[Ca^{2+}]_i$ rise. The two shaded areas were time integrals (for 200 s) of the $Ca^{2+}$ signal in TEA alone and in combination of TEA and adenosine respectively. *C*, example of a type I cell in which TEA did not affect the resting $[Ca^{2+}]_i$. Note that adenosine could still trigger $[Ca^{2+}]_i$ rise. $[Ca^{2+}]_i$ was measured with fura-2 $Ca^{2+}$ imaging.

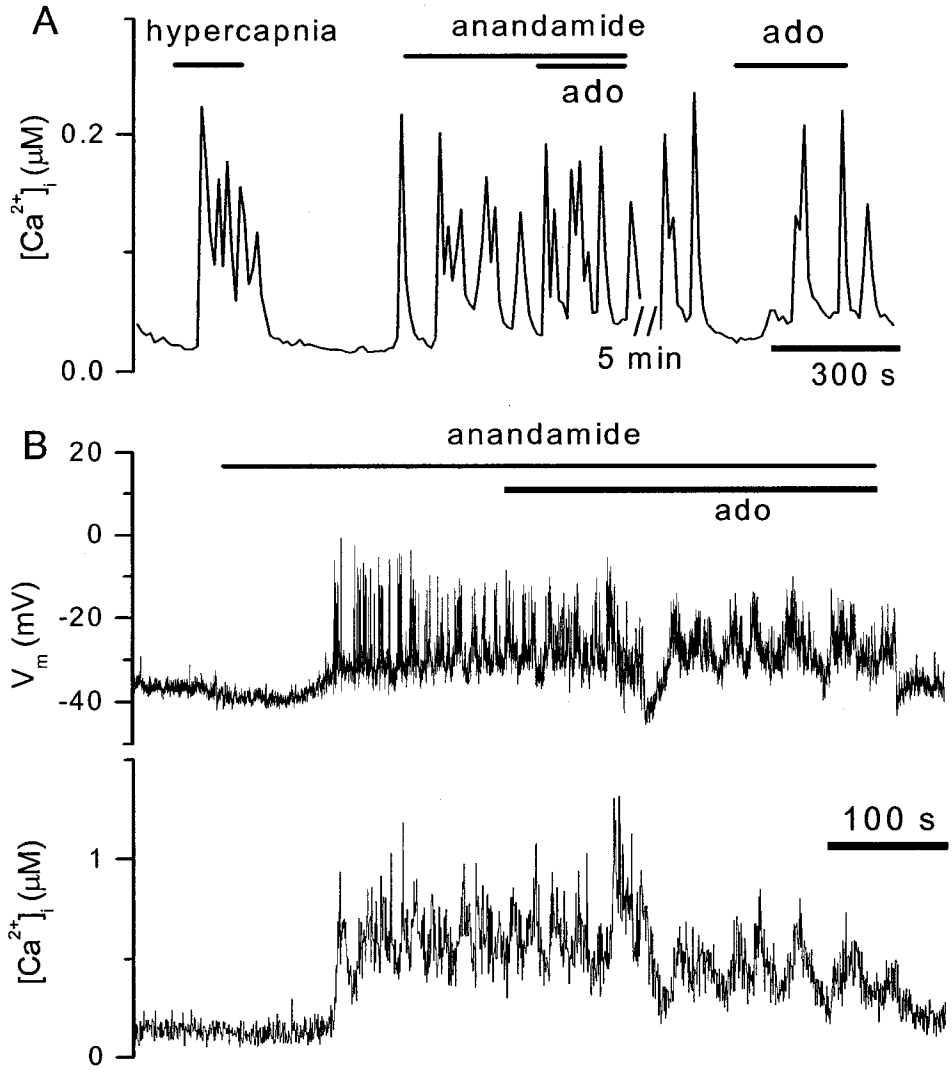


**Figure 4-6** The adenosine response involved inhibition of the TASK-like background $K^+$ channels. *A*, anandamide (5 μM), an inhibitor of TASK-like $K^+$ channels triggered $[Ca^{2+}]_i$ rise. In the presence of anandamide, adenosine did not cause any further increase in $[Ca^{2+}]_i$. $[Ca^{2+}]_i$ was measured with fura-2 $Ca^{2+}$ imaging. *B*, simultaneous measurement of $[Ca^{2+}]_i$ (indo-1 fluorometry) and membrane potential showed that the anandamide-mediated $[Ca^{2+}]_i$ rise was accompanied by depolarization and firing of action potentials. In the presence of anandamide, adenosine did not cause any further depolarization.

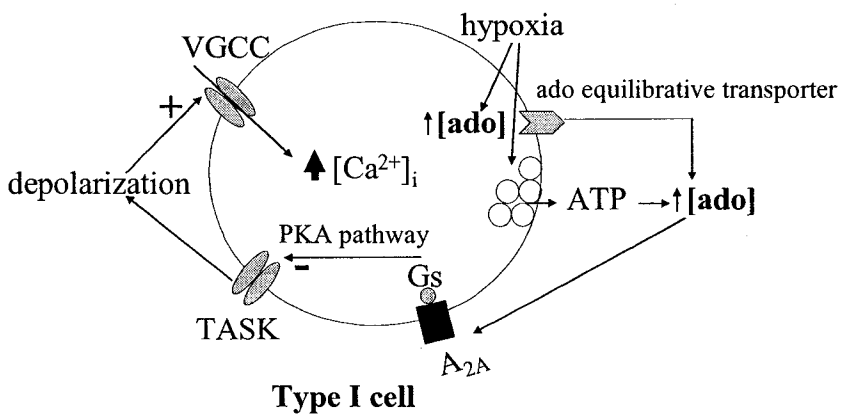


**Figure 4-7** Summary of the actions of adenosine on rat type I cells. During hypoxia, the adenosine level near type I cells increases due to the catabolism of ATP into adenosine and to adenosine efflux via adenosine equilibrative transporter. Adenosine acts on $A_{2A}$ receptors coupled to cAMP-dependent PKA pathway and inhibits TASK-like $K^+$ current. This leads to membrane depolarization and activation of VGCC. $Ca^{2+}$ entry via VGCC elevates $[Ca^{2+}]_i$ in type I cells.

## References


Buckler K. J. (1997) A novel oxygen-sensitive potassium current in rat carotid body type I cells. *J Physiol* **498 ( Pt 3),** 649-662.

Buckler K. J. and Vaughan-Jones R. D. (1994a) Effects of hypercapnia on membrane potential and intracellular calcium in rat carotid body type I cells. *J Physiol* **478 ( Pt 1),** 157-171.

Buckler K. J. and Vaughan-Jones R. D. (1994b) Effects of hypoxia on membrane potential and intracellular calcium in rat neonatal carotid body type I cells. *J Physiol* **476,** 423-428.

Chen J., Dinger B., and Fidone S. J. (1997) cAMP production in rabbit carotid body: role of adenosine. *J Appl Physiol* **82,** 1771-1775.

Choi J., Choi B. H., Hahn S. J., Yoon S. H., Min D. S., Jo Y., and Kim M. (2001) Inhibition of Kv1.3 channels by H-89 (N--[2-(p-bromocinnamylamino)ethyl]-5-isoquinolinesulfonamide) independent of protein kinase A. *Biochem Pharmacol* **61,** 1029-1032.

Conde S. V. and Monteiro E. C. (2004) Hypoxia induces adenosine release from the rat carotid body. *J Neurochem* **89,** 1148-1156.

Dale N., Pearson T., and Frenguelli B. G. (2000) Direct measurement of adenosine release during hypoxia in the CA1 region of the rat hippocampal slice. *J Physiol* **526 Pt 1,** 143-155.

Dunwiddie T. V. and Masino S. A. (2001) The role and regulation of adenosine in the central nervous system. *Annu Rev Neurosci* **24,** 31-55.

Fearon I. M., Zhang M., Vollmer C., and Nurse C. A. (2003) GABA mediates autoreceptor feedback inhibition in the rat carotid body via presynaptic GABAB receptors and TASK-1. *J Physiol* **553,** 83-94.

Fieber L. A. and McCleskey E. W. (1993) L-type calcium channels in type I cells of the rat carotid body. *J Neurophysiol* **70,** 1378-1384.

Fitzgerald R. S., Shirahata M., Wang H. Y., Balbir A., and Chang I. (2004) The impact of adenosine on the release of acetylcholine, dopamine, and norepinephrine from the cat carotid body. *Neurosci Lett* **367,** 304-308.

Gauda E. B. (2000) Expression and localization of A2a and A1-adenosine receptor genes in the rat carotid body and petrosal ganglia. A2a and A1-adenosine receptor mRNAs in the rat carotid body. *Adv Exp Med Biol* **475,** 549-558.

Hussain M., Drago G. A., Bhogal M., Colyer J., and Orchard C. H. (1999) Effects of the protein kinase A inhibitor H-89 on $Ca^{2+}$ regulation in isolated ferret ventricular myocytes. *Pflugers Arch* **437,** 529-537.

Klotz K. N. (2000) Adenosine receptors and their ligands. *Naunyn Schmiedebergs Arch Pharmacol* **362,** 382-391.

Kobayashi S., Conforti L., and Millhorn D. E. (2000) Gene expression and function of adenosine A(2A) receptor in the rat carotid body. *Am J Physiol Lung Cell Mol Physiol* **279,** L273-L282.

Kobayashi S., Conforti L., Pun R. Y., and Millhorn D. E. (1998) Adenosine modulates hypoxia-induced responses in rat PC12 cells via the A2A receptor. *J Physiol* **508 ( Pt 1),** 95-107.

Leonoudakis D., Gray A. T., Winegar B. D., Kindler C. H., Harada M., Taylor D. M., Chavez R. A., Forsayeth J. R., and Yost C. S. (1998) An open rectifier potassium channel with two pore domains in tandem cloned from rat cerebellum. *J Neurosci* **18,** 868-877.

Lopes C. M., Gallagher P. G., Buck M. E., Butler M. H., and Goldstein S. A. (2000) Proton block and voltage gating are potassium-dependent in the cardiac leak channel Kcnk3. *J Biol Chem* **275,** 16969-16978.

Maingret F., Patel A. J., Lazdunski M., and Honore E. (2001) The endocannabinoid anandamide is a direct and selective blocker of the background K(+) channel TASK-1. *EMBO J* **20,** 47-54.

Marunaka Y. and Niisato N. (2003) H89, an inhibitor of protein kinase A (PKA), stimulates $Na^+$ transport by translocating an epithelial $Na^+$ channel (ENaC) in fetal rat alveolar type II epithelium. *Biochem Pharmacol* **66,** 1083-1089.

McQueen D. S. and Ribeiro J. A. (1981) Effect of adenosine on carotid chemoreceptor activity in the cat. *Br J Pharmacol* **74,** 129-136.

McQueen D. S. and Ribeiro J. A. (1983) On the specificity and type of receptor involved in carotid body chemoreceptor activation by adenosine in the cat. *Br J Pharmacol* **80,** 347-354.

McQueen D. S. and Ribeiro J. A. (1986) Pharmacological characterization of the receptor involved in chemoexcitation induced by adenosine. *Br J Pharmacol* **88,** 615-620.

Monteiro E. C. and Ribeiro J. A. (1987) Ventilatory effects of adenosine mediated by carotid body chemoreceptors in the rat. *Naunyn Schmiedebergs Arch Pharmacol* **335,** 143-148.

Monteiro E. C., Vera-Cruz P., Monteiro T. C., and Silva e Sousa MA (1996) Adenosine increases the cAMP content of the rat carotid body in vitro. *Adv Exp Med Biol* **410,** 299-303.

Pardal R., Ludewig U., Garcia-Hirschfeld J., and Lopez-Barneo J. (2000) Secretory responses of intact glomus cells in thin slices of rat carotid body to hypoxia and tetraethylammonium. *Proc Natl Acad Sci U S A* **97,** 2361-2366.

Poucher S. M., Keddie J. R., Singh P., Stoggall S. M., Caulkett P. W., Jones G., and Coll M. G. (1995) The in vitro pharmacology of ZM 241385, a potent, non-xanthine A2a selective adenosine receptor antagonist. *Br J Pharmacol* **115,** 1096-1102.

Ralevic V. and Burnstock G. (1998) Receptors for purines and pyrimidines. *Pharmacol Rev* **50,** 413-492.

Riesco-Fagundo A. M., Perez-Garcia M. T., Gonzalez C., and Lopez-Lopez J. R. (2001) O(2) modulates large-conductance Ca(2+)-dependent K(+) channels of rat chemoreceptor cells by a membrane-restricted and CO-sensitive mechanism. *Circ Res* **89,** 430-436.

Rocher A., Gonzalez C., and Almaraz L. (1999) Adenosine inhibits L-type $Ca^{2+}$ current and catecholamine release in the rabbit carotid body chemoreceptor cells. *Eur J Neurosci* **11,** 673-681.

Runold M., Cherniack N. S., and Prabhakar N. R. (1990) Effect of adenosine on isolated and superfused cat carotid body activity. *Neurosci Lett* **113,** 111-114.

Shibuya I. and Douglas W. W. (1992) Calcium channels in rat melanotrophs are permeable to manganese, cobalt, cadmium, and lanthanum, but not to nickel: evidence provided by fluorescence changes in fura-2-loaded cells. *Endocrinology* **131,** 1936-1941.

Vandier C., Conway A. F., Landauer R. C., and Kumar P. (1999) Presynaptic action of adenosine on a 4-aminopyridine-sensitive current in the rat carotid body. *J Physiol* **515 ( Pt 2),** 419-429.

Williams B. A. and Buckler K. J. (2004) Biophysical properties and metabolic regulation of a TASK-like potassium channel in rat carotid body type 1 cells. *Am J Physiol Lung Cell Mol Physiol* **286,** L221-L230.

Williams S. E., Wootton P., Mason H. S., Bould J., Iles D. E., Riccardi D., Peers C., and Kemp P. J. (2004) Hemoxygenase-2 is an oxygen sensor for a calcium-sensitive potassium channel. *Science* **306,** 2093-2097.

Wyatt C. N. and Peers C. (1995) $Ca(^{2+})$-activated $K^+$ channels in isolated type I cells of the neonatal rat carotid body. *J Physiol* **483 ( Pt 3),** 559-565.

# Chapter 5

## PACAP Stimulates $O_2$-Sensing Type I Cells of Rat Carotid Bodies via inhibition of a Background TASK-like $K^+$ Current

## 5.1 Introduction

PACAP belongs to the vasoactive intestinal peptide (VIP)-glucagon-growth hormone releasing factor-secretin family. PACAP is widely distributed in the brain and peripheral organs and has been shown to have important roles in many physiological functions, including smooth muscle regulation, hormonal secretion and regulation of circadian rhythm (Sherwood et al. 2000; Vaudry et al. 2000). PACAP is also implicated in the regulation of breathing. PACAP is a potent bronchodilator (Linden et al. 1999) and stimulator of airway mucus secretion (Liu et al. 1999). PACAP receptors are present in many levels of the respiratory tract, including the lungs and bronchioles (Vaudry et al. 2000), as well as areas in the brain that are involved in the regulation of respiratory rhythm and respiratory chemosensitivity (Hannibal 2002). Recent studies have shown that PACAP-deficient mice exhibited reduced respiratory response to hypoxia and hypercapnia (Cummings et al. 2004) and were more prone to sudden neonatal death (Cummings et al. 2004; Gray et al. 2001; Gray et al. 2002). Carotid bodies are the major peripheral sensory organs for monitoring the arterial level of $O_2$ and $CO_2$. The reduction of respiratory chemoresponse in the PACAP-deficient mice raised the possibility that PACAP may contribute to the chemosensory transduction in the carotid bodies. Consistent with a role of PACAP in the regulation of carotid body function, intravenous injection of PACAP in dogs caused an increase in ventilation and the transection of the CSN abolished the action of PACAP (Runcie et al. 1995).

The carotid body comprises clusters of ovoid type I cells which are surrounded by glial-like type II cells (Gonzalez et al. 1994; Gronblad 1983). The type II cells resemble glial cells of the peripheral nervous system (Kameda 1996) and were traditionally viewed as passive supportive structures. However, studies in our laboratory have shown that ATP can evoke intracellular $Ca^{2+}$ release from type II cells (Xu et al. 2003). PACAP has also been reported to mobilize intracellular $Ca^{2+}$ stores in glial cells (Tatsuno and Arimura 1994). Therefore, it is possible that PACAP may affect type I and/or type II cells of the carotid body. In the current study, we examined the action of PACAP on type I and type II cells isolated from rat carotid bodies. We found that PACAP did not evoke any $Ca^{2+}$ signal in the type II cells. In contrast, for type I cells, PACAP, acting via the $PAC_1$ receptor-coupled adenylate cyclase and PKA pathway, reduced the background TASK-like $K^+$ current, triggering depolarization and $[Ca^{2+}]_i$ rise. During moderate hypoxia, the effect of PACAP and hypoxia on $[Ca^{2+}]_i$ in type I cell was additive. Thus, PACAP may have an important role in augmenting the response of carotid type I cells to moderate hypoxia. This mechanism may partly account for the reduction in chemoresponse to hypoxia and sudden neonatal death in the PACAP-deficient mice.

## 5.2 Results

### *5.2.1 PACAP triggered $[Ca^{2+}]_i$ elevation in type I cells*

PACAP is present in two biologically active forms: PACAP-38 and PACAP-27. The two forms of PACAP have similar affinity to the two types of PACAP

receptors (Vaudry et al. 2000). PACAP-38 was employed in the current study. Using the fura-2 $Ca^{2+}$ imaging technique, we examined the action of PACAP on $[Ca^{2+}]_i$ in single cells isolated from adult rat carotid bodies. In the current study, we identified individual type I cells based on their $Ca^{2+}$ response to hypoxia challenge. Figure 5-1A shows that application of PACAP (100 nM) to a hypoxia-sensitive type I cell also triggered a rise in $[Ca^{2+}]_i$. In 101 type I cells which exhibited a $[Ca^{2+}]_i$ rise in response to hypoxia, PACAP (100 nM) induced a $[Ca^{2+}]_i$ rise in ~80% of the cells. The mean amplitude of the $Ca^{2+}$ signal evoked by 100 nM PACAP was 114 ± 6 nM (n = 81), which was significantly smaller than the peak $[Ca^{2+}]_i$ rise evoked by moderate hypoxia in the same cells (150 ± 8 nM). We found that PACAP at 10 nM could also trigger a $Ca^{2+}$ response in type I cells (e.g. Figure 5-2B). In 88 type I cells examined, the mean amplitude of the $Ca^{2+}$ signal evoked by 10 nM PACAP was 110 ± 5 nM, not significantly different from that triggered by 100 nM PACAP (114 ± 6 nM; n = 81). Thus, 10 nM PACAP was sufficient to trigger the maximum response in type I cells. Since the PACAP response was smaller than that mediated by hypoxia, we examined whether the effects of PACAP and hypoxia on $[Ca^{2+}]_i$ in type I cell were additive by comparing the $Ca^{2+}$ response mediated by PACAP alone and that evoked by a combination of PACAP and hypoxia in the same cell. Figure 5-1B shows that following the $[Ca^{2+}]_i$ rise evoked by PACAP (100 nM), hypoxia could cause a further increase in $[Ca^{2+}]_i$. In 40 type I cells examined, the mean time integral (for 100 s) of the $Ca^{2+}$ signal (shaded areas in Figure 5-1B) triggered in the presence of a combination of PACAP and hypoxia was 11.1 ± 0.7 μM s, significantly larger than that triggered by PACAP alone (5.8 ± 0.4 μM s). Figure 5-1C shows that in the

presence of moderate hypoxia, PACAP (100 nM) evoked a further increase in $[Ca^{2+}]_i$. In 41 cells, the mean time integral (for 100s) of the $Ca^{2+}$ signal in hypoxia alone (shaded areas in Figure 5-1C) was 9.9 ± 0.6 μM s and increased to 14.0 ± 0.4 μM s when the same cells were subsequently challenged with PACAP in the continued presence of hypoxia. Thus, during moderate hypoxia, the action of PACAP was additive to the hypoxia response. We also examined the possible action of PACAP on type II cells. In contrast to type I cells, the type II cells do not express any VGCC (Urena et al. 1989; Xu et al. 2003). However, we have shown previously that ATP can repetitively trigger intracellular $Ca^{2+}$ release from type II, but not type I cells (Xu et al. 2003). Therefore, to examine whether PACAP affects $[Ca^{2+}]_i$ in type II cells, we first identified type II cells based on their $Ca^{2+}$ response to ATP. Figure 5-1D shows an example of the rise in $[Ca^{2+}]_i$ in a type II cell when challenged with ATP (100 μM). Note that PACAP (100 nM) failed to trigger any $[Ca^{2+}]_i$ rise in the same cell (Figure 5-1C). In 16 type II cells examined, ATP (100 μM) raised $[Ca^{2+}]_i$ by 252 ± 37 nM. Application of PACAP (100 nM) at 350s (n=10) or 800s (n=6) after the ATP challenge failed to trigger any $[Ca^{2+}]_i$ elevation in the same cells. Note that the lack of PACAP response in type II cells cannot be due to depletion of intracellular $Ca^{2+}$ stores by ATP, as a previous study in our lab (Xu et al. 2003) has shown that repetitive application of 100 μM ATP (at ~400 s apart) can trigger robust $Ca^{2+}$ signals in type II cells (in the presence of extracellular $Ca^{2+}$). Thus, in contrast to type I cells, PACAP did not trigger any $Ca^{2+}$ signal in type II cells.

*5.2.2 The PACAP response in type I cells is mediated via $PAC_1$ receptors and the PKA pathway*

Two main types of PACAP receptors are reported in the literature (Sherwood et al. 2000; Vaudry et al. 2000). The type I receptor, $PAC_1$, binds to both PACAP-38 and PACAP-27 with greater (100-1000 fold) affinity than vasointestinal polypeptide (VIP). The type II receptors have two subtypes ($VPAC_1$ and $VPAC_2$) and bind PACAP and VIP with equal affinity. To examine the receptor subtypes involved in the PACAP-mediated $[Ca^{2+}]_i$ rise in type I cells, we tested whether VIP could mimic the PACAP response. Figure 5-2A shows that VIP (100 nM) failed to trigger any $[Ca^{2+}]_i$ rise in a type I cell. Subsequent challenge of the same cell with PACAP (100 nM) could still evoke a robust $Ca^{2+}$ response. In 19 out of 21 type I cells examined, VIP (100 nM) did not evoke any $[Ca^{2+}]_i$ rise while PACAP (100 nM) triggered $[Ca^{2+}]_i$ rise in every cell (mean amplitude of $[Ca^{2+}]_i$ rise = 137 ± 13 nM; n = 21). In the remaining 2 cells, VIP (100 nM) triggered a small $[Ca^{2+}]_i$ rise (76 ± 9 nM). The poor response to VIP in the type I cells suggests that PACAP acts via the $PAC_1$ receptors. To further examine the type of receptors involved, we employed PACAP 6-38, which is a potent ($IC_{50}$ = 14 nM) antagonist of $PAC_1$ receptors (Harmar et al. 1998). PACAP 6-38 has negligible effect on $VPAC_1$ receptor but antagonizes $VPAC_2$ receptors with an $IC_{50}$ of 170 nM (Dickinson et al. 1997). Figure 5-2B shows that in the presence of PACAP 6-38 (100 nM), PACAP (10 nM) failed to trigger any significant rise in $[Ca^{2+}]_i$. After the removal of PACAP 6-38, PACAP (10 nM) was able to trigger a robust $Ca^{2+}$ signal in the same cell. In the presence of PACAP 6-38 (100 nM), the peak amplitude of $[Ca^{2+}]_i$ rise evoked by PACAP (10 nM) was only 20

± 4 nM (n = 91). Following the removal of PACAP 6-38, subsequent challenge of PACAP (10 nM) to the same cells elevated $[Ca^{2+}]_i$ by 108 ± 5 nM (n = 94). Since PACAP 6-38 antagonizes $VPAC_2$ receptors with an $IC_{50}$ value of 170 nM, the strong inhibitory action of 100 nM PACAP 6-38 observed in the experiments of Figure 5-2B further supports the involvement of $PAC_1$ receptors in the PACAP-mediated $Ca^{2+}$ response in type I cells.

$PAC_1$ receptors have been shown to be coupled to the adenylate cyclase as well as the phospholipase C (PLC) pathways (Vaudry et al. 2000). These two pathways can elevate $[Ca^{2+}]_i$ via distinct mechanisms. The PLC pathway leads to the release of $Ca^{2+}$ from the intracellular stores. To determine whether the PACAP-mediated $Ca^{2+}$ response in type I cells involves intracellular $Ca^{2+}$ release, we examined whether the removal of extracellular $Ca^{2+}$ affected the PACAP response. Figure 5-3A shows that the PACAP-mediated $[Ca^{2+}]_i$ elevation was abolished when the standard bath solution was replaced by a $Ca^{2+}$-free solution (which also contained 1 mM of a $Ca^{2+}$ chelator, EGTA). The PACAP-mediated $[Ca^{2+}]_i$ rise was restored upon perfusion of the $Ca^{2+}$-containing standard bath solution. In the 52 cells examined, the $Ca^{2+}$-free solution completely abolished the PACAP-mediated $[Ca^{2+}]_i$ rise. Thus, the action of PACAP in type I cells required the presence of extracellular $Ca^{2+}$. Since $PAC_1$ receptors are coupled to adenylate cylase in many cell types (Sherwood et al. 2000;Vaudry et al. 2000), we tested the involvement of the adenylate cylcase/PKA pathway using a PKA inhibitor, H89. Figure 5-3B shows that in the presence of H89 (10 μM), PACAP (100 nM) caused a very small elevation in $[Ca^{2+}]_i$. Following the removal of H89, PACAP (100 nM) was able to evoke a robust $Ca^{2+}$

response in the same cell. In 51 cells examined, PACAP (100 nM) triggered a very small $[Ca^{2+}]_i$ rise (7 ± 4 nM) in the presence of H89 (10 μM). For the same cells, application of PACAP (100 nM) prior to or following H89 removal elevated $[Ca^{2+}]_i$ by 135 ± 12 nM (n = 51). Thus, the PACAP response in type I cells involves the PKA pathway.

### *5.2.3 The PACAP response was mediated via membrane depolarization and inhibition of TASK-like $K^+$ channels*

Since the effect of PACAP on type I cells is strongly dependent on the presence of extracellular $Ca^{2+}$ (Figure 5-3A), we examined whether the PACAP-mediated $[Ca^{2+}]_i$ rise involved changes in membrane excitability. In these experiments, we simultaneously monitored $[Ca^{2+}]_i$ (indo-1 fluorometry) and membrane potential (perforated patch recording) in type I cells. As shown in Figure 5-4A, following the application of PACAP, the membrane potential depolarized and there was some firing of action potentials. Note that the membrane depolarization was accompanied by $[Ca^{2+}]_i$ rise (Figure 5-4A). In 16 cells examined, PACAP (100 nM) depolarized the membrane potential from -42 ± 4 mV to a plateau value of -29 ± 3 mV and the mean increase in peak $[Ca^{2+}]_i$ in the same cells was 246 ± 24 nM. Consistent with the notion that the PACAP-mediated membrane depolarization in turn leads to activation of voltage-gated $Ca^{2+}$ entry, Figure 5-4B shows that the PACAP-triggered $[Ca^{2+}]_i$ rise could be reversibly inhibited by the VGCC blocker, $Ni^{2+}$ (2.5 mM; n = 32). Note that we did not employ $Cd^{2+}$, another common VGCC blocker in this experiment because $Cd^{2+}$ but not $Ni^{2+}$ was reported to enter cells and

cause quenching of the fluorescence of the $Ca^{2+}$ indicator (Shibuya and Douglas 1992). In separate experiments, we also confirmed that $Ni^{2+}$ did not affect the membrane potential of type I cells (n = 5).

Hypoxia has been shown to excite type I cells via inhibition of BK channels (Riesco-Fagundo et al. 2001; Williams et al. 2004; Wyatt and Peers 1995). To investigate the involvement of BK channels in the PACAP response, we examined whether the PACAP response could be attenuated by TEA, which is a blocker of a number of voltage-dependent $K^+$ channels, including BK channels (Pardal et al. 2000). In ~55% of type I cells examined (n = 86), TEA (10 mM) triggered transient increases in $[Ca^{2+}]_i$ (e.g. Figure 5-5A). Application of PACAP (100 nM) in the continued presence of TEA evoked a more sustained $[Ca^{2+}]_i$ rise (Figure 5-5B). The time integral (for 200 s) of the $Ca^{2+}$ signal (see Figure 5-5A for example) triggered in the presence of a combination of TEA and PACAP (17 ± 2 μM s; n = 47) was significantly larger than that triggered by TEA alone (9 ± 1 μM s) in the same cells. In cells that TEA did not trigger any $[Ca^{2+}]_i$ elevation (e.g. Figure 5-5B), application of PACAP (100 nM) in the presence of TEA could still trigger a robust $[Ca^{2+}]_i$ rise (121 ± 12 nM; n = 39). Overall, the above results suggest that TEA-sensitive $K^+$ currents did not contribute significantly to the PACAP response.

To further investigate the ionic mechanism underlying the PACAP response in type I cells, we examined whether PACAP affected the current of type I cells under voltage-clamp condition. Since our results above indicate that the TEA-sensitive current did not contribute to the PACAP response (Figure 5-5), we included TEA (10 mM) and $Cd^{2+}$ (0.2 mM) in the standard bath solution to block the delayed rectifier,

BK current as well as any $Ca^{2+}$-activated current. Type I cells also express a 4-AP-sensitive $K^+$ current (Vandier et al. 1999) but 4-AP (5 mM) did not affect the membrane potential (Buckler 1997; Vandier et al. 1999) or $[Ca^{2+}]_i$ of type I cells (Xu et al. 2006). Thus, it is unlikely that the 4-AP-sensitive $K^+$ current is involved in the action of PACAP on type I cells. Therefore, we also included 4-AP (5 mM) in our bath solution. In this set of experiments, single type I cell was voltage-clamped at -60 mV and voltage steps (200 ms in duration) to potentials between -70 and +50 mV were applied. Figure 5-6A & B show the family of currents evoked from a cell before (Figure 5-6A) and in the presence of PACAP (100 nM; Figure 5-6B). The amplitude of the current at different potentials was measured by averaging the current during the last 20 ms of the voltage steps. The current-voltage relation before and in the presence of PACAP for the same cell is plotted in Figure 5-6C. Note that PACAP caused a significant reduction in the outward current evoked at positive potentials. In 8 cells examined, PACAP (100 nM) reduced the outward current evoked at -10 mV in these cells by 20 $\pm$ 5%. As described earlier, the resting membrane potential of the type I cells is ~-40 mV. This value is similar to that described by our previous study (Xu et al. 2006) and comparable to those reported previously in adult rat type I cells (Fieber and McCleskey 1993) and neonatal rat type I cells (Buckler and Vaughan-Jones 1994). As shown in Figure 5-6, the amplitude of the currents evoked at -40 mV was small (< 5 pA). The small amplitude of the current hindered a clear analysis of the action of PACAP on the current near the resting potential of the type I cells. Therefore, we repeated the above experiment using a bath solution which contained 140 mM $K^+$, as well as TEA, 4-AP and $Ni^{2+}$ (see chapter 2). Cells were voltage

clamped at -60 mV and voltage steps (20 ms in duration) were applied to various potentials (-60 to +60 mV in 20 mV increments). Figure 5-7A shows the families of currents evoked from a type I cell before and in the presence of PACAP (100 nM). The amplitude of the current at different potentials was measured by averaging the last 10 ms of the voltage steps. The current voltage relations before and in the presence of PACAP for the same cell were plotted in Figure 5-7B. Note that PACAP reduced the current at a wide range of potentials. In 6 cells examined, PACAP reduced the current at -40 mV by 37 ± 10%.

The PACAP-sensitive current (Figure 5-7B) resembles the TEA-insensitive background TASK-like $K^+$ current, which has been shown to be an important mechanism underlying hypoxia-mediated membrane depolarization and $[Ca^{2+}]_i$ rise in rat type I cells (Buckler 1997). The expression of multiple TASK-like channels (including TASK-1, TASK-2, TASK-3) has been reported in rat type I cells (Yamamoto et al. 2002). We have shown previously that anandamide, a selective TASK-1 $K^+$ channel blocker (Maingret et al. 2001), triggered robust $[Ca^{2+}]_i$ rise and depolarization in rat type I cells (Figure 4-6B). Thus, the TASK-1 channel is an important regulator of the electrical excitability in rat type I cells. To determine whether the action of PACAP involves TASK-1 channels, we examined whether anandamide could attenuate the inhibitory action of PACAP on the background $K^+$ current. In this set of experiments, the background $K^+$ current was recorded in 140 mM extracellular $K^+$ as described in Figure 5-7A. Cells were challenged with anandamide (5 μM) and then with a combination of anandamide and PACAP (100 nM). The current voltage relations recorded from a cell in control condition, in the

presence of anandamide (5 μM), and in the presence of anandamide and PACAP were shown in Figure 5-7C (different cell from Figure 5-7B). Note that anandamide reduced the background current at all potentials. In the continued presence of anandamide, PACAP did not cause any further reduction in the background current (Figure 5-7C). In 4 cells examined, anandamide (5 μM) reduced the background $K^+$ current at -40 mV by 68 ± 3%, and PACAP (100 nM) did not cause any further reduction of the current. Thus, anandamide occluded the inhibitory action of PACAP on the background $K^+$ current. This result is consistent with the notion that a reduction of the TASK-1 background $K^+$ current is the major mechanism underlying the PACAP-mediated $Ca^{2+}$ signal in type I cells.

## 5.3 Discussion

The findings here demonstrate that PACAP has stimulatory actions on the $O_2$ sensing type I cells in the rat carotid body. In the majority of type I cells (identified by their $Ca^{2+}$ response to hypoxia), PACAP triggered a rise in $[Ca^{2+}]_i$. PACAP at 10 or 100 nM triggered a similar increase in $[Ca^{2+}]_i$ in type I cells, suggesting that a maximal response could be achieved by 10 nM PACAP. In ~20% of the hypoxia-responding cells, PACAP failed to elicit any $[Ca^{2+}]_i$ rise. Since the PACAP-mediated $[Ca^{2+}]_i$ rise was dependent on depolarization and activation of VGCC (Figure 5-4), it is possible that the PACAP-mediated depolarization in some type I cells that may be insufficient to trigger significant VGCC activation and $Ca^{2+}$ entry. Although PACAP has been reported to stimulate intracellular $Ca^{2+}$ release in glial cells (Tatsuno and

Arimura 1994), PACAP did not evoke any $Ca^{2+}$ signal in the glial-like type II cells in carotid body (Figure 5-1C). The PACAP-mediated $[Ca^{2+}]_i$ rise in type I cells could be antagonized by PACAP 6-38 (100 nM; Figure 5-2B). Although PACAP 6-38 affects both $PAC_1$ and $VPAC_2$ receptors (Dickinson et al. 1997), the concentration of PACAP 6-38 employed in the current study was only ~60% of the $IC_{50}$ value of PACAP 6-38 for $VPAC_2$ receptors (Dickinson et al. 1997). Thus, a significant involvement of the $VPAC_2$ receptor in the PACAP response can be ruled out. Consistent with the involvement of $PAC_1$ receptors, the PACAP response in type I cells could not be mimicked by the VPAC receptor agonist, VIP (Figure 5-2A).

PACAP has been reported to trigger $Ca^{2+}$ signal in many cell types and multiple mechanisms have been implicated. For example, in suprachiasmatic neurons (Kopp et al. 1999) and pituitary gonadotropes (Alarcon and Garcia-Sancho 2000; Rawlings et al. 1994), PACAP was reported to trigger intracellular $Ca^{2+}$ release from the inositol trisphosphate ($IP_3$) stores. On the other hand, in chromaffin cells (Tanaka et al. 1998) and intracardiac neurons (DeHaven and Cuevas 2004), PACAP was reported to trigger $Ca^{2+}$ release from the ryanodine/caffeine-sensitive stores. Although type I cells contain both $IP_3$- (Dasso et al. 1997) and caffeine-sensitive (Buckler and Vaughan-Jones 1994) stores, we found that the removal of extracellular $Ca^{2+}$ completely abolished the PACAP-mediated $[Ca^{2+}]_i$ rise (Figure 5-3A). Thus, the primary involvement of intracellular $Ca^{2+}$ release in the PACAP response in type I cells can be ruled out. PACAP has also been reported to increase the electrical excitability in many types of neurons (Beaudet et al. 2000; Di Mauro et al. 2003). Consistent with this, we also found that the PACAP-mediated $[Ca^{2+}]_i$ rise in type I

cells was accompanied by depolarization and firing of action potentials (Figure 5-4). Multiple ionic mechanisms have been reported to underlie the PACAP-mediated increase in electrical excitability, including a reduction of the delayed rectifier current (Mei et al. 2004) as well as activation of a hyperpolarization-activated non-selective cation current (Merriam et al. 2004;Sun et al. 2003). Here, we found that PACAP reduced a background $K^+$ current which was insensitive to TEA and 4-AP, and exhibited little voltage dependence (Figure 5-7B). These properties of the PACAP-sensitive current resembled those reported for the $O_2$-sensitive TASK-like $K^+$ current in type I cells (Buckler 1997). Consistent with the notion that PACAP reduced the TASK-like $K^+$ current in type I cells, the TASK-1 channel blocker anandamide occluded the inhibitory action of PACAP on the background $K^+$ current (Figure 5-7C). Activation of PKA by forskolin and IBMX has been shown to reduce TASK-like $K^+$ current (Leonoudakis et al. 1998; Lopes et al. 2000). In a previous study, we have shown that forskolin (but not the inactive analog of forskolin) could trigger $[Ca^{2+}]_i$ rise in type I cells (Xu et al. 2006). Here, we found that inhibition of PKA by H89 attenuated the PACAP-mediated $[Ca^{2+}]_i$ rise (Figure 5-3B). Overall, our results suggest that stimulation of $PAC_1$ receptor in rat type I cell activates PKA, which in turn inhibits the TASK-like $K^+$ channels and leads to depolarization, activation of VGCC and $[Ca^{2+}]_i$ elevation (Figure 5-8).

Note that even at high concentration of PACAP (100 nM), the peak amplitude of the PACAP-mediated $[Ca^{2+}]_i$ rise was significantly smaller than that triggered by moderate hypoxia in the same cells (114 vs. 150 nM). Although the TASK-like channel is a common target for both PACAP and hypoxia, hypoxia is also known to

inhibit the BK channels (Riesco-Fagundo et al. 2001; Williams et al. 2004). Moreover, the inhibitory action of PACAP on the TASK-like current was smaller than that elicited by anandamide (38 vs. 68% at -40 mV). Thus, it is likely that PACAP can inhibit only a fraction of the TASK-like current in type I cells. In the presence of PACAP, hypoxia should cause a further reduction of the TASK-like current as well as inhibition of BK current, resulting in more depolarization and a larger $[Ca^{2+}]_i$ rise. Consistent with this, Figure 5-1B shows that in the presence of PACAP (100 nM), a moderate hypoxic challenge could trigger additional increase in $[Ca^{2+}]_i$. The additive effects of PACAP and moderate hypoxia raises the possibility that at near the threshold level of tissue $P_{O_2}$ for activation of type I cells, PACAP may augment the hypoxia-mediated $[Ca^{2+}]_i$ elevation in type I cells. The loss of this mechanism in PACAP-deficient mice may contribute to the reduction in chemoresponse to hypoxia and sudden neonatal death in these animals.

## 5.4 Acknowledgements

I performed all of the experiments in this chapter. Some of the findings of this chapter have been published as a book chapter in Adv Exp Med Biol. A manuscript of this study was accepted by J Neurochem in November, 2006.

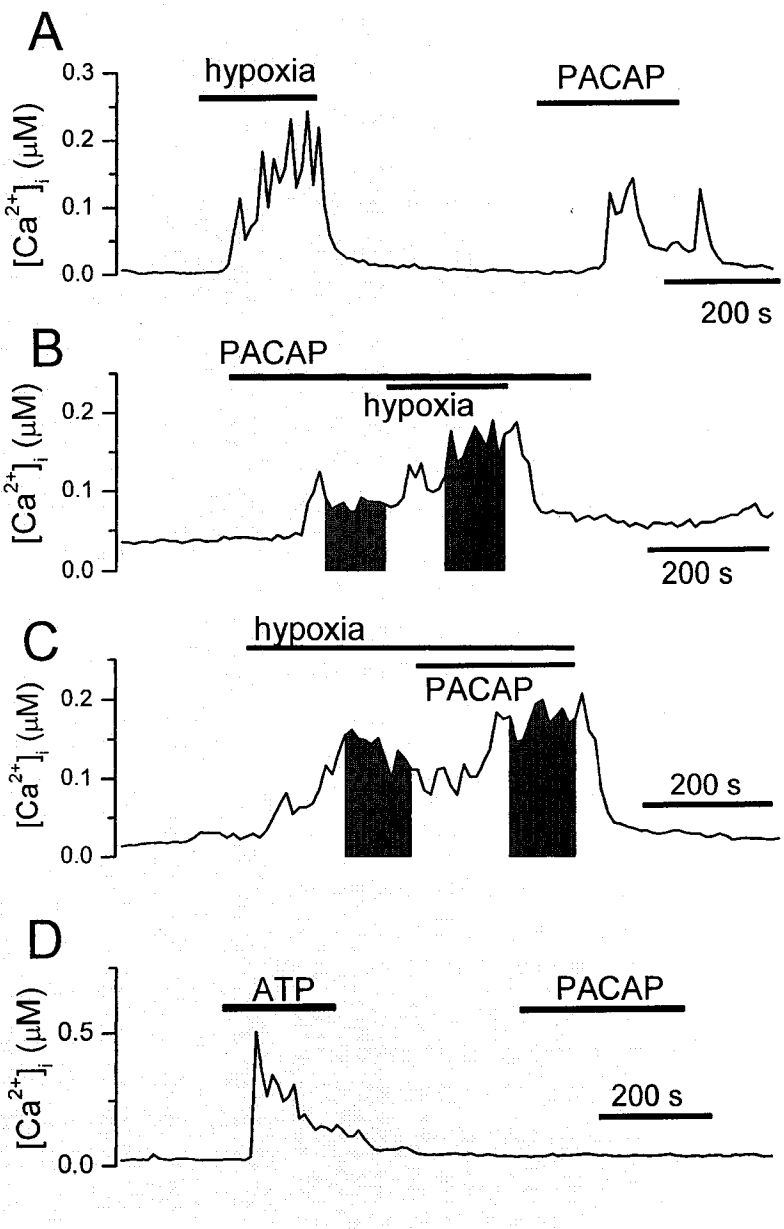


**Figure 5-1** PACAP induced $[Ca^{2+}]_i$ rise in the $O_2$-sensing type I cells but not the type II cells. *A*, PACAP (100 nM) triggered $[Ca^{2+}]_i$ rise in a type I cell that was identified by its $Ca^{2+}$ response to hypoxia. *B*, In the presence of PACAP (100 nM), hypoxia could trigger additional increase in $[Ca^{2+}]_i$. The two shaded areas were time integrals (for 100 s) of the $Ca^{2+}$ signal in PACAP (100 nM) alone and PACAP in combination with hypoxia respectively. *C*, In the presence of hypoxia, PACAP (100 nM) could trigger additional increase in $[Ca^{2+}]_i$. The two shaded areas were time integrals (for 100 s) of the $Ca^{2+}$ signal in hypoxia alone and PACAP in combination with hypoxia respectively. *D*, PACAP failed to trigger any $[Ca^{2+}]_i$ rise in a type II cell that was identified by its $Ca^{2+}$ response to ATP (100 μM).

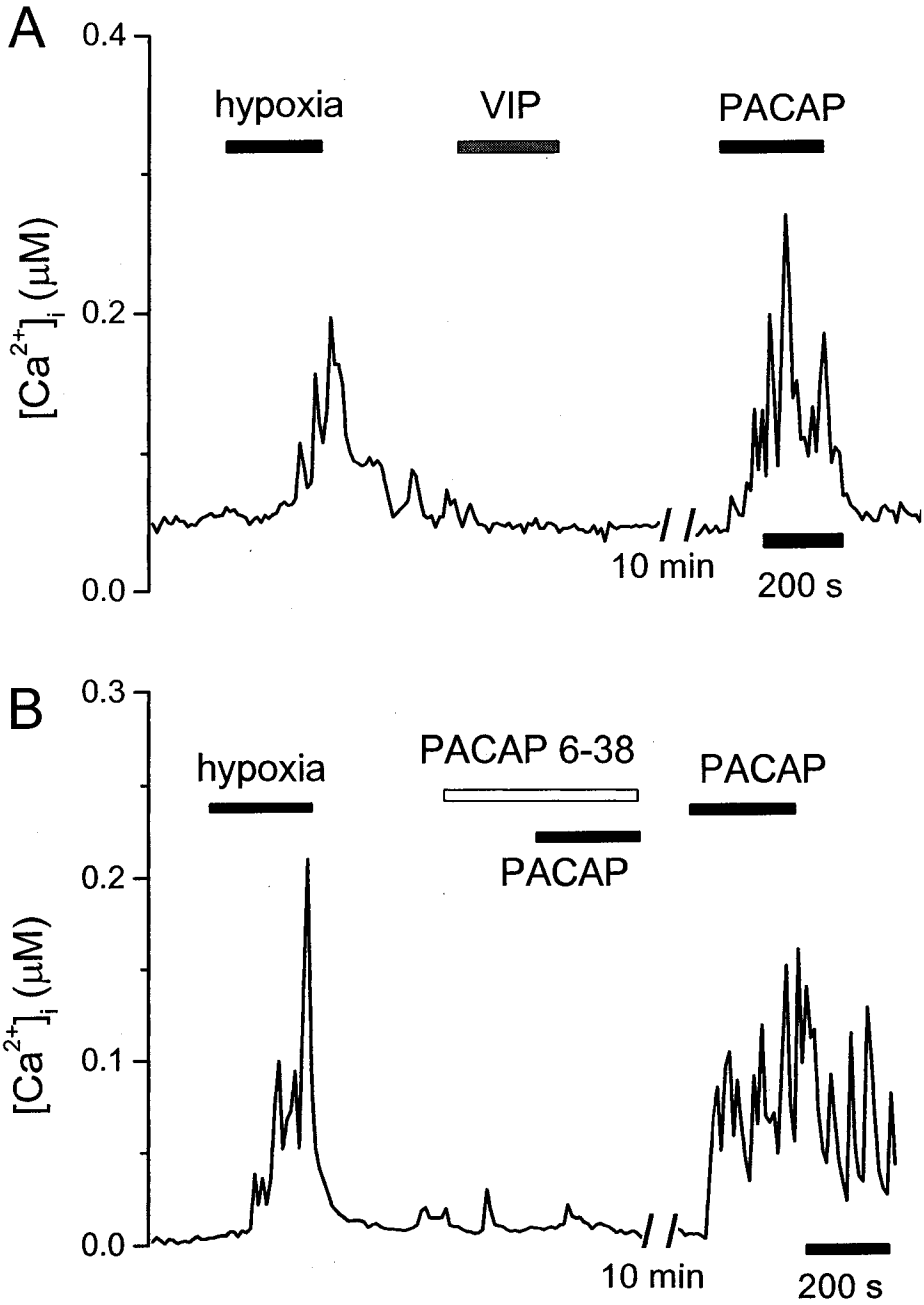


**Figure 5-2** The action of PACAP on type I cell was mediated via $PAC_1$ receptors. *A*, the selective $VPAC_2$ receptor agonist, VIP (100 nM) could not mimic the PACAP. Subsequent challenge of the same cell to PACAP (100 nM) could still evoke a $Ca^{2+}$ signal. *B*, In the presence of the antagonist, PACAP 6-38 (100 nM), PACAP (10 nM) failed to trigger a rise in $[Ca^{2+}]_i$. After the removal of PACAP 6-38, PACAP (10 nM) was able to trigger a robust $Ca^{2+}$ signal in the same cell. $[Ca^{2+}]_i$ was measured with fura-2 $Ca^{2+}$ imaging.

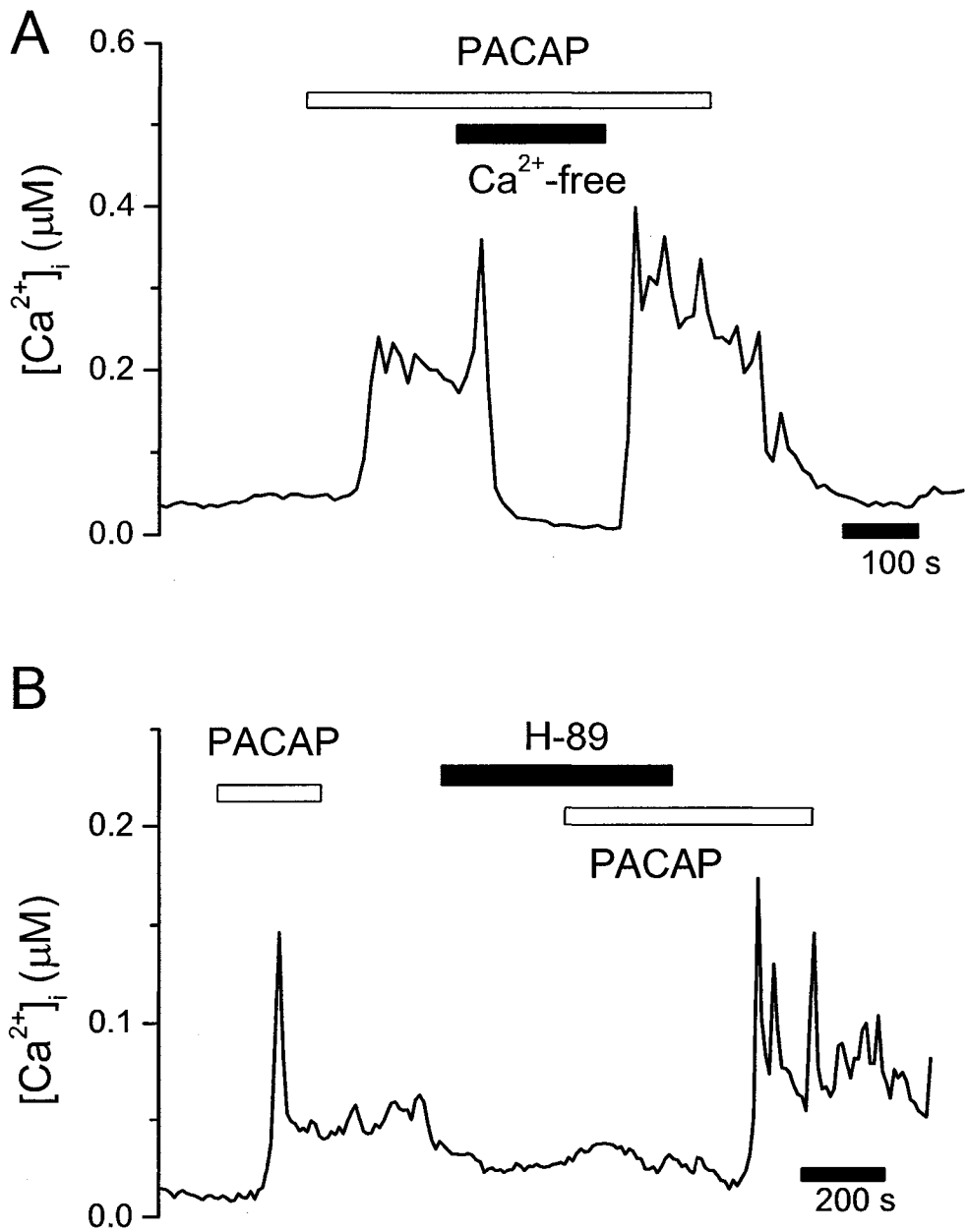


**Figure 5-3** The PACAP response was mediated via the adenylate cyclase/PKA pathway. *A*, The PACAP response did not involve intracellular $Ca^{2+}$ release. The removal of extracellular $Ca^{2+}$ reversibly abolished the PACAP-mediated $[Ca^{2+}]_i$ rise. *B*, In the presence of the PKA inhibitor, H89 (10 μM), PACAP (100 nM) failed to trigger any $[Ca^{2+}]_i$ rise. Following the removal of H89, the PACAP response was restored. $[Ca^{2+}]_i$ was measured with fura-2 $Ca^{2+}$ imaging.

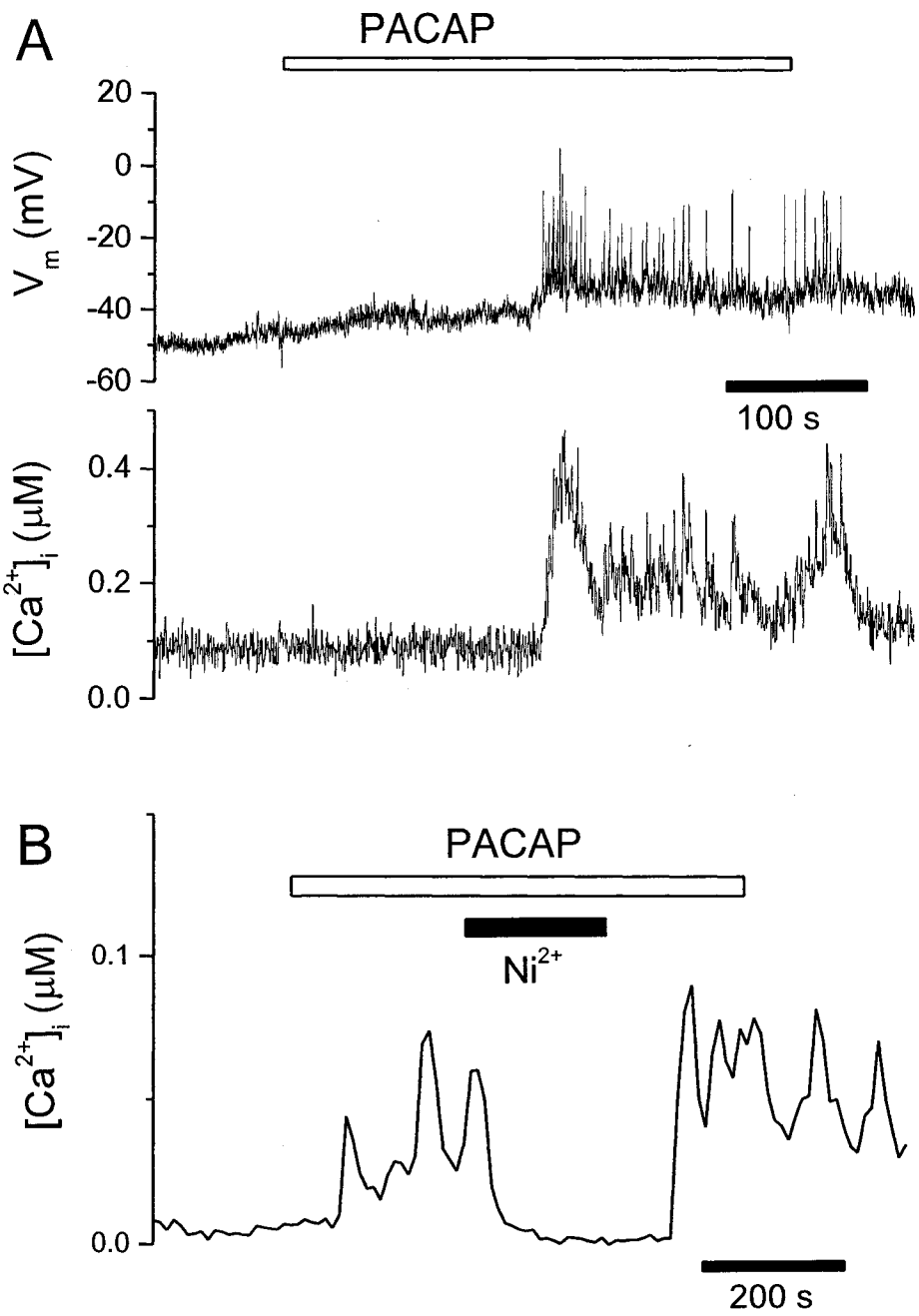


**Figure 5-4** The PACAP-mediated $[Ca^{2+}]_i$ rise in type I cell was accompanied by membrane depolarization and activation of VGCC. *A*, simultaneous measurement of membrane potential (perforated patch recording) with $[Ca^{2+}]_i$ (indo-1 fluorometry). PACAP (100 nM) caused depolarization and firing of action potentials. Note that the bursts of actions potentials were accompanied by transient increases in $[Ca^{2+}]_i$. *B*, the PACAP-mediated $[Ca^{2+}]_i$ rise was reversibly inhibited by the VGCC blocker, $Ni^{2+}$ (2.5 mM). $[Ca^{2+}]_i$ was measured with fura-2 $Ca^{2+}$ imaging.

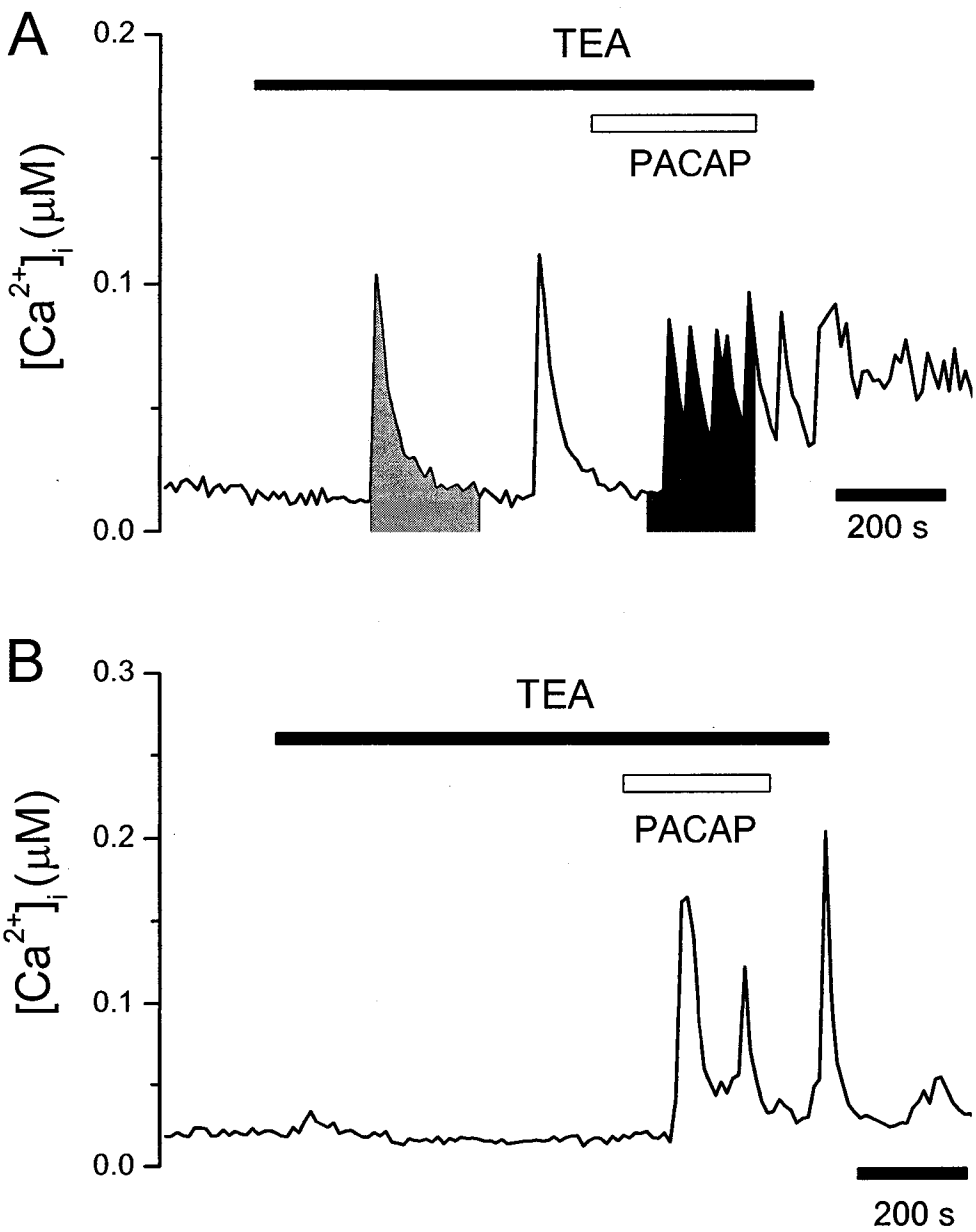


**Figure 5-5** The PACAP response could not be attenuated by TEA. *A*, example of a type I cell in which TEA (10 mM) triggered $[Ca^{2+}]_i$ rise. The two shaded areas were time integrals (for 200 s) of the $Ca^{2+}$ signal in TEA alone, and TEA in combination with PACAP, respectively. *B*, example of a type I cell in which TEA (10 mM) did not affect the resting $[Ca^{2+}]_i$. Note that in the presence of TEA, PACAP (100 nM) could still trigger $[Ca^{2+}]_i$ rise. $[Ca^{2+}]_i$ was measured with fura-2 $Ca^{2+}$ imaging.

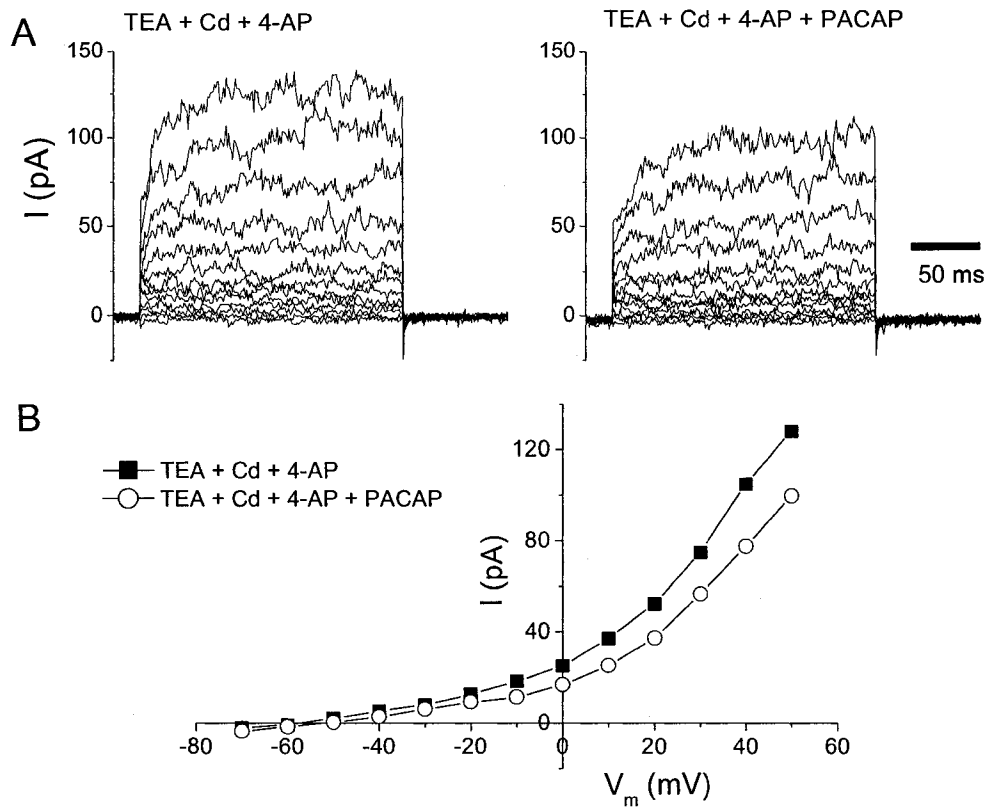


**Figure 5-6** PACAP reduced a TEA, 4-AP insensitive current. *A* & B, superimposed current records from a cell elicited by 200 ms voltage steps from -70 to 50 mV (in 10 mV increments) before (*A*) and in the presence of 100 nM PACAP (*B*). *C*, the current-voltage relation before and in the presence of PACAP for the same cell. The cell was held at -60 mV and the current amplitude at different potentials was measured by averaging the current during the last 20 ms of the voltage steps. The bath solution contained 10 mM TEA, 5 mM 4-AP and 0.2 mM $Cd^{2+}$.

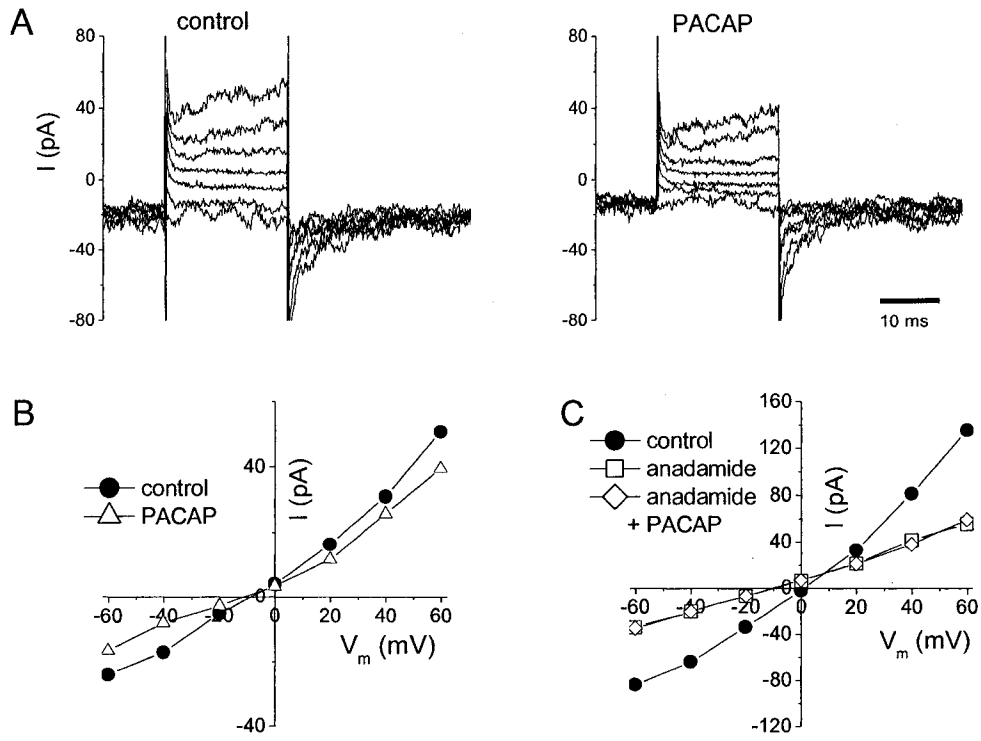


**Figure 5-7** PACAP reduced a TASK-like background $K^+$ current. *A*, superimposed current records elicited by 20 ms voltage steps from -60 to +60 mV in 20 mV increments before and in the presence of 100 nM PACAP. *B*, the current-voltage relations before and in the presence of PACAP for the same cell as shown in *A*. *C*, example of the current-voltage relations obtained from a cell recorded in control condition, in the presence of anandamide (5 μM) and in the presence of a combination of anandamide (5 μM) and PACAP (100 nM). Note that this is not the same cell as shown in Figure 7*A-B*. In this series of experiments, a single cell was held at -60 mV and the current amplitude at different potentials was measured by averaging the current during the last 10 ms of the voltage steps. The bath solution contained 140 mM $K^+$, 10 mM TEA-Cl, 5 mM 4-AP and 2.5 mM $Ni^{2+}$.

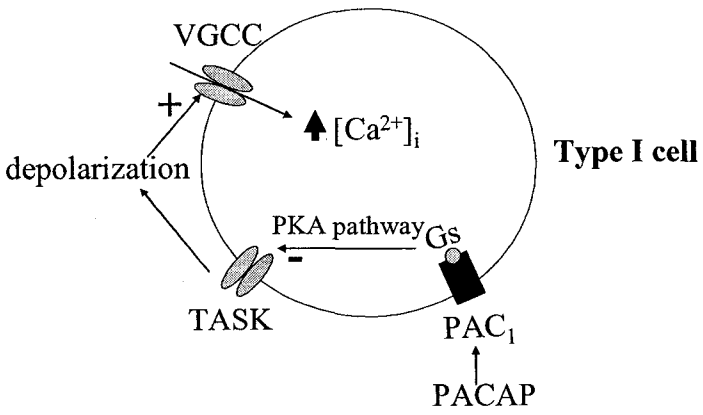


**Figure 5-8** Summary of actions of PACAP on rat type I cells. PACAP, acting via $PAC_1$ receptors coupled to adenylate cyclase/PKA pathway, causes membrane depolarization which activates VGCC. The influx of $Ca^{2+}$ via VGCC elevates $[Ca^{2+}]_i$ in type I cells.

## References


Alarcon P. and Garcia-Sancho J. (2000) Differential calcium responses to the pituitary adenylate cyclase-activating polypeptide (PACAP) in the five main cell types of rat anterior pituitary. *Pflugers Arch* **440,** 685-691.

Beaudet M. M., Parsons R. L., Braas K. M., and May V. (2000) Mechanisms mediating pituitary adenylate cyclase-activating polypeptide depolarization of rat sympathetic neurons. *J Neurosci* **20,** 7353-7361.

Buckler K. J. (1997) A novel oxygen-sensitive potassium current in rat carotid body type I cells. *J Physiol* **498 ( Pt 3),** 649-662.

Buckler K. J. and Vaughan-Jones R. D. (1994) Effects of hypercapnia on membrane potential and intracellular calcium in rat carotid body type I cells. *J Physiol* **478 ( Pt 1),** 157-171.

Cummings K. J., Pendlebury J. D., Sherwood N. M., and Wilson R. J. (2004) Sudden neonatal death in PACAP-deficient mice is associated with reduced respiratory chemoresponse and susceptibility to apnoea. *J Physiol* **555,** 15-26.

Dasso L. L., Buckler K. J., and Vaughan-Jones R. D. (1997) Muscarinic and nicotinic receptors raise intracellular Ca2+ levels in rat carotid body type I cells. *J Physiol* **498 ( Pt 2),** 327-338.

DeHaven W. I. and Cuevas J. (2004) VPAC receptor modulation of neuroexcitability in intracardiac neurons: dependence on intracellular calcium mobilization and synergistic enhancement by PAC1 receptor activation. *J Biol Chem* **279,** 40609-40621.

Di Mauro M., Cavallaro S., and Ciranna L. (2003) Pituitary adenylate cyclase-activating polypeptide modifies the electrical activity of CA1 hippocampal neurons in the rat. *Neurosci Lett* **337,** 97-100.

Dickinson T., Fleetwood-Walker S. M., Mitchell R., and Lutz E. M. (1997) Evidence for roles of vasoactive intestinal polypeptide (VIP) and pituitary adenylate cyclase activating polypeptide (PACAP) receptors in modulating the responses of rat dorsal horn neurons to sensory inputs. *Neuropeptides* **31,** 175-185.

Fieber L. A. and McCleskey E. W. (1993) L-type calcium channels in type I cells of the rat carotid body. *J Neurophysiol* **70,** 1378-1384.

Gonzalez C., Almaraz L., Obeso A., and Rigual R. (1994) Carotid body chemoreceptors: from natural stimuli to sensory discharges. *Physiol Rev* **74,** 829-898.

Gray S. L., Cummings K. J., Jirik F. R., and Sherwood N. M. (2001) Targeted disruption of the pituitary adenylate cyclase-activating polypeptide gene results in early postnatal death associated with dysfunction of lipid and carbohydrate metabolism. *Mol Endocrinol* **15,** 1739-1747.

Gray S. L., Yamaguchi N., Vencova P., and Sherwood N. M. (2002) Temperature-sensitive phenotype in mice lacking pituitary adenylate cyclase-activating polypeptide. *Endocrinology* **143,** 3946-3954.

Gronblad M. (1983) Function and structure of the carotid body. *Med Biol* **61,** 229-248.

Hannibal J. (2002) Pituitary adenylate cyclase-activating peptide in the rat central nervous system: an immunohistochemical and in situ hybridization study. *J Comp Neurol* **453,** 389-417.

Harmar A. J., Arimura A., Gozes I., Journot L., Laburthe M., Pisegna J. R., Rawlings S. R., Robberecht P., Said S. I., Sreedharan S. P., Wank S. A., and Waschek J. A. (1998) International Union of Pharmacology. XVIII. Nomenclature of receptors for vasoactive intestinal peptide and pituitary adenylate cyclase-activating polypeptide. *Pharmacol Rev* **50,** 265-270.

Kameda Y. (1996) Immunoelectron microscopic localization of vimentin in sustentacular cells of the carotid body and the adrenal medulla of guinea pigs. *J Histochem Cytochem* **44,** 1439-1449.

Kopp M. D., Schomerus C., Dehghani F., Korf H. W., and Meissl H. (1999) Pituitary adenylate cyclase-activating polypeptide and melatonin in the suprachiasmatic nucleus: effects on the calcium signal transduction cascade. *J Neurosci* **19,** 206-219.

Leonoudakis D., Gray A. T., Winegar B. D., Kindler C. H., Harada M., Taylor D. M., Chavez R. A., Forsayeth J. R., and Yost C. S. (1998) An open rectifier potassium channel with two pore domains in tandem cloned from rat cerebellum. *J Neurosci* **18,** 868-877.

Linden A., Cardell L. O., Yoshihara S., and Nadel J. A. (1999) Bronchodilation by pituitary adenylate cyclase-activating peptide and related peptides. *Eur Respir J* **14,** 443-451.

Liu Y. C., Khawaja A. M., and Rogers D. F. (1999) Effect of vasoactive intestinal peptide (VIP)-related peptides on cholinergic neurogenic and direct mucus secretion in ferret trachea in vitro. *Br J Pharmacol* **128,** 1353-1359.

Lopes C. M., Gallagher P. G., Buck M. E., Butler M. H., and Goldstein S. A. (2000) Proton block and voltage gating are potassium-dependent in the cardiac leak channel Kcnk3. *J Biol Chem* **275,** 16969-16978.

Maingret F., Patel A. J., Lazdunski M., and Honore E. (2001) The endocannabinoid anandamide is a direct and selective blocker of the background K(+) channel TASK-1. *EMBO J* **20,** 47-54.

Mei Y. A., Vaudry D., Basille M., Castel H., Fournier A., Vaudry H., and Gonzalez B. J. (2004) PACAP inhibits delayed rectifier potassium current via a cAMP/PKA transduction pathway: evidence for the involvement of I k in the anti-apoptotic action of PACAP. *Eur J Neurosci* **19,** 1446-1458.

Merriam L. A., Barstow K. L., and Parsons R. L. (2004) Pituitary adenylate cyclase-activating polypeptide enhances the hyperpolarization-activated nonselective cationic conductance, Ih, in dissociated guinea pig intracardiac neurons. *Regul Pept* **123,** 123-133.

Pardal R., Ludewig U., Garcia-Hirschfeld J., and Lopez-Barneo J. (2000) Secretory responses of intact glomus cells in thin slices of rat carotid body to hypoxia and tetraethylammonium. *Proc Natl Acad Sci U S A* **97,** 2361-2366.

Rawlings S. R., Demaurex N., and Schlegel W. (1994) Pituitary adenylate cyclase-activating polypeptide increases [Ca2]i in rat gonadotrophs through an inositol trisphosphate-dependent mechanism. *J Biol Chem* **269,** 5680-5686.

Riesco-Fagundo A. M., Perez-Garcia M. T., Gonzalez C., and Lopez-Lopez J. R. (2001) O(2) modulates large-conductance Ca(2+)-dependent K(+) channels of rat chemoreceptor cells by a membrane-restricted and CO-sensitive mechanism. *Circ Res* **89,** 430-436.

Runcie M. J., Ulman L. G., and Potter E. K. (1995) Effects of pituitary adenylate cyclase-activating polypeptide on cardiovascular and respiratory responses in anaesthetised dogs. *Regul Pept* **60,** 193-200.

Sherwood N. M., Krueckl S. L., and McRory J. E. (2000) The origin and function of the pituitary adenylate cyclase-activating polypeptide (PACAP)/glucagon superfamily. *Endocr Rev* **21,** 619-670.

Shibuya I. and Douglas W. W. (1992) Calcium channels in rat melanotrophs are permeable to manganese, cobalt, cadmium, and lanthanum, but not to nickel: evidence provided by fluorescence changes in fura-2-loaded cells. *Endocrinology* **131,** 1936-1941.

Sun Q. Q., Prince D. A., and Huguenard J. R. (2003) Vasoactive intestinal polypeptide and pituitary adenylate cyclase-activating polypeptide activate hyperpolarization-activated cationic current and depolarize thalamocortical neurons in vitro. *J Neurosci* **23,** 2751-2758.

Tanaka K., Shibuya I., Uezono Y., Ueta Y., Toyohira Y., Yanagihara N., Izumi F., Kanno T., and Yamashita H. (1998) Pituitary adenylate cyclase-activating

polypeptide causes Ca2+ release from ryanodine/caffeine stores through a novel pathway independent of both inositol trisphosphates and cyclic AMP in bovine adrenal medullary cells. *J Neurochem* **70,** 1652-1661.

Tatsuno I. and Arimura A. (1994) Pituitary adenylate cyclase-activating polypeptide (PACAP) mobilizes intracellular free calcium in cultured rat type-2, but not type-1, astrocytes. *Brain Res* **662,** 1-10.

Urena J., Lopez-Lopez J., Gonzalez C., and Lopez-Barneo J. (1989) Ionic currents in dispersed chemoreceptor cells of the mammalian carotid body. *J Gen Physiol* **93,** 979-999.

Vandier C., Conway A. F., Landauer R. C., and Kumar P. (1999) Presynaptic action of adenosine on a 4-aminopyridine-sensitive current in the rat carotid body. *J Physiol* **515 ( Pt 2),** 419-429.

Vaudry D., Gonzalez B. J., Basille M., Yon L., Fournier A., and Vaudry H. (2000) Pituitary adenylate cyclase-activating polypeptide and its receptors: from structure to functions. *Pharmacol Rev* **52,** 269-324.

Williams S. E., Wootton P., Mason H. S., Bould J., Iles D. E., Riccardi D., Peers C., and Kemp P. J. (2004) Hemoxygenase-2 is an oxygen sensor for a calcium-sensitive potassium channel. *Science* **306,** 2093-2097.

Wyatt C. N. and Peers C. (1995) Ca(2+)-activated K+ channels in isolated type I cells of the neonatal rat carotid body. *J Physiol* **483 ( Pt 3),** 559-565.

Xu F., Xu J., Tse F. W., and Tse A. (2006) Adenosine stimulates depolarization and rise in cytoplasmic [Ca2+] in type I cells of rat carotid bodies. *Am J Physiol Cell Physiol* **290,** C1592-C1598.

Xu J., Tse F. W., and Tse A. (2003) ATP triggers intracellular $Ca^{2+}$ release in type II cells of the rat carotid body. *J Physiol* **549,** 739-747.

Yamamoto Y., Kummer W., Atoji Y., and Suzuki Y. (2002) TASK-1, TASK-2, TASK-3 and TRAAK immunoreactivities in the rat carotid body. *Brain Res* **950,** 304-307.

# Chapter 6

# General Discussion

All the experiments described in this thesis were performed on enzymatically dissociated single type I or type II cells of rat carotid bodies. Since the $Ca^{2+}$ signal in type I cells has been shown to be tightly coupled to CSN discharge (Roy et al. 2000), we focused on the actions of three transmitters (ATP, adenosine, and PACAP) on our preparation of single type I cells, using a combination of $[Ca^{2+}]_i$ measurement and electrophysiological techniques. This chapter will summarize the findings in the preceding chapters and propose some future perspectives on exploring possible physiological significance of my findings. It will then discuss the strengths and limitations of the experiments.

## 6.1 Summary and physiological implications of our findings on ATP and adenosine

Although synaptic contacts have been detected between nerve endings and type I cells (Mcdonald, 1977), neurotransmitter release from type I cells appears to occur from most of the cell surface. For example, catecholamine release can be detected by carbon fibers placed randomly on the cell surface of type I cells (Urena et al. 1994; Pardal et al. 2000). Since ATP is colocalized with catecholamines in many cells, it is likely that ATP is also released from the entire surface of the type I cells during hypoxia. Moreover, type I cells exist in clusters and are encapsulated by type II cells in the carotid body, and the extracellular space between these cells is very

small (~1-3 μm, as shown in figures 3-4B & C). Thus, during hypoxia, the local concentration of ATP near the type I cells is probably very high. During hypoxia the average ATP concentration in carotid body slices can reach 0.5 μM (Buttigieg and Nurse, 2004). Due to the small extracellular space, we expect the local concentration of ATP to be at least several fold higher. We found that even for 1 μm ATP, ~60% of the hypoxia-mediated $Ca^{2+}$ signal would be inhibited (Figure 3-4A). Thus, under physiological conditions, ATP released from a type I cell is likely to have both autocrine action (on type I cell itself) as well as paracrine action (on neighboring type I cells). As shown by our study (Chapter 3) ATP, acting via $P2Y_1$ receptors, causes a hyperpolarization in type I cells. This hyperpolarization opposes the hypoxia-induced membrane depolarization and prevents hypoxia-mediated $[Ca^{2+}]_i$ rise (Figure 6-1). Thus, ATP exerts negative feedback action on type I cells. This action of ATP may play an important physiological role during prolonged hypoxic challenge. For example, at high altitudes, where the $P_{O_2}$ is low, the prolonged hypoxic stimulation may cause a sustained elevation of $[Ca^{2+}]_i$ in type I cells. Excessive and sustained $[Ca^{2+}]_i$ rise has been suggested to trigger apoptosis (Asada et al. 2000; Chow et al. 1992). Thus, the inhibition of hypoxia-induced $[Ca^{2+}]_i$ rise by ATP may be a protective mechanism to prevent excessive and sustained $[Ca^{2+}]_i$ rise in type I cells during prolonged hypoxia. The feedback inhibition of ATP on the hypoxia-induced $[Ca^{2+}]_i$ rise will inhibit further release of ATP from type I cells. The resultant drop in local ATP concentration will in turn remove the inhibitory action on type I cells. If

the hypoxic stimulation is still present at this time, $[Ca^{2+}]_i$ in the disinhibited type I cells can rise again. Thus, our results raise the possibility that the $Ca^{2+}$ signal in type I cells may be oscillatory. The oscillation of the $Ca^{2+}$ signal may trigger periodic release of ATP from type I cells. ATP would in turn stimulate CSN activity via P2X receptors (Zhang et al. 2000; Prasad et al. 2001).

Multiple experimental approaches can be used to better understand how ATP affects the $Ca^{2+}$ signal in type I cells during chronic hypoxia. For example, $[Ca^{2+}]_i$ can be monitored in intact carotid body slice preparation in the presence of a $P2Y_1$ receptor antagonist, such as MRS2179. Inhibition of the negative feedback action of ATP during prolonged hypoxia is expected to cause a more sustained $[Ca^{2+}]_i$ rise in type I cells. During hypoxia, type I cells may also release other neurotransmitters, such as dopamine, ACh, and histamine, and these neurotransmitters may also have feedback effects on type I cells. In order to inhibit the actions of other neurotransmitters such as dopamine, ACh, histamine, etc., antagonists of the receptors for these transmitters should be also included. Since the $Ca^{2+}$ signal in type I cells is tightly coupled to CSN activity, our results raise the possibility that during chronic hypoxia, the CSN activity may also occur in oscillatory bursts.

Following the release of ATP from type I cells during hypoxia, ATP in the extracellular space may be broken down into adenosine by ecto-nucleotidases (Dunwiddie and Masino 2001). Hypoxia also stimulates intracellular adenosine efflux via adenosine equilibrative transporters (Conde and Monteiro 2004). Thus, during

chronic hypoxia, a rise in adenosine concentration in the extracellular space near type I cells is expected. As shown in Figure 6-1, we found that adenosine, acting via $A_{2A}$ receptors, inhibits the background TASK-like $K^+$ channels and thus causes membrane depolarization, which activates VGCC. The $Ca^{2+}$ influx via VGCC results in $[Ca^{2+}]_i$ elevation. As discussed earlier, during chronic hypoxia, the negative feedback action of ATP is expected to cause an oscillating $Ca^{2+}$ signal in type I cells. When the ATP level in the extracellular space is subsequently lowered, the stimulatory action of adenosine will further help type I cells to oppose the previous inhibitory action of ATP. Therefore, adenosine may contribute to increase the frequency of $Ca^{2+}$ oscillations in type I cells during chronic hypoxia, and thus shorten the interval between bursts of CSN activity.

In order to better understand how adenosine shapes the $Ca^{2+}$ signal in type I cells, the effects of $A_{2A}$ receptor agonists (CGS21680) or antagonists (ZM241385) can be examined by monitoring $[Ca^{2+}]_i$ in clusters of type I cells in a carotid body slice during chronic hypoxia. $A_{2A}$ receptors agonists would be expected to increase the frequency of $Ca^{2+}$ oscillation. In contrast, $A_{2A}$ receptor antagonists would be expected to decrease the frequency of $Ca^{2+}$ oscillation in type I cells.

Thus, our experiments, together with other studies, indicate that ATP and its metabolite adenosine play multiple roles in the carotid body (summarized in Figure 6-2). In addition to the $P2Y_1$-receptor-mediated inhibitory action of ATP and $A_{2A}$-receptor-mediated stimulatory action of adenosine on type I cells, a recent study

by Campanucci et al. (2006) showed that application of ATP in a co-culture preparation of type I cell clusters and GPN neurons caused depolarization and evoked inward currents in GPN neurons, but caused hyperpolarization in type I cells. In our experiments, we observed a similar effect of ATP on single type I cells. Campanucci et al. (2006) found that the hyperpolarization of type I cells was abolished by an NO scavenger, and also found that GPN neurons express multiple P2X receptor subtypes. Thus, they suggested that activation of P2X receptors on GPN neurons by ATP leads to $Ca^{2+}$ influx and activation of NOS, which synthesizes NO. NO, released from GPN endings, may in turn cause membrane hyperpolarization in type I cells (Campanucci et al. 2006). The above mechanism is expected to work in parallel with our finding that ATP caused negative feedback action directly on type I cells.

A previous study from our lab also found that ATP can act on $P2Y_2$ receptors on the glial-like type II cells of the carotid body, and can trigger intracellular $Ca^{2+}$ release from these cells (Xu et al. 2003). The role of the ATP-induced $Ca^{2+}$ signal in type II cells is unclear. Although type II cells do not contain any dense-core granules, they may release amino acids, arachidonic acid, or ATP (Haydon and Carmignoto, 2006; Zonta and Carmignoto, 2002). It is possible that some of these molecules modulate chemotransduction by acting on neighboring type I cells or on nerve endings.

In summary, ATP exerts multiple actions on the different cell components in the carotid body. The paracrine and autocrine actions of ATP suggest that ATP is an important neurotransmitter in the regulation of chemotransduction in the carotid body.

## 6.2 Summary and physiology implications of our findings on PACAP

We found that the circulating peptide PACAP, acting via $PAC_1$ receptors, causes membrane depolarization by inhibition of the background TASK-like $K^+$ channels (Figure 6-1). The PACAP-induced depolarization in turn activates VGCC, and $Ca^{2+}$ entry via these channels elevates $[Ca^{2+}]_i$. Our study also showed that the action of PACAP on $[Ca^{2+}]_i$ is additive to a moderate hypoxia response (Figure 5-1B & C). Recently, Cummings et al. (2006) have also shown that PACAP causes an increase in CSN discharge in the carotid body. All of the results summarized above suggest that under moderate hypoxia, PACAP may augment the hypoxia-induced $[Ca^{2+}]_i$ rise in type I cells which in turn leads to an increase in CSN discharge. The stimulatory action of PACAP on type I cells may enhance the response of type I cells during weak or moderate hypoxia. Consistent with this, Cummings et al (2004) found that PACAP-deficient mice have a reduced response to hypoxia or hypercapnia.

Interestingly, PACAP-deficient mice also have a higher susceptibility to sudden death during neonatal period (Cummings et al. 2004). This suggests that PACAP may be critical for carotid body chemotransduction in neonatal animals. In

neonatal animals, the carotid body exhibits poor response to hypoxia (Donnelly 2000). Thus, for neonatal animals, where the hypoxic response of the carotid body is not fully developed, the enhancing action of PACAP on the hypoxia-mediated $Ca^{2+}$ signal in type I cells may have an important role in response to hypoxia. However, it is not known, in either neonatal rats or adult rats, whether the PACAP level in the carotid body is indeed increased during hypoxia. It is also not clear whether PACAP is released from nerve terminals in the carotid body or reaches carotid body cells through the blood vessels. These issues should be addressed in future studies.

## 6.3 Role of BK and TASK-like $K^+$ channels in the hypoxic response

In rat type I cells, two $K^+$ channels have been implicated in the hypoxia-induced depolarization: TASK (mainly TASK-1)-like $K^+$ channels (Buckler 1997; Buckler 1999; Buckler et al. 2000) and BK channels (Peers 1990; Riesco-Fagundo et al. 2001). In our study, application of TEA (a BK channel blocker) or anandamide (a TASK-1 like $K^+$ channel blocker) caused membrane depolarization and $[Ca^{2+}]_i$ rise in type I cells. We found that inhibition of BK channels with TEA caused transient $[Ca^{2+}]_i$ rise in about 50% of the cells (Figure 4-5B & Figure 5-5A). In contrast, application of the TASK-1 $K^+$ channel blocker anandamide always caused a reduction in TASK-like background $K^+$ current (Figure 5-7C), leading to membrane depolarization and sustained $[Ca^{2+}]_i$ rise (Figure 4-6B). These results suggest that the

opening probability of TASK-like $K^+$ channels is higher than that of BK channels at resting membrane potentials in rat type I cells. TASK-like $K^+$ channels are background $K^+$ channels that are active at resting membrane potentials. Activation of BK channels, on the other hand, depends on both depolarization (to ~-20 mV) and $[Ca^{2+}]_i$ elevation (to ~μM) (Donnelly 1999; Vergara et al. 1998). In our studies involving simultaneous measurement of membrane potential (perforated patch-recording technique) and $[Ca^{2+}]_i$ (indo-1 fluorometry), the mean values of resting membrane potential in type I cells are ~-40 mV ± 3mV and the resting $[Ca^{2+}]_i$ are 216 ± 18 nM (n= 23; Chapter 4.2.2 & Chapter 5.2.3). Under these conditions, the overall probability of BK channel opening is expected to be low. Note that however, the resting membrane potential and $[Ca^{2+}]_i$ did not rule out the possibility that some BK channels are open at rest. Activation of HO-2 has been suggested to regulate the activity of BK channels (Prabhakar and Overholt 2000; Williams et al. 2004). Under normoxic condition, CO, generated by the activity of HO-2, is suggested to maintain a negative resting membrane potential probably by promoting the opening of BK channels (Kemp 2005; Williams et al. 2004). Thus, the activation of BK channels depends on the activity of HO-2, which may vary among cells. In summary, we speculate that TASK-like $K^+$ channels may contribute more toward the initial depolarization and $[Ca^{2+}]_i$ rise during hypoxia in rat type I cells, and as the membrane potential becomes more positive, the inhibition of BK channels becomes more important.

## 6.4 Strengths and limitations of the experiments

### *6.4.1 Strengths of the experiments*

As mentioned in Chapter 1.3.2, the interpretation of the actions of the neurotransmitters in intact carotid body preparation is complicated by the expression of multiple receptors on type I cells, type II cells and different types of nerve endings. To better understand how transmitters modulate the chemotransduction in the carotid body, it is essential to first understand the actions of transmitters on the level of individual cell types. Thus, enzymatically dissociated single type I or type II cells were used in this study. A major difficulty in the study of isolated type I cells is the loss of sensitivity to hypoxia. Thus, several precautions were taken in our study to ensure that the cells are healthy. First, during the removal of carotid body, the Tyrode solution was bubbled continuously with $O_2$. This procedure minimizes any hypoxia in the tissue, as hypoxia will elevate basal $[Ca^{2+}]_i$ in type I cells and this may lead to cell damage. Second, after enzymatic cell dissociation, cells were left to recover for 2-6 hours before the experiments. We found that after ~2 hours, dissociated cells can respond to hypoxia. Third, the majority of type I cells cultured overnight became unresponsive to hypoxia. Therefore we use only short-term cultured single type I cells (12 h at most) to circumvent this problem. Fourth, type I, type II carotid cells, as well as blood cells, are round or ovoid immediately following dissociation, and thus

cannot be distinguished morphologically. Therefore, in our study, hypoxia or hypercapnia was used to identify type I cells. Only type I cells, but not the type II cells or blood cells, respond to hypoxia or hypercapnia with $[Ca^{2+}]_i$ rise. Fifth, we employed adult animals in our study. Although the dissection of carotid body in neonatal rats is much easier (due to the fact that there is less connective tissue), neonatal rats may have a poorer hypoxic response, as the carotid body is not fully developed. This may explain why we can consistently detect the hypoxia response in type I cells. Sixth, we used a low concentration of $Ca^{2+}$ indicator in all our experiments. Since $Ca^{2+}$ indicator also acts as $Ca^{2+}$ buffer, our procedure allows us to detect the relatively small changes in $[Ca^{2+}]_i$ during adenosine and PACAP challenge. Finally, perforated patch clamp is used in our experiments to reduce any loss of important cytosolic components in the type I cells. We know that our recording conditions never result in accidental whole cell because the fluorescent indo-1 dye (for $[Ca^{2+}]_i$ measurement) never suddenly leaves the cell during prolonged recording.

### *6.4.2 Limitations of the experiments*

Since we can consistently detect hypoxia response at room temperature, we performed all the experiments at room temperature (20-23°C) instead of at physiological temperature (37°C). A major advantage is that the perforated patch-clamp recording is more stable at room temperature. However, we must also take into consideration the temperature dependence of certain biological processes.

It is well known that the voltage-gated $Ca^{2+}$ current is temperature-dependent (Allen, 1996; Williams and Kelly, 1995). In dorsal raphe neurons, increasing the temperature enhanced the amplitude of high voltage-activated $Ca^{2+}$ current and accelerated the activation rate of the $Ca^{2+}$ current (Williams and Kelly, 1995). As well, lowering the temperature reduced the L-type $Ca^{2+}$ current in single guinea pig ventricular myocytes (Allen, 1996). Thus, it is likely that the amplitude of the $Ca^{2+}$ current in our study is lower than that at the physiological temperature.

The release of hormones and neurotransmitters is also sensitive to temperature (Renstrom et al. 1996; Ohta et al. 1990). Although we did not examine the secretion of transmitters from type I cells, it is likely that the amount of ATP released from type I cells at room temperature is less than that released at physiological temperature. Since our studies focused on the effects of applied ATP, adenosine, and PACAP on isolated type I cells, and the cells were exposed to known concentration of the transmitters, the effect of temperature would probably not affect our conclusion about the actions of ATP, adenosine and PACAP on type I cells of rat carotid bodies. Nevertheless, as described below, the effect of temperature would be an important factor in intact preparations.

There are several limitations in extending our findings in dissociated single cells to an intact carotid body preparation. First, although we speculate that the local ATP concentrations near type I cells might be very high during hypoxia due to the small extracellular space in the cell cluster, the actual local concentration of ATP or

adenosine near type I cells during hypoxia is not known. Second, the time course of ATP release and its enzymatic conversion to adenosine (which is highly temperature dependent) can not be estimated from our single cell experiments. Third, our single cell studies cannot address how type I cells interact with type II cells or the CSN, GPN nerve endings. Finally, how the multiple actions of ATP interact to shape the CSN output is not known. Thus, future experiments with carotid body slice and *in vitro* carotid body with specific antagonists of $P2Y_1$, $P2Y_2$ and adenosine receptors are needed to clarify the precise action of ATP in a physiological context.

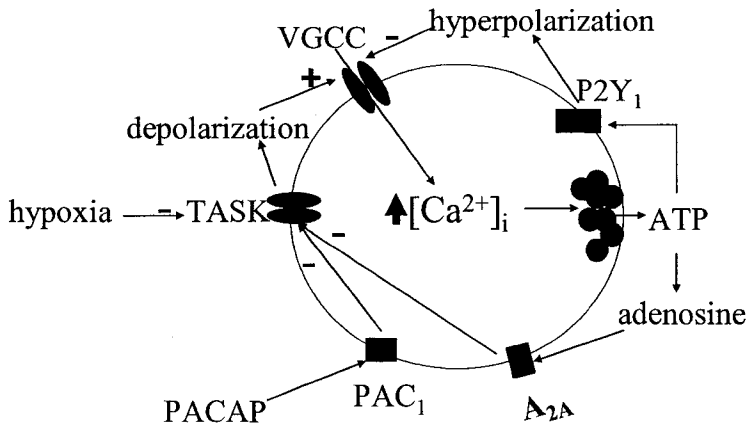


**Figure 6-1** Summary of the actions of ATP, adenosine and PACAP on type I cells of rat carotid body. ATP, a neurotransmitter released from type I cells during hypoxia, acting via $P2Y_1$ receptors, causes a hyperpolarization in type I cells which in turn opposes hypoxia-mediated membrane depolarization and $Ca^{2+}$ entry via VGCC. The ATP metabolite adenosine, acting via $A_{2A}$ receptors, inhibits TASK-like $K^+$ channels and thus causes membrane depolarization and $Ca^{2+}$ influx via VGCC. PACAP also triggered a $[Ca^{2+}]_i$ rise in type I cells. The action of PACAP was mediated via $PAC_1$ receptors and inhibition of TASK-like $K^+$ channels.

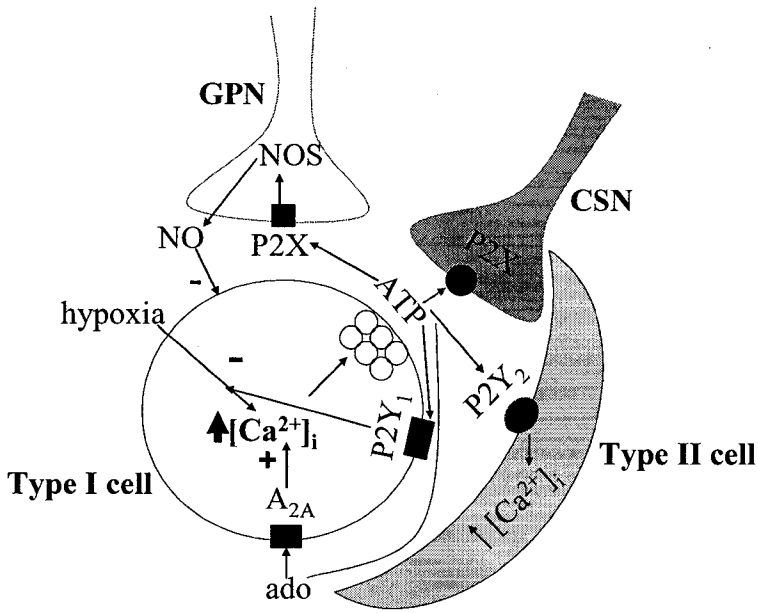


**Figure** 6-2 Autocrine and paracrine actions of ATP and adenosine in rat carotid body. During hypoxia, ATP is released from type I cells and will then act on the cells themselves, or on type II cells or nerve endings. ATP can mediate negative feedback action on type I cells via receptors on GPN endings or via $P2Y_1$ receptors in type I cells. At the GPN nerve endings, ATP binds to P2X receptors and stimulates the activity of NOS which produces NO. NO exerts inhibitory action on type I cells by causing membrane hyperpolarization. ATP can directly cause hyperpolarization in type I cells via $P2Y_1$ receptors, and thus inhibit hypoxia-mediated membrane depolarization and $[Ca^{2+}]_i$ rise. ATP has stimulatory actions on both CSN and type II cells by acting on P2X and $P2Y_2$ receptors, respectively. Finally, the ATP metabolite adenosine causes $[Ca^{2+}]_i$ rise in type I cells via $A_{2A}$ receptors.

## References


Allen T.J. (1996) Temperature dependence of macroscopic L-type calcium channel currents in single guingea pig ventricular myocytes. *J Cardiovasc Electrophysiol* **7(4),** 307-321.

Asada S., Fukuda K., Nishisaka F., Matsukawa M. and Hamanisi C. (2001) Hydrogen peroxide induces apoptosis of chondrocytes: involvement of calcium ion and extracellular signal-regulated protein kinase. *Inflamm Res.* **50 (1),** 19-23.

Buckler K. J. (1997) A novel oxygen-sensitive potassium current in rat carotid body type I cells. *J Physiol* **498 ( Pt 3),** 649-662.

Buckler K. J. (1999) Background leak K+-currents and oxygen sensing in carotid body type 1 cells. *Respir Physiol* **115,** 179-187.

Buckler K. J., Williams B. A., and Honore E. (2000) An oxygen-, acid- and anaesthetic-sensitive TASK-like background potassium channel in rat arterial chemoreceptor cells. *J Physiol* **525 Pt 1,** 135-142.

Buttigieg J. and Nurse C.A. (2004) Dectection of hypoxia-evoked ATP release from chemoreceptor cells of the rat cartoid body. *Biochemical and Biophysical Research Communications* **332,** 82-87.

Campanucci V. A., Zhang M., Vollmer C., and Nurse C. A. (2006) Expression of multiple P2X receptors by glossopharyngeal neurons projecting to rat carotid body O2-chemoreceptors: role in nitric oxide-mediated efferent inhibition. *J Neurosci* **26,** 9482-9493.

Chow S.C., Kass G.E. McCabe J.J. and Orrenius S. (1992) Tributylin increases cytosolic free Ca2+ concentration in thymocytes by mobilizing intracellular Ca2+, activating a Ca2+ entry pathway, and inhibiting Ca2+ efflux. *Arch Biochem Biophys* **298(1),** 143-149.

Conde S. V. and Monteiro E. C. (2004) Hypoxia induces adenosine release from the rat carotid body. *J Neurochem* **89,** 1148-1156.

Cummings K. J., Pendlebury J. D., Sherwood N. M., and Wilson R. J. (2004) Sudden neonatal death in PACAP-deficient mice is associated with reduced respiratory chemoresponse and susceptibility to apnoea. *J Physiol* **555,** 15-26.

Cummings K.J., Day T., and Wilson R.J.A. (2006) PACAP stimulates the carotid body leading to an increase in neuronal ventilation. Abstract, the Xth Oxford Conference on Modeling and Control of Breathing, Lake Louise, Canada

Donnelly D. F. (1999) K+ currents of glomus cells and chemosensory functions of carotid body. *Respir Physiol* **115,** 151-160.

Donnelly D.F. (2000) Developmental aspects of oxygen sensing by the carotid body. J. Appl. Physiol 88 (6), 2296-2301.

Dunwiddie T. V. and Masino S. A. (2001) The role and regulation of adenosine in the central nervous system. *Annu Rev Neurosci* **24,** 31-55.

Haydon P.G. and Carmignoto G. (2006) Astrocyte control of synaptic transmission and neurovascular coupling. *Physiol Rev* **86(3),** 1009-1031.

Kemp P. J. (2005) Hemeoxygenase-2 as an O2 sensor in K+ channel-dependent chemotransduction. *Biochem Biophys Res Commun* **338,** 648-652.

Mcdonald D.M. Structure-function relationships of chemoreceptive nerves in the carotid body. *American Review of Respiratory Disease* **115(6 Pt 2),** 193-207.

Ohta M., Nelson D., Nelson J., Meglasson M.D., and Erecinska M. (1990) Oxygen and temperature dependence of stimulated insulin secretion in isolated rat islets of langerhans. *J of Bio Chem.* **265(29),** 17525-17532.

Pardal, R., Ludewig U., Hirschfeld, J.G. and Loopez-Barneo J. (2000) Secretory responses of intact glomus cells in thin slices of rat cartoid body to hypoxia and tetraethylammonium. *Proc Natl Acad Sci* **97(5),** 2361-2366.

Peers C. (1990) Hypoxic suppression of K+ currents in type I carotid body cells: selective effect on the Ca2(+)-activated K+ current. *Neurosci Lett* **119,** 253-256.

Prabhakar N. R. and Overholt J. L. (2000) Cellular mechanisms of oxygen sensing at the carotid body: heme proteins and ion channels. *Respir Physiol* **122,** 209-221.

Prasad M., Fearon I. M., Zhang M., Laing M., Vollmer C. and Nurse C. A. (2001) Expression of P2X2 and P2X3 receptor subunits in rat carotid body afferent neurones: role in chemosensory signalling. *J. Physiol.* **537,** 667-677.

Renstrom E., Eliasson L., Bokvist K. and Rorsman P. (1996) Cooling inhibits exocytosis in single mouse pancreatic B-cells by suppression of granule mobilization. *J of Physiol.* **494 (1),** 41-52.

Riesco-Fagundo A. M., Perez-Garcia M. T., Gonzalez C., and Lopez-Lopez J. R. (2001) O(2) modulates large-conductance Ca(2+)-dependent K(+) channels of rat chemoreceptor cells by a membrane-restricted and CO-sensitive mechanism. *Circ Res* **89,** 430-436.

Roy A., Rozanov C., Mokashi A., and Lahiri S. (2000) P(O(2))-P(CO(2)) stimulus interaction in [Ca(2+)](i) and CSN activity in the adult rat carotid body. *Respir Physiol* **122,** 15-26.

Vergara C., Latorre R., Marrion N. V., and Adelman J. P. (1998) Calcium-activated potassium channels. *Curr Opin Neurobiol* **8,** 321-329.

Urena J., Chacon R.F., Benot A.R., Toledo G.A., and Lopez-Barneo J. Hypoxia induces voltage-dependent Ca2+ entry and quantal dopamine secretion in carotid body glomus cells. *Proc Natl Acad Sci* **91(21),** 10208-10211.

Williams S. E., Wootton P., Mason H. S., Bould J., Iles D. E., Riccardi D., Peers C., and Kemp P. J. (2004) Hemoxygenase-2 is an oxygen sensor for a calcium-sensitive potassium channel. *Science* **306,** 2093-2097.

Williams R.H.M. and Kelly J.S. (1995) The temperature dependence of high-threshold calcium channel currents recorded from adult rat dorsal raphe neurones. *Neuropharmacology* **34(11),** 1479-1490.

Xu J., Tse F. W., and Tse A. (2003) ATP triggers intracellular $Ca^{2+}$ release in type II cells of the rat carotid body. *J Physiol* **549,** 739-747.

Zonta M. and Carmignoto G. (2002) Calcium oscillations encoding neuron-to astrocyte communication. *J Physiol Paris* **96(3-4),** 193-198.

Zhang M., Zhong H., Vollmer C., and Nurse C. A. (2000) Co-release of ATP and ACh mediates hypoxic signalling at rat carotid body chemoreceptors. *J Physiol* **525 Pt 1,** 143-158.